Simplified and dynamic calculation method for a façade with double glazing and internal shading device

Univeristy	Aalborg University
Theme	Master thesis project
Autors	Izabela Ewa Wysocka
	Juan Llop Chocarro
	Laurentiu Stefan Lungu
Date	13th of June 2016

AALBORG UNIVERSITET

Aalborg University
Engineering and Science
Sofiendalsvej 9-11
9200 Aalborg SV
Phone No.: 99 40 84 84
http://www.byggeri.aau.dk

Title:
Simplified and dynamic calculation method for a façade with double glazing and internal shading devices.

Project period:
01-11-2015 to 13-06-2016

Project group:
3

Participants:
Izabela Ewa Wysocka
Juan Llop Chocarro
Laurentiu Stefan Lungu

Supervisor:
Olena Kalyanova Larsen
Mingzhe Liu

Number of pages: 87
Number of appendices: 12
Completed: 13.06.2016

Synopsis:

Nowadays, it is crucial to find an appropriate solution for the shade control in the buildings which in current architecture trend are mostly totally glazed. Internal shading control is assumed to be a reasonable, effective and cheap solution, however its proper evaluation is needed. Current numerical simulations require a deep understanding of the processes involved and are not easy to use. Therefore, the aim of this thesis is further development of the simplified calculation method for double glazing façade with implementation of internal shading devices This thesis is based on already developed 1D model for double glazed façade presented in Mingzhe Liu work. Thermal and solar properties of assigned system are evaluated. Investigation and model development are done by using two types of internal shading devices (White Pearl and Charcoal Grey solar shading). Calculation method is based on standards EN410, EN673, EN 13363-1, EN 13363-2, ISO 15099 and other literature review. Model is verified by full-scale façade element test facility at Aalborg University. Developed calculation method allows to calculate whole year performance at different time steps. That makes it a simple and accurate tool for the design purposes at early stage for glazing façade under control strategy using internal shading devices.

1 Abstract

Today newly constructed buildings have to fulfil strict energy consumption requirements, due to the necessity of reducing fossil fuel based energy dependency. In order to do so, passive strategies are implemented by maximizing the use of daylight, natural heating, cooling and ventilation. These strategies require a balance to guarantee proper indoor comfort and low energy consumption. They have to be implemented in such a way that their advantages will not turn into disadvantages. Highly glazed buildings with intelligent façades are a good solution, where natural light gains can be combined with shading devices to avoid undesired heat gains.

Simulation programs are needed during the design phase of the building, to accurately estimate energy consumption and thermal comfort throughout the year. Highly glazed façades require specific simulation treatment because of high solar angle dependency of both, glazing and shading devices. There exist many simulation programs that accurately calculate angle dependency properties of glazing with shading devices. However they require high computing power and very specific knowledge of the glazing and shading properties.

Therefore the purpose of this work is to develop a simplified calculation method, that determines heating and cooling energy consumption as well as temperatures, to evaluate thermal comfort in a room with a glazed façade and an internal shading device. Two different approaches are followed to develop the calculation method. First one is based on the solar heat gain coefficient in the room and is referred to as "SHGC-model". Second one considers more in detail angular properties of the glazing and blind, as well as more precise analysis of the air in the cavity between the glazing and the blind. This approach is called "Detail model" in the project.

SHGC-model is a simpler model where solar heat gains are implemented in the air of the cavity and the room, and incident radiation angular dependency is considered by using an empirical method. By using the solar heat gain coefficient, special knowledge about the properties of the glazing nor the blind is needed. This model calculates room and cavity air temperatures, but local discomfort cannot be evaluated due to the fact that the façade surfaces' temperatures are not simulated.

Detail model analyses the two panes of the glazing individually and the blind, considering

angle dependent properties of all of them. Additionally, air movement in the cavity is also simulated based on temperature gradient and pressure losses in the cavity, and between the cavity and the room. Regarding the solar gains, they are considered through the absorbed energy in each of the surfaces of the elements. Besides air temperatures, temperatures in the façade's elements can be obtained, so local discomfort can also be evaluated.

Results obtained from the simulations are compared with full scale measurements in order to validate them. In terms of energy consumption, both approaches provide accurate results, although there is certain deviation from the measurements that can be related to overestimated heat losses. Detail model is more sensitive to the type of blind used, which loses accuracy when using more reflective blinds. Regarding calculated temperatures, both models indicate good agreement with the experiment when calculating room air temperature. This is due to the fact that the controller is set in the air of the room. However SHGC-model is calculating high temperatures in the cavity while detail model results are closer to the measurements. Based on obtained results, the sensitivity analysis is performed and several influencing parameters are evaluated.

All in all, from the analysis of obtained simulation results, it is highlighted that further work is needed in terms of developing a simplified calculation tool for double glazed façades with internal shading devices. Project indicates vulnerabilities of the models and the most influencing parameters, from which the cavity and blind treatment have the biggest impact.

Preface 2

This is the master thesis project for the "Indoor Environmental and Energy Engineering" study programme by the School of Engineering and Science at Aalborg University. The project is called "Simplified and dynamic calculation method for a façade with double glazing and internal shading device" and is made in the period from the 1^{st} of November 2015 to the 14^{th} of June 2016.

The project is ordered in five parts. Part one explains general theory used in the thesis. The second part consists on the investigation work carried out with an explanation of the most relevant aspects. Part three explains the experiment facilities, set-up, conditions and data treatment. In the fourth part the mathematical model is developed and is validated with experimental measurements. Afterwards a sensitivity analysis of the model is performed. The last part includes a discussion and a conclusion about the obtained results.

All references in the report are listed in the reference list in the end. Books are listed with author and publisher. Websites are listed with URL address. Figures, tables and equations are enumerated according to the chapter. If no references are given, the figures and tables have been produced by the group members.

Appendices are attached in the back. Furthermore, electronic appendices are enclosed on a CD.

Izabela Ewa Wysocka	Juan Llop Chocarro	Laurentiu Stefan Lungu

Table of contents

Introduction 3

The Limits to Growth [1] written in 1972 predicted that resources on Earth would be finished after 100 years if the increase of population, industrialisation, pollution, food production and resources consumption continues in the same way. Society is nowadays aware about climate change and the urgent need of environmental policies and energy consumption reduction. According to the United Nations [2] buildings use around 40% of global energy and resources, 60% of world's electricity and responsible of 10% of global GDP emissions. Therefore, governments politics are oriented towards building energy reduction.

Building energy consumption during its lifetime is of great importance, depending on heating, cooling, lighting and ventilation. However, building design has to be done so the indoor comfort is achieved with minimum energy use. In order to do so, simulation programs are developed to help architects and engineers with buildings design. The most influencing part over energy consumption in buildings is the envelope, where windows have an important role. An effective way of reducing energy cooling demand is shading implementation, and a lot of research has been done in order to develop simulation models that would perform accurately [3].

There are three major types of shading solutions for buildings: external, integrated and internal shading devices. In this project, investigation around internal shading devices is handled. This choice has been made due to a lower purchase price, its user-friendliness and low maintenance costs are involved during the life time of the building. [4] Considering these features as a surpassing over another solutions, only this type is investigated in this report.

It is known that glazings' physical properties are strongly dependent on solar angle of incidence. However it has been also proved in [4] that the system conformed by a glazing with an internal shading device is also very dependent on the angle of incidence. In this work standard EN-13363-1 is used, where a simple equation including both glazing and shading is proposed to calculate the energy transmittance through the system. However as suggested in this same standard, this equation leads to conservative values [5]. Standard ISO 15099 proposes a more advanced calculation method where heat transfer through the window is considered as well as air circulation within the glazing and the blind [6].

However little investigation is available about blinds angle dependency and some of it

has been analysed in [7]. It has been found that there exist semi-empirical methods to calculate the corresponding off-normal properties for a given solar optical properties of any fabric (shading device) at normal incidence. Model developed by [8] measures the spectral properties of the blind at the range of incident angle from 0° to 60° and is in agreement with the experimental data provided. This methodology is used in the model developed in this work.

Most of the studies are focused on determining the indoor thermal environmental conditions when having a glazed façade with internal shading device. Some calculate a thermal model with obtained solar optical properties and different heat transfer coefficients [9], thermal comfort as radiant temperature asymmetry [10] or mean radiant temperature [11]. Other papers as [12], [13] and [14], focus on the visual comfort by measuring the illumination level on the working area and controlling the shading position. Nonetheless there are few studies related to energy consumption simulation when implementing internal roller shading device. A recent study [15] for the internal roller shades analyses the effectiveness of various types used, where some of the influential characteristics are distance between the glazing and the shading, their temperature difference, fabric type, color and thickness.

In [16] simplified method is developed in order to calculate solar gains into a double glazing. Having the weather conditions, this hourly-based simplified method calculates energy consumption needed for cooling and heating, as well as indoor air and surfaces temperatures. This method is based on standard ISO-13790 [17], where solar gains are assumed to be in the construction elements' surfaces. However when implementing an internal shading device, air in the cavity between glazing and blind is heated up by the solar radiation which may have an important impact over heat transfer. Standard DIN-18599-2 [18] proposes a methodology where solar gains in a building with an adjacent unheated sun space, are considered into the air of the two spaces. This analysis can be extrapolated into the air in the cavity and air in the room.

Aim

Because there is a necessity to calculate heat transfer through a glazing with internal shading device considering angle dependency, the aim of this work is to develop a simplified calculation method for a façade with a double glazing and internal shading devices. Method is developed based on a nodal approach using MATLAB [19] and validated through several experiments provided in full-scale test facility at Aalborg University called "The Cube". Developed model aims to provide consultants with a simple calculation tool which can be used in early stages of the design, evaluating energy consumption in buildings with increased accuracy in an hourly-based method.

Methodology

This project focuses on the development of a simple simulation program for glazing with internal shading, considering heat energy transfer. Investigation work is done in order to summarize and compare existing calculation methodologies concerning both glazing and shading device properties. Those properties are also explained in the theory part, as well as the physical phenomena involved. Analysis of the cavity in between the glazing and shading is done as well.

Model is developed according to two different approaches depending on how detailed the glazing analysis is. First approach considers the total heat transfer through the glazing while the second one takes into account each of the glazing panes and its physical properties.

The models are validated with experimental measurements obtained from real scale set up. Experiment is run under different weather conditions provided in May, with two shading devices. After validation is done a sensitivity analysis is evaluated. Sketch of the methodology is presented on figure 3.1.

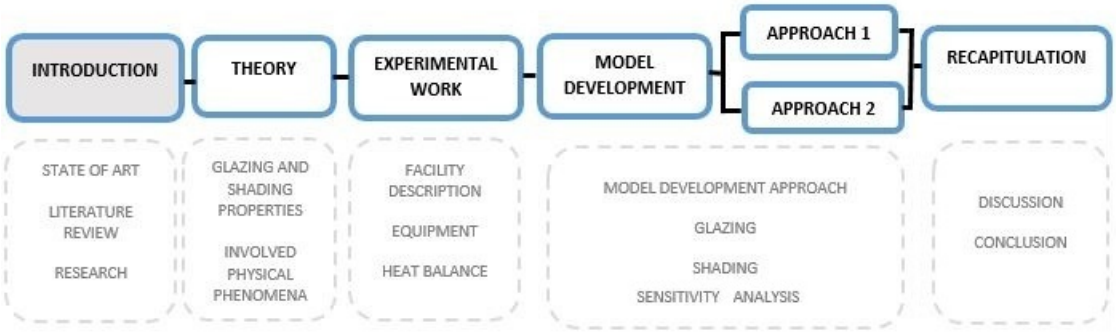

Figure 3.1. Followed methodology in the project

Part I

Theory

Window and shading - theoretical evaluation 4

The project emphasises on the evaluation of processes happening in the glazing with internal shading devices. To do so, the description of physical phenomena with specific parameters which determine the window and shading are needed. Therefore, presentation of theory behind considered system is presented.

4.1 Physical phenomena

In the examined system the main process involved is the heat transfer which is the exchange of thermal energy between different systems. The role of heat transfer in the thermal science is to add thermodynamic analysis, which considers only systems in equilibrium (closed systems), with additional laws that allow prediction of time rates of energy transfer[20]. Fundamental parts of the energy transport by heat are: conduction, convection and radiation. Detailed description of the mentioned processes is presented in Appendix A.

4.2 Thermal transmittance (U-value)

U-value is the parameter which characterizes the heat transfer through the materials per temperature difference between the environmental temperatures on each side of the analysed system. It is given in watts per square meter kelvin [$\frac{W}{m^2K}$].

According to European Standard EN673 [21] thermal transmittance of the glass in the building is determined in the following way:

$$\frac{1}{U} = \frac{1}{h_e} + \frac{1}{h_t} + \frac{1}{h_i} \tag{4.1}$$

Thermal transmittance is considered as a combination of heat transfer coefficients. The first and the last terms (h_e and h_i) are the external and internal heat transfer coefficients whereas the middle one (h_t) corresponds to the total thermal conductance of the considered system.

Heat transfer coefficient h_t for a considered system is calculated according to equation 4.2:

$$\frac{1}{h_t} = \sum_{1}^{N} \frac{1}{h_s} + \sum_{1}^{M} d_j r_j \tag{4.2}$$

Where:

h_t	thermal conductance for the window, $[\frac{\mathrm{W}}{\mathrm{m^2K}}]$
h_s	thermal conductance of each gas space, $[\frac{\mathrm{W}}{\mathrm{m^2K}}]$
N	number of spaces, [−]
d_j	thickness of each material layer, [m]
r_j	thermal resistivity of each material, $[\frac{\mathrm{mK}}{\mathrm{W}}]$
M	number of material layers, [−]

$$h_s = h_r + h_g \tag{4.3}$$

Where:

h_r	radiation conductance, $[\frac{\mathrm{W}}{\mathrm{m^2K}}]$
h_g	gas conductance, $[\frac{\mathrm{W}}{\mathrm{m^2K}}]$

$$h_r = 4\sigma_s(\frac{1}{\epsilon_1} + \frac{1}{\epsilon_2} - 1)^{-1} T_m^3 \tag{4.4}$$

Where:

σ_s	Stefan-Boltzmann's constant, $[\frac{\mathrm{W}}{\mathrm{m^2K^4}}]$
T_m	mean absolute temperature of the gas space, [K]
ϵ_1 & ϵ_2	corrected emissivities at T_m [−]

$$h_g = Nu\frac{\lambda_{gas}}{s} \tag{4.5}$$

Where:

s	width of the space, [m]
λ_{gas}	thermal conductivity of the gas, $[\frac{\mathrm{W}}{\mathrm{mK}}]$
Nu	Nusselt Number, [−]

4.3 Total solar energy transmittance (g-value)

The total solar energy transmittance describes the total fraction of incident solar energy that is transmitted through a building component [22]. Solar radiation analysis and necessary calculation for angle of incidence are presented in Appendix B.

Solar energy can be divided into three main components. In this project, a window with internal solar shading device is considered, therefore on figure 4.1 representation of solar energy components is presented for such system.

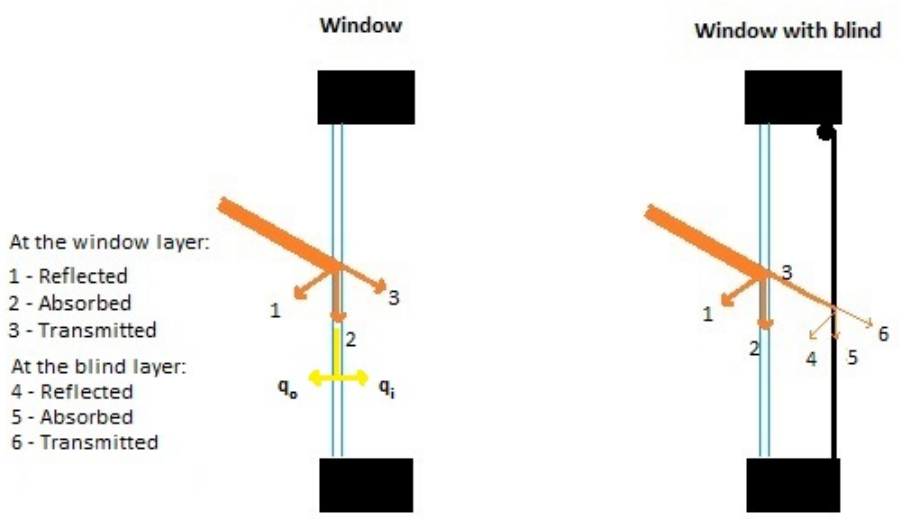

Figure 4.1. The reflectance, absorbtance and transmittance of the incident solar radiation when reaching the window component and window with internal shading device.

As presented on the figure above division solar energy is divided into:

- ρ - reflected part
- α - absorbed part
- τ - transmitted part
- q_i - secondary heat transfer factor
- q_0 - absorbed heat re emitted outdoors

According to [23] the relations between the mentioned characteristics are:

$$\tau + \rho + \alpha = 1 \tag{4.6}$$

$$g = \tau + q_i \tag{4.7}$$

Where g is a g-value or solar heat gain coefficient (SHGC).

In the case without shading device, g-value for a window can be obtained from the equation:

$$g_w = \frac{Q_{suni}}{Q_{sune}} \tag{4.8}$$

Where:

g_w	g-value of the window, $[-]$
Q_{sune}	Solar radiation reaching exterior of the window, $[\frac{\mathrm{W}}{\mathrm{m}^2}]$
Q_{suni}	Solar heat gain in the room, $[\frac{\mathrm{W}}{\mathrm{m}^2}]$

This equation gives a simplified approach for calculation of g-value of the window.

In case of the window with solar shading device, the solar energy is primarily split on the window panes and then the transmitted part is secondarily split into three characteristic parts. The situation presented on figure 4.1 is simplified in order to give a better overview and understanding of the processes taking place.

In order to properly evaluate the exact value of solar energy transmittance, the boundary conditions on which the g-value depends need to be identified [22]:

- Position of the blind (in investigated case it is internal)
- Type of glazing and blind
- Room characteristics
- Wind conditions
- Ventilation of the gap between the glazing and blind, and in the room
- Angle of incidence
- Reflection of solar radiation from the ground and surroundings

As stated above, the total solar energy transmittance depends on incidence angle of the sun. Several researches have been made around that topic, and an example of how glazing properties are influenced by the angle of incidence is presented on figure below.

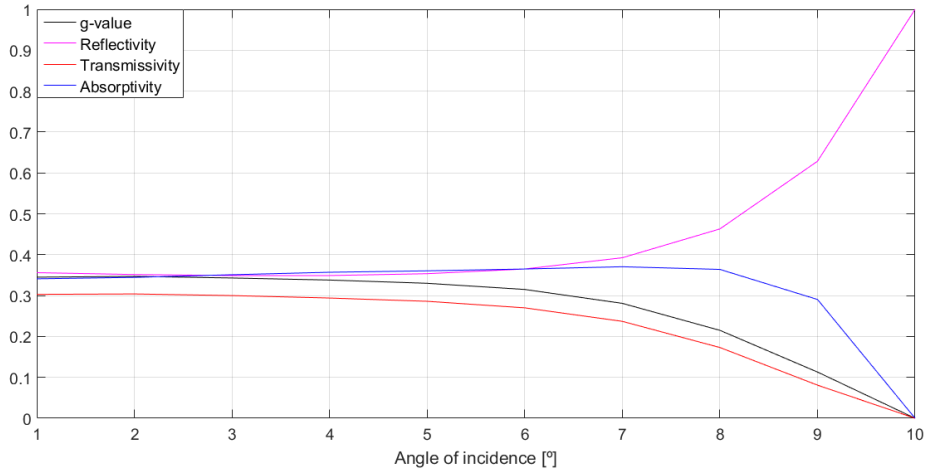

Figure 4.2. Glazing system angular properties obtained from WINDOW. [40]

Figure 4.2 shows the properties of a double glazed window with coating obtained from WINDOW software. However, it needs to be stated that the properties vary from one type of window to another.

As it can be seen, for normal incident angles transmissivity, absorptivity and reflectivity do not vary significantly. The more oblique the incident angle is, the less is transmitted. Absorptivity increases at first for incident angles close to 60°- 70°, whereas it decreases for higher angles. Reflectivity is varying in the opposite way as absorptivity does. The difference between total solar heat gain coefficient and transmissivity represents the secondary heat transfer factor, from the re-emitted heat from the glazing towards the inside.

4.4 Shading device angle dependency

Standard ISO 15099:2003 [6] gives necessary description of the solar-optical parameters of shading devices as well as information about how the shading device should be treated in the calculations procedures.

The standard is restricted to those kinds of shading devices which are or may be treated as a layer parallel to the panes of the window, by proper approximations. This additional layer exchanges heat with other components and/or environment and its thermal-optical interaction is, to a great extent, similar to the panes or films. Thus it can be defined as a layer between two gaps (or gap and environment). Due to usually a porous structure of the blind, the shading device is not only partially transmittant for solar radiation, but also for thermal (long wave) radiation.

Proper approximations are considered in order to sufficiently accurately evaluate thermal effects.

Incident beam radiation on the shading device surface is split into two portions:

- an undistributed portion - transmitted through the opening (specular transmission and reflection)
- a distributed portion (some of which will be scattered in the forward direction - transmitted, or scattered in the reverse direction - reflected)

Distributed portion is approximated as diffuse regardless of its directional nature.

Consequently, the following solar properties of a solar shading device are described and required for its description.

- $\tau_{dir,dir}$ - direct-direct (specular) transmittance; constitutes the undistributed portion and at normal incidence angle $\tau_{dir,dir}$ is equivalent to an openness factor A_0
- $\tau_{dir,dif}$ - direct-diffuse transmittance; portion of distributed radiation that is not absorbed by the shading device;
- $\tau_{dif,dif}$ - diffuse-diffuse transmittance; incident diffuse radiation remains diffuse in transmission (or reflection)

The sum of $\tau_{dir,dir}$ and $\tau_{dir,dif}$ is equal to direct hemispherical transmittance $\tau_{dir,h}$.

$$\tau_{dir,h} = \tau_{dir,dir} + \tau_{dir,dif} \tag{4.9}$$

Similarly, following properties are required for the reflectance ($\rho_{dir,dir}$, $\rho_{dir,dif}$, $\rho_{dif,dif}$, $\rho_{dir,h}$).

Solar absorption is calculated according to the formulas:

$$\alpha_{dir} = 1 - \tau_{dir,dir} - \rho_{dir,dir} - \tau_{dir,dif} - \rho_{dir,dif} \tag{4.10}$$

$$\alpha_{dif} = 1 - \tau_{dif,dif} - \rho_{dif,dif} \tag{4.11}$$

With consideration of presented description of solar properties for shading device, calculations shall be proceeded similarly to this for the glazing separately.

There is no existing standardized method for the calculation of the above-mentioned off-normal and diffuse optical parameters of shading device. However, there has been developed models for its evaluation [7]. According to referred paper which compares four existing models, semi-empirical model developed by [8] showed good agreement with experimental data. Therefore, detail evaluation of this model is going to be presented further in this paper.

4.5 Ventilated air space

By implementing an internal shading device an air gap space is created, which is connected to the interior environment. Since investigation provided in this project does not consider

shading as opaque, neither completely homogeneous the created air space should no be considered as non-vented gap. It is assumed that ventilation in it is thermally-driven. Therefore, calculation process presented in ISO 15099:2003 [6] is followed for thermally-driven ventilated air space. Detailed procedure is presented in the next part where calculation models are developed.

Part II

Experimental work

The need of experimental measurements

The developed method aims to simulate the heat transfer through a glazing towards a room, when an internal roller shading device is used to avoid solar radiation. Calculation methods need to be compared with experimental measurements so that the results and accuracy of the method can be evaluated.

Theory involved in this physical phenomena has been explained in previous part to facilitate its understanding. In this part, the way how the measurements are performed is explained. Test facility consists on a real scale room called "the Cube", where glazed façade is facing South orientation. This part describes the test facility, used measuring instruments and control equipment. Two main set ups are carried out, where both a highly reflective and highly absorptive blinds are tested. At the end of this part heat balance is calculated in order to validate the measurements.

Experimental work part within the organization of the project is shadowed in the figure below.

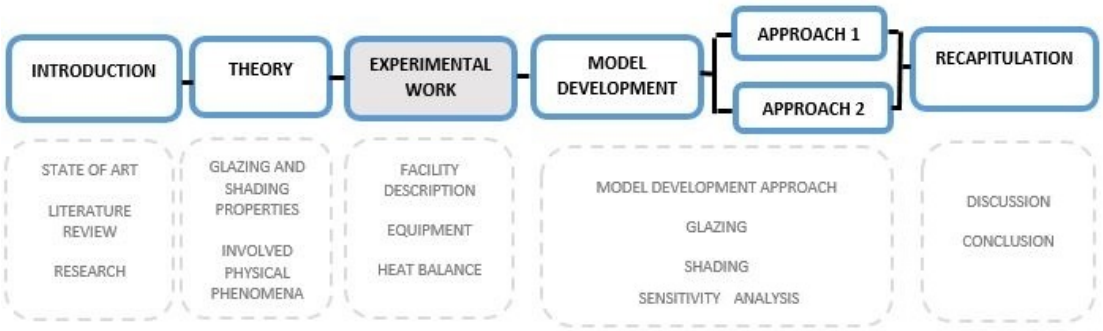

Figure 4.3. Followed methodology in the project

Experimental work 5

5.1 Description of the test facility

'The Cube' is a test facility used during the whole thesis work time, however due to various technical difficulties just a reduced time period is used for measurements. The building is adapted for full-scale measurements of the double glazed window along with an internal shading device. The test facility is placed in the south-east part of Aalborg, near the main university campus of AAU. Figure 5.1 shows the location of 'the Cube' on a map. [24]

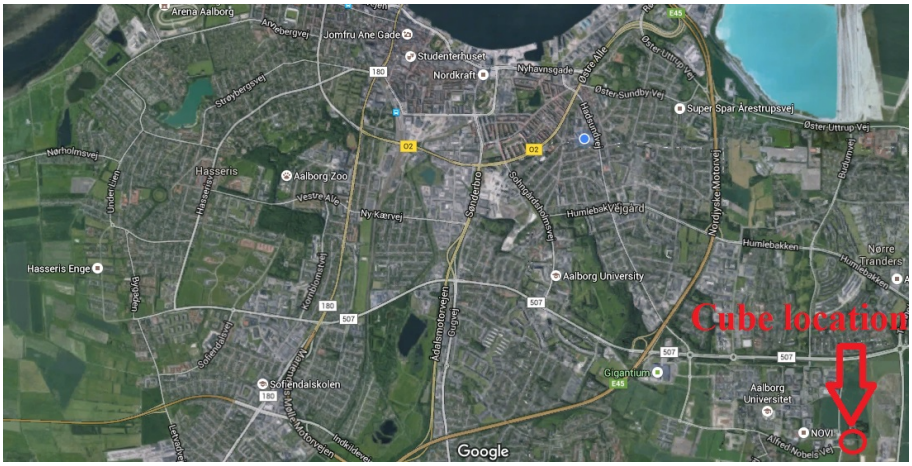

Figure 5.1. The Cube's location in Aalborg , Postgårdsvej

The dimensions of the building used for experimental work are presented in table 5.1 and the drawn representation, viewed from the top, is shown in figure 5.3 on the following page.

Zone room	**Length,** m	**Width,** m	**Height,** m	**Floor area,** m^2	**Volume,** m^3
1 (test zone)	3.6	2.76	2.75	9.94	27.32
2 (guarding zone)	5.17	4.96	5.8	25.64	148.71
3 (equipment room)	3.5	3	3	10.5	31.5
4 (engine room)	3.6	1.96	3	7.06	21.16

Table 5.1. Data for the Cube

Figure 5.2. The Cube facility

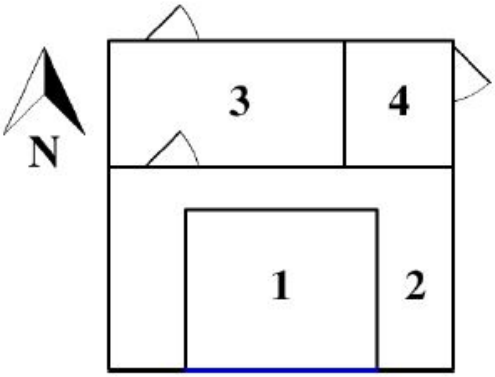

Figure 5.3. Top view of the Cube

The Cube is divided in four distinct zones in order to create the indoor climate necessary for the experiment. Zone 1 is constituted by the test zone, where the only connection with the exterior is through the south oriented façade. Aside the double glazed window, which is preponderant on the south orientation, the zone 2 or guarding zone, envelops the zone 1. In order to confirm that there are no infiltrations from the test zone towards the guarded zone pressure difference is measured and being close to zero. The other zones, instrument and engine rooms are an extension of the Cube on the North side.

The room's interior is painted mainly in white, which results in high reflectivity of the surfaces for wall, floor and ceiling. In the middle of the room there is an air inlet diffuser for the ventilation system. [24]

In this document a double glazed window with a solar shading device is analysed. The window corresponds to a Pilkington model with two glass layers separated by a mix of gases. The gas gap between the two panes is composed by 90 % argon and 10 % air. General information about the window properties is given in table 5.2, and more detailed information is available from providers' technical data sheet in Appendix D.

Type	**Length,** [m]	**Height,** [m]	**U-value,**$[\frac{\mathrm{W}}{\mathrm{m^2K}}]$	**g-value**, [−]
Pilkinton	2.75	1.55	1.2	0.36

Table 5.2. Window properties

The solar shading for the window consists of an internal type of blind, which is placed at 45 cm from the glazing creating a cavity in between them. In the experiment, two samples of internal blinds are used from Mermet manufacturer. Figure 5.4 shows the two coloured utilized blinds. One has a light grey nuance in order to have a high reflective surface and the other is dark to obtain a high absorbing one. The first blind is named White Pearl and the second Charcoal Grey. General blinds' properties can be seen on table 5.3 on the facing page. Detailed information can be found in Appendix D

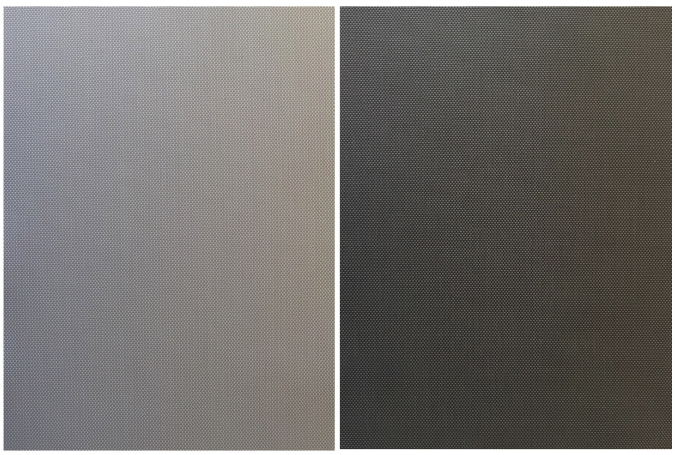

Figure 5.4. White Pearl and Charcoal Grey blinds

Blind type	**Length,** [m]	**Height,** [m]	$\tau_{blind}, [-]$	$\rho_{blind}[-]$	$\alpha_{blind}[-]$
White Pearl	2.75	1.55	0.17	0.52	0.31
Charcoal Grey	2.75	1.55	0.09	0.11	0.80

Table 5.3. Blinds' properties

5.2 Control equipment

A crucial aspect for the experiment is to be able to control the systems for the Cube. The testing space requires cooling, heating and ventilation to get the desired indoor conditions in terms of thermal comfort. The facility controller should be able to keep the indoor environment as close to the steady state condition as possible. This will ease the use of data and also it will influence the accuracy of the results. By keeping steady state conditions energy heat storage is avoided in the air of the room. Figure 5.5 on the next page presents the equipments used for this matter.

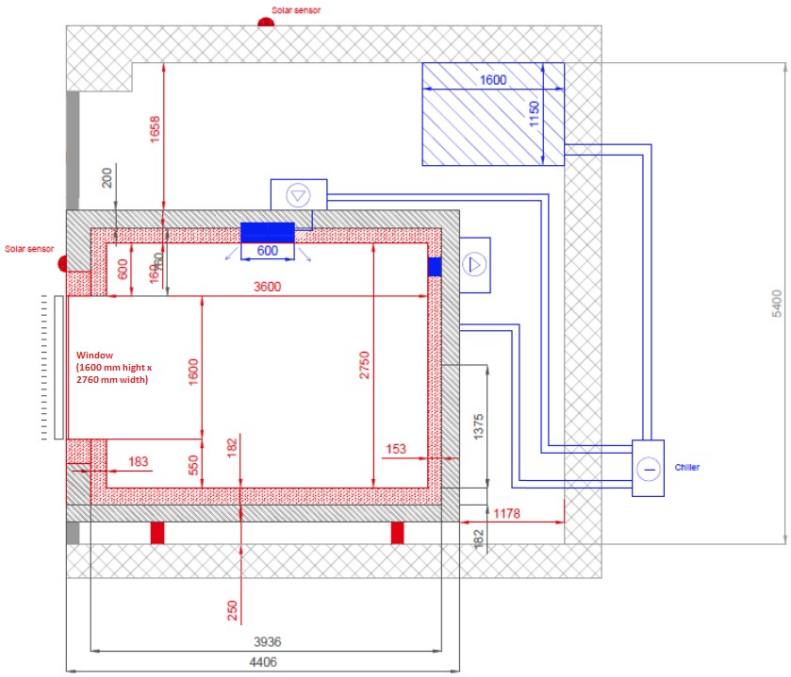

Figure 5.5. Side view of the test and guarding zone with the control equipment

The cooling in the Cube is performed with a chiller that connects to two distinct systems. The cooling is done by circulating cooled distilled water through the pipes. The agent is supplied through tubes inside of the radiant wall giving a cooling power of 400 W. Brunata equipment measures the water flow and its temperature difference in order to determine the cooling power for six of the channels going to the wall. The water from these pipes decreases the temperature of the wall and generates radiative cooling inside the room. Another device connected to the water circulation system is a cooling coil with a maximum power of 500 W for the ventilation system situated in the upper part of the test zone. This channel helps to cool down the air that enters in the experimental zone from the guarding zone. Due to technical problems cooling systems are functioning at full capacity and the Brunata devices values are logged through Labview software.

The heating of the test zone is assured by using an electrical radiator that is placed in the middle of the room. The maximum heating power of the radiator is close to 1700 W and it is measured by using a powermeter. The heater is regulated through a controller and an electrical fuse then connected to the computer. The internal air temperature is controlled only by using the heating system, through National Instruments - modular hardware platform and system design software. [25] Temperature sensor for the controller is placed in the pole in the middle of the room at a height 1.1m.

In terms of ventilation, the Cube needs two different systems for the two important zones on the building. The guarding zone's ventilation is assured when needed with a big ventilation system in order to supply fresh air from outside. For the experimental room, the ventilation system is taking the inlet air from the guarding zone and the exhaust comes back into the same space. [4] [24]

5.3 Measurement set up

In this section it is explained briefly how measurements are performed. The test zone is presented in figure 5.6 with a schematic drawing of the equipment involved in measurements. In the side view of the room there are presented a series of thermocouples that are used to measure the surface temperature. The type K thermocouples are put on each side of the window and shading.

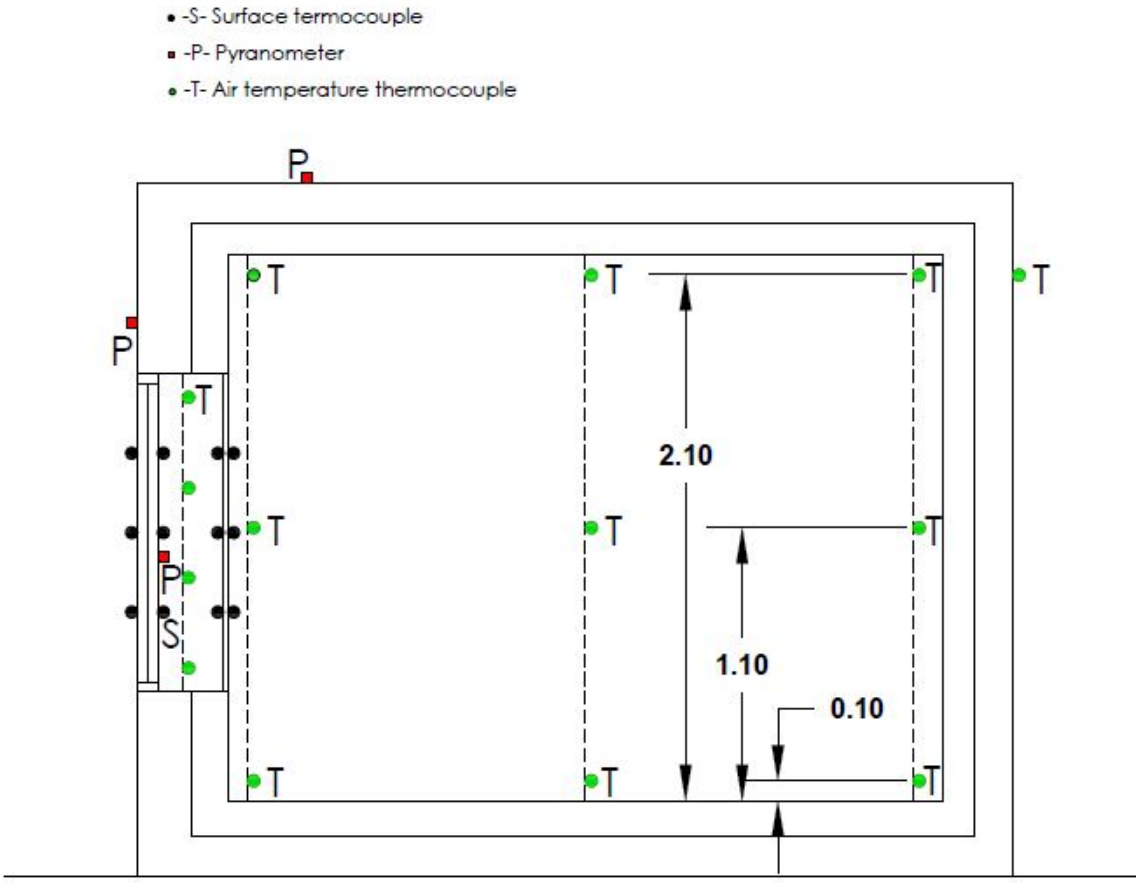

Figure 5.6. Placement of the measuring equipment

A schematic drawing of the thermocouples placement on window and blind surfaces is done in figure 5.7 on the next page. The thermocouples are fixed on surfaces with thermal paste and then covered by a reflective tape in order to protect the equipment from measurement error that might be caused during solar radiation. The same setup is followed in both glazings and both sides of the shading.

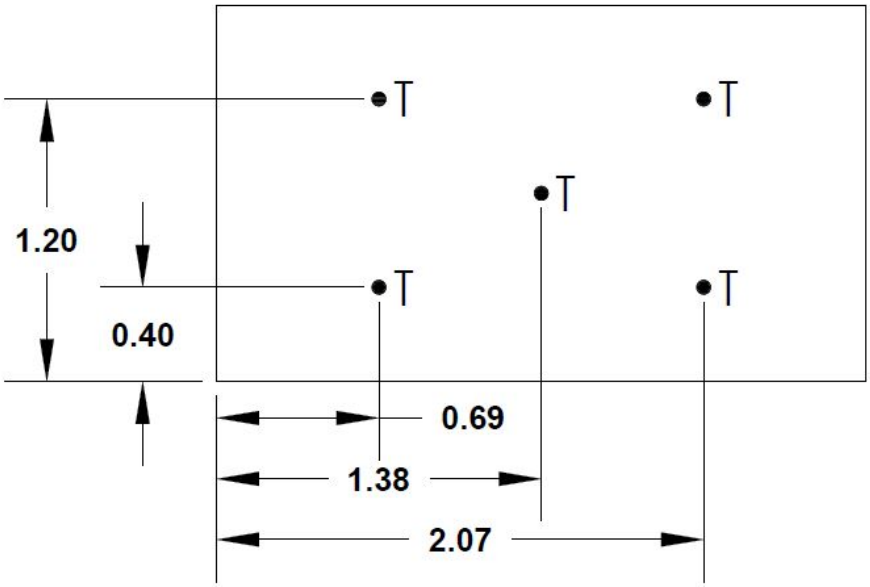

Figure 5.7. Schematics of thermocouples position on window and shading

The test room's temperature is measured with a series of three poles placed at different distances from the window. On the pole there will be put three type K thermocouples with silver tubes and fan to determine the air temperatures at different heights from the floor to the ceiling. Beside the room, the thermal zone formed between the window and the shading has to be evaluated as well. The cavity is holding also a number of eight thermocouples in order to understand the thermal behaviour of the air under sun influence, and are distributed evenly along the height of the cavity in two poles.

A couple of type K thermocouples are situated in the guarding zone and two more outdoors in order to measure the air temperature.

A CMP pyranometer is placed in the cavity in order to collect data about the solar radiation. Two others are place outside, one in the facade and another horizontally in the roof.

Two pressure transducers are installed in the Cube. One measures the pressure difference in between the test room and guarding zone while second measures pressure difference in orifice plate from ventilation supply in order to get the ventilation air flow.

Figure 5.8. Blind in the test room

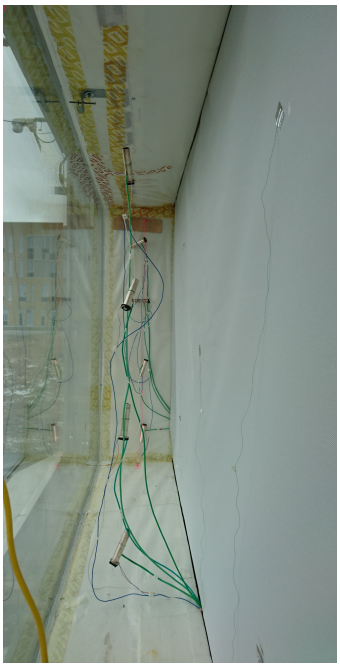

Figure 5.9. Cavity side view

More information about the equipment and also about the calibration details can be found in Appendix C. In figure on the next page it is presented whole set up connection for the experiments performed in the Cube.

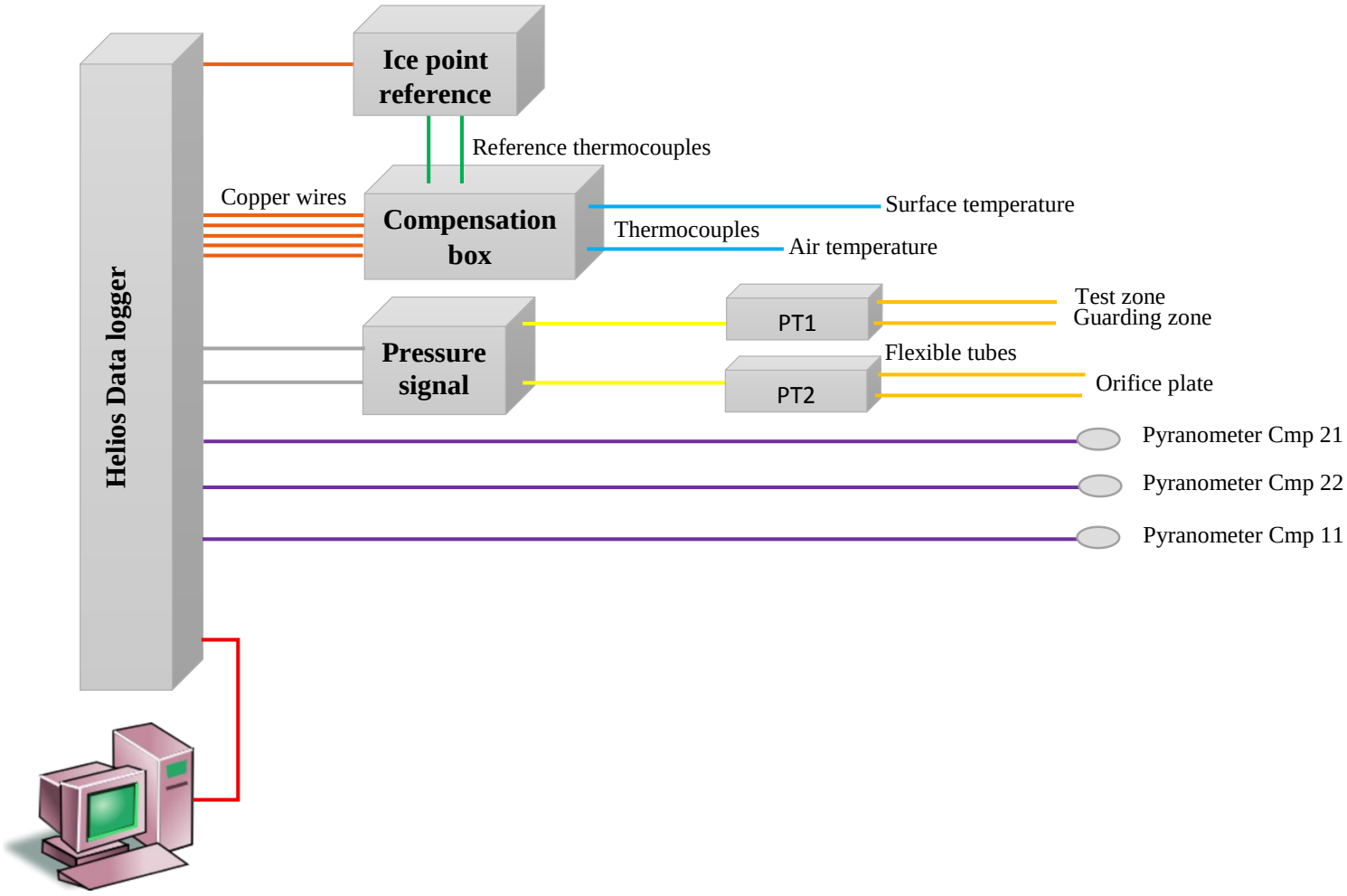
Helios Data logger
Ice point reference
Reference thermocouples
Copper wires
Compensation box
Surface temperature
Thermocouples
Air temperature
Pressure signal
PT1
Test zone
Guarding zone
Flexible tubes
PT2
Orifice plate
Pyranometer Cmp 21
Pyranometer Cmp 22
Pyranometer Cmp 11

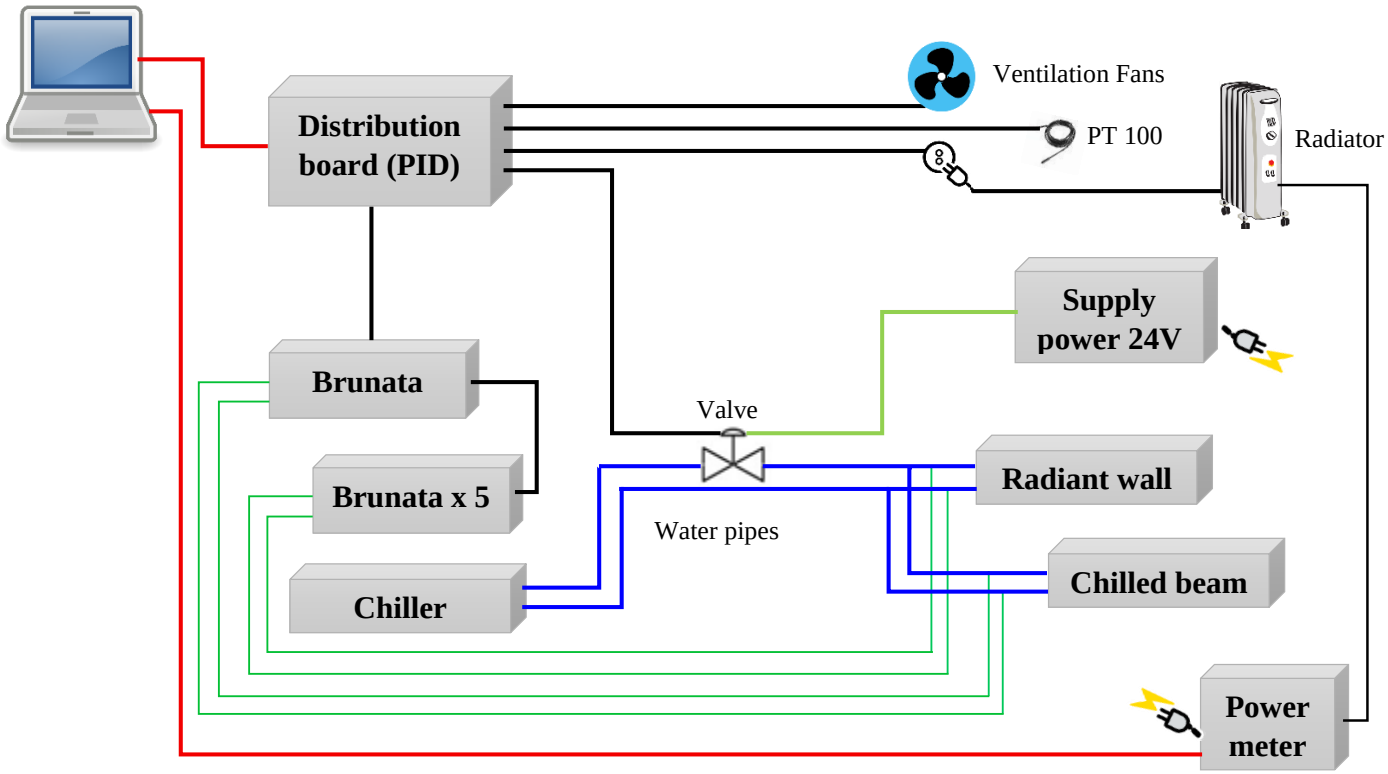
Distribution board (PID)
Ventilation Fans
PT 100
Radiator
Supply power 24V
Brunata
Valve
Brunata x 5
Radiant wall
Water pipes
Chiller
Chilled beam
Power meter

5.4 Measurement plan

The main reason for the experimental setup is to gather information in order to validate the simplified developed models.

Along the experimental measurements there are necessary two sets of experiments for consecutive days considering two types of shadings, White Pearl (W-P) and Charcoal Grey (C-G). Additionally, an experiment is conducted in order to compare the model just for the double glazed window Table 5.4 displays the detailed data about the periods for measurements.

Time period	Description	Conditions
7-8 May 2016	Measurement with C-G	Partial sunny - 1st day, sunny - 2nd day
10-15 May 2016	Measurement with W-P	Sunny - 1st to 3rd day, Partial sunny - 4th to 6th day
17-19 May 2016	Measurement glazing	Clear and sunny day
25-26 May 2016	Measurement with C-G	Overcast - 1st day, sunny - 2nd day

Table 5.4. Measurements plan

5.5 Heat balance

Temperature in the room is maintained constant all over the measurements so it is assumed not to have heat storage in the air of the room. Set point temperature for the heating system is set to 27 °C and cooling is set constant. By calculating the heat balance for the air in the room, experimental data can be validated and solar gains can be calculated.

Heat balance is done according to equation 5.1. Data treatment from the obtained measurements is explained in Appendix E.

$$Q_{air} = Q_{controlled-heating} + Q_{uncontrolled-heating} + Q_{controlled-cooling} + Q_{uncontrolled-cooling} \tag{5.1}$$

Q_{air} refers to the stored heat in the air due to temperature variation over the time. It can be calculated as:

$$Q_{air} = V_{room} \rho_{air} Cp_{air} \frac{\partial T}{\partial t} \tag{5.2}$$

Where:

V_{room}	is the volume of the room, 27.32 m^3
∂T	is the temperature variation over time
∂t	is the time step

$Q_{controlled-heating}$ refers to the heat gains due to the heating system. It is measured by the power meter installed in the experimental set up.

$Q_{uncontrolled-heating}$ refers to solar gains. They can not be calculated in a direct way, but by calculating all the others and doing the heat balance in equation 5.1.

$Q_{controlled-cooling}$ refers both to the cooling from the coil and ventilation of the room. They are calculated as follows:

$$Q_{cooling-coil} = q_{water}\rho_{water}Cp_{water}(T_{water,in} - T_{water,out}) \tag{5.3}$$

Where:

q_{water}	is water flow through the coil, $[\frac{\mathrm{m}^3}{\mathrm{h}}]$
$T_{water,in}$	forward temperature of the cooling coil, [K]
$T_{water,out}$	return temperature of the cooling coil, [K]

$$Q_{vent} = q_{air}\rho_{air}Cp_{air}(T_{air,in} - T_{air,out}) \tag{5.4}$$

Where:

q_{air}	is air flow into the room, 2.6 $[\frac{\mathrm{l}}{\mathrm{s}}]$
$T_{air,in}$	temperature of the air going into the room, [K]
$T_{air,out}$	temperature of the air going out of the room, [K]

$Q_{uncontrolled-cooling}$ refers to undesired cooling due to infiltration losses, transmission losses and thermal bridges. Transmission and infiltration losses from the room towards the guarded zone have been neglected. They are calculated as follows,

$$Q_{inf} = q_{inf}\rho_{air}Cp_{air}(T_o - T_i) \tag{5.5}$$

Where:

q_{inf}	is infiltration air flow into the room, 0.0009 $[\frac{\mathrm{m}^3}{\mathrm{s}}]$
T_o	external air temperature, [K]
T_i	air temperature inside the room, [K]

$$Q_{trans} = U_w A_{facade}(T_o - T_i) \tag{5.6}$$

Where:

U_w	is the total heat transfer coefficient of the window, 0.8706 $[\frac{\mathrm{W}}{\mathrm{m}^2\mathrm{K}}]$
A_{facade}	is the area of the glazing
q_{inf}	is infiltration air flow into the room, 0.0009 $[\frac{\mathrm{m}^3}{\mathrm{s}}]$
T_o	external air temperature, [K]
T_i	air temperature inside the room, [K]

$$Q_{L-Loss} = \psi_w p_w (T_o - T_i) \tag{5.7}$$

Where:

ψ_w	is the linear loss through the frame of the window, 0.3 $[\frac{\mathrm{W}}{\mathrm{K}}]$
p_w	is the perimeter of the window, 8.6 [m]
T_o	external air temperature, [K]
T_i	air temperature inside the room, [K]

The heat balance calculation is done for the measurements in order to validate them. Here are shown experiment results during days 7th and 8th of May, where data has been averaged for every hour. The heat balance from the experiments for the other time periods is included in appendix G on page 108 as there is necessary to check if the measurements are precise.

Regarding air temperature variation in the room, it can be seen that apart from the few peaks, there is no variation bigger than ± 2 W. The temperature used for the heat balance corresponds to a single sensor placed in the middle of the pole.

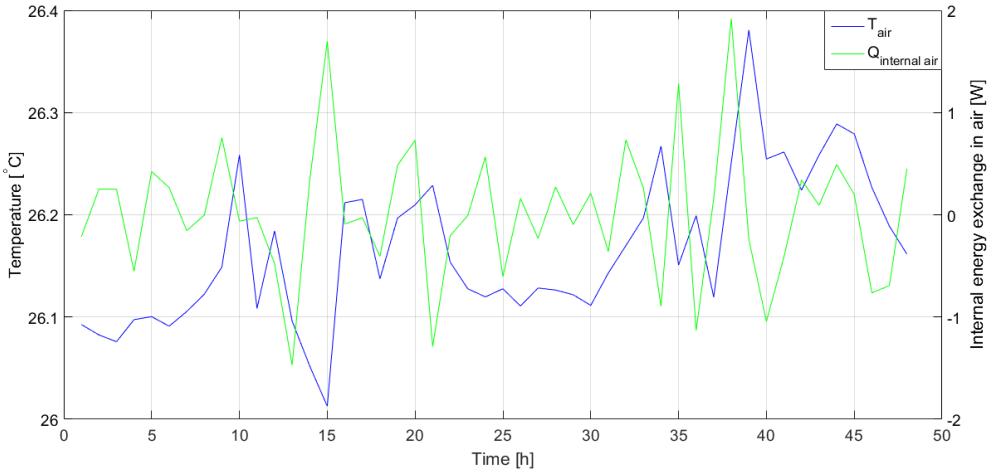

Figure 5.10. Energy storage in the air of the room

Next figure shows controlled cooling where ventilation has little effect. Cooling from the coil is more or less constant between 400 W and 500 W. The radiant wall keeps mostly a steady value close to 300 W.

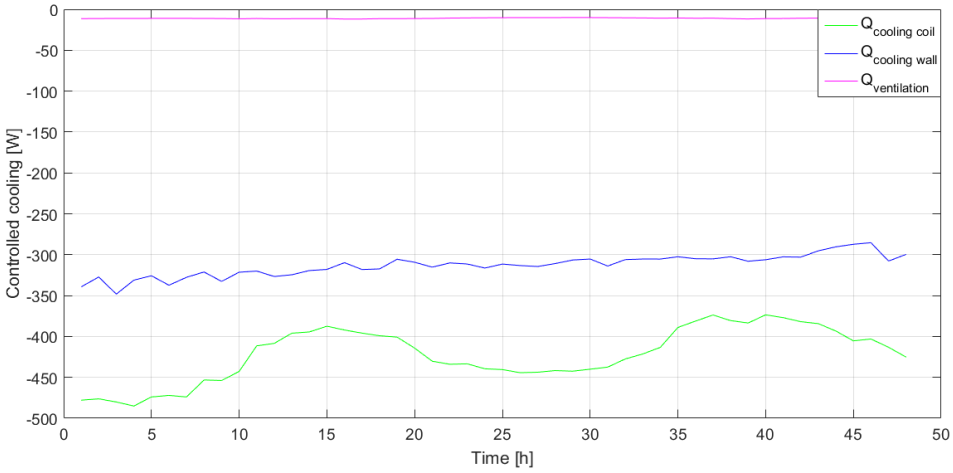

Figure 5.11. Controlled cooling of the room

Next figure shows uncontrolled cooling due to transmission, infiltration and linear losses. Infiltration loss is small due to the small infiltration rate defined. Transmission loss has been calculated only through the glazing towards outside, and the others thermal bridges have been neglected. The variation of the uncontrolled cooling load is directly related with the temperature difference between outdoors and indoors air and at certain times they might be similar, resulting in no or low heat exchange.

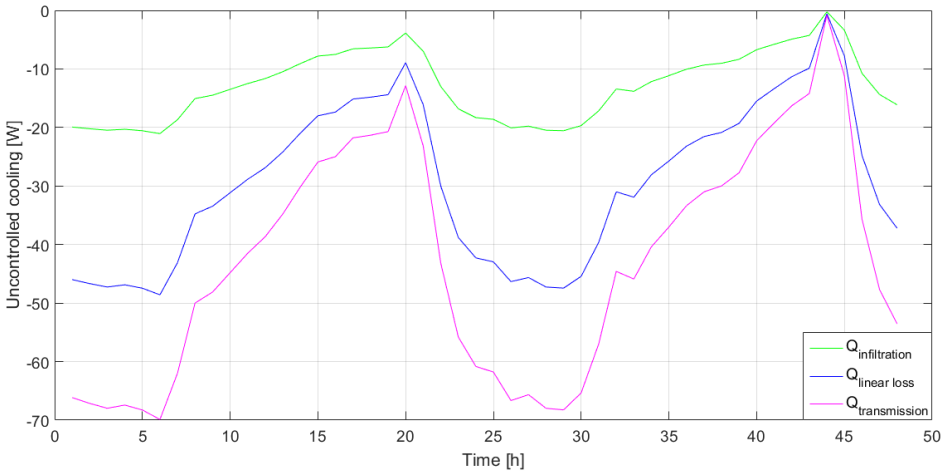

Figure 5.12. Uncontrolled cooling of the room

Figure 5.13 on the next page shows measured power consumption, solar radiation inside the cavity and calculated heat gains. The difference between the measured and calculated solar radiation comes from the blind as the measured value is inside the cavity and the calculated value is inside the room.

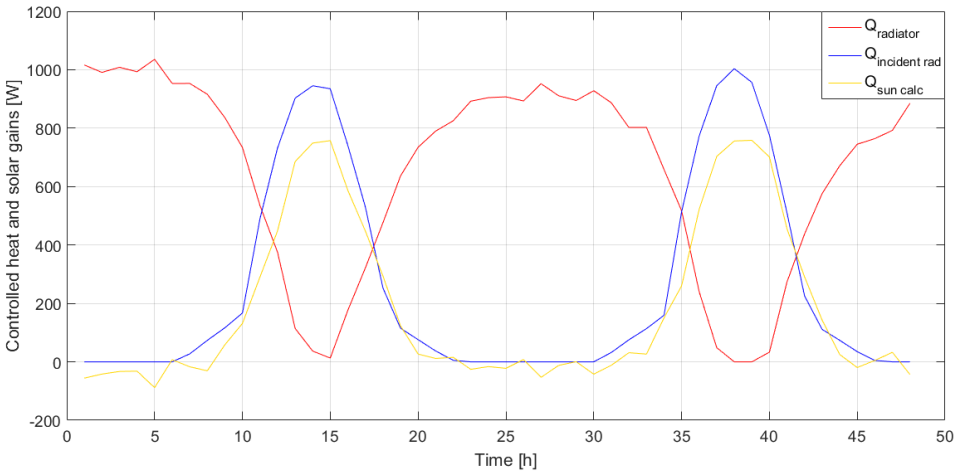

Figure 5.13. Heat balance for 7-8th of May

Part III

Model developement

Model development approach 6

The goal of this project is to implement a simple simulation model which calculates accurately the energy heat transfer through a glazing with internal shading towards a room. Additionally, required energy consumption is calculated from an hourly based calculation. All simulations are based on the nodal approach model presented in the first section of this chapter called "Basis model", which follows standard ISO 13790 [17] .

As previously mentioned in experimental part, two main approaches for the model development are handled in this project. These approaches have been chosen after deep analysis and literature review of previous works which have been done around the topic of modelling internal shading devices. Appropriate informations has been selected and grouped in these two specific paths. These are shown in box diagram in figure 6.1 on the following page and later on, are explained in detail in this chapter.

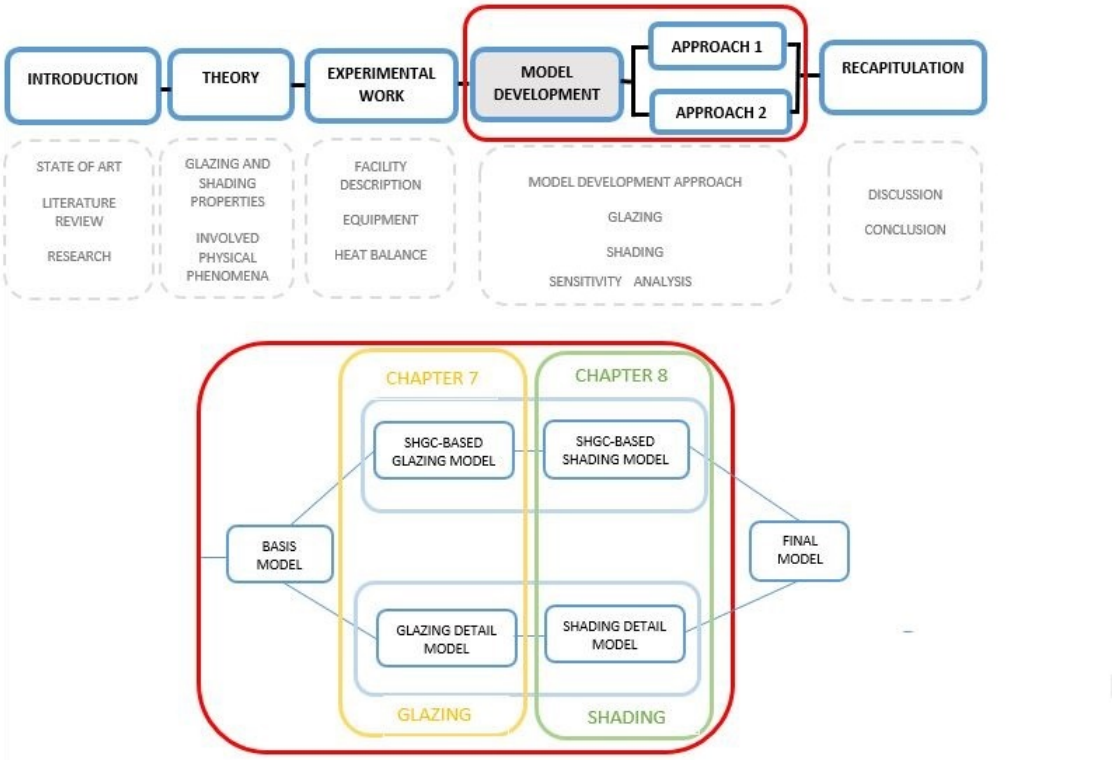

Figure 6.1. Model developement approach

Red box represents the two chosen paths of model development mentioned before. Both of them are separated into two sections: the glazing part and the shading, and this is represented by the yellow and green boxes respectively.

For all developed models the starting point is the "Basis model" which is depending on nodal approach where internal nodes in the room are common to the different developed models. Those are, one node for the air volume in the room, one node for the internal surface areas and one node for the walls' mass.

After defining the basis model, first step in both approaches focuses on glazing itself (yellow box on 6.1). Depending on how the heat transfer through the glazing is calculated, are defined the two initial approaches. In the SHGC-based model, heat transfer through the window from outdoors towards indoors is calculated by using the g-value parameter. In the detailed model based on [16], the glazing is treated more accurately by implementing several nodes on the panes. A grid dependency analysis is performed under unsteady state conditions, in order to validate the model and apply the obtained results in further steps. In both cases incident angle dependency can be treated with different accuracy, and the obtained results are compared. Detailed explanation of this step is presented in chapter 7.

After validation of the glazing model the focus is put on internal shading device implementation (green box on 6.1), which detail explanation is presented in chapter 8. SHGC-based model considers on one hand the total heat transfer coefficient including

blind properties and on the other implementation of the shading device by adding more nodes to the heat balance. Detail model includes at first the shading device by treating all the system as a triple glazed window. Then, angular properties of the blind are assigned to this node. Next the cavity is treated as a ventilated space and air movement is performed.

The models are compared between them and validated with measurements from full scale experiment introduced in chapter 5. Measured weather data is introduced as boundary condition and temperatures in the nodes and energy consumption are compared.

6.1 Basis model

Standard ISO-13790 [17] proposes a model that calculates the influence of glazing façade over the heating and cooling energy demand of the room, based on the heat transfer by transmission and ventilation. It is an hourly model where both internal and solar heat gains are considered and distributed to the different nodes. Figure 6.2, shows an RC (Resistance Capacitance) heat flow network with three nodes and the external temperature as boundary conditions: room air, surfaces and room's mass temperatures.

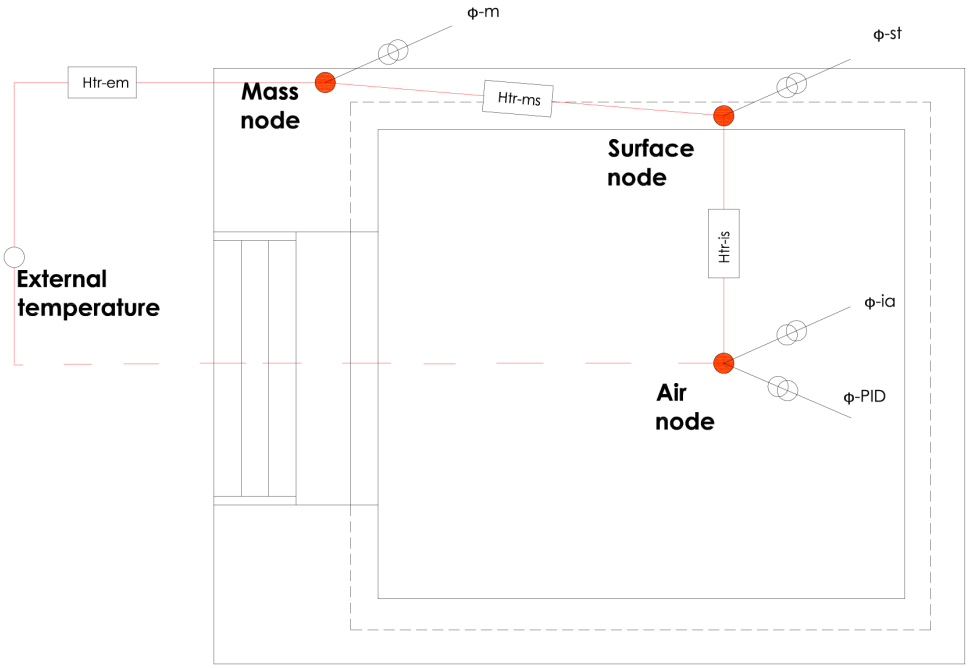

Figure 6.2. RC network heat flow of the room.

ϕ_{ia}, ϕ_{st} and ϕ_m are considering how internal and solar heat gains are split between the air, surface and mass nodes.

$$\phi_{ia} = 0.5\phi_{int} \tag{6.1}$$

$$\phi_m = \frac{A_m}{A_t}(0.5\phi_{int} + \phi_{sol}) \tag{6.2}$$

$$\phi_{st} = (1 - \frac{A_m}{A_t} - \frac{H_{tr,w}}{9.1A_t})(0.5\phi_{int} + \phi_{sol}) \tag{6.3}$$

Where:

ϕ_{ia}	heat gain in the air node, [W]
ϕ_{st}	heat gain in the surface node, [W]
ϕ_m	heat gain in the mass node, [W]
A_m	effective mass area, [m^2]
A_t	total internal surface area except glazed façade: 50.604 [m^2]
ϕ_{int}	internal heat gain, [W]
ϕ_{sol}	solar gain, [W]
$H_{tr,w}$	thermal transmission coefficient [$\frac{W}{K}$]

In order to calculate solar heat gains in the room, total energy transmittance through the window must be calculated.

$$\phi_{SOL} = \phi_{dir} g_{dir} + \phi_{dif} g_{dif} \tag{6.4}$$

In developed models no internal heat gains are considered, and effective mass area is assumed to be zero so all gains in the walls are included in the surface node. Gains from heating, cooling and ventilation are assumed to be added to the air node, and are represented by ϕ_{PID}. Heating and cooling consumptions are calculated in the model by implementing a PI controller. Gain from ventilation is calculated as follows:

$$Q_{ven} = q_{ven}\rho_{air}C_p\Delta T \tag{6.5}$$

Where:

q_{ven}	air change rate:2,6 $\cdot$ 10^{-2}[$\frac{m^3}{s}$]
ρ_{air}	air density, [$\frac{kg}{m^3}$]
C_p	specific heat capacity of the air, [$\frac{J}{kgK}$]
ΔT	difference between air supply temperature and room's air temperature, [K]

Heat transfer coefficients in between those nodes are defined as follows:

$$H_{tr-is} = h_{is}A_t \tag{6.6}$$

Where:

H_{tr-is}	heat transfer between internal surface and air node, [$\frac{W}{K}$]
h_{is}	heat transfer coefficient between surface and air: 3.45 [$\frac{W}{m^2K}$]

$$H_{tr-ms} = h_{ms}A_t \tag{6.7}$$

Where:

H_{tr-ms}	heat transfer between internal surface and mass nodes, $[\frac{\mathrm{W}}{\mathrm{K}}]$
h_{ms}	heat transfer coefficient between surface and air: $9.1\,[\frac{\mathrm{W}}{\mathrm{m^2K}}]$

$$H_{tr-em} = (\frac{1}{H_{tr-op}} - \frac{1}{H_{tr-ms}})^{-1} \tag{6.8}$$

Where:

H_{tr-em}	heat transfer between mass node and outdoors, $[\frac{\mathrm{W}}{\mathrm{K}}]$
H_{tr-op}	heat transfer through the external wall, $[\frac{\mathrm{W}}{\mathrm{K}}]$

$$H_{tr-op} = h_{op} A_{wall-out} \tag{6.9}$$

Where:

h_{op}	heat transmittance through the external wall: $0.09\,[\frac{\mathrm{W}}{\mathrm{m^2K}}]$
$A_{wall-out}$	area of the external wall, $[\mathrm{m}^2]$

This way is defined the room by three nodes as basis model for further models development.

Glazing 7

The examination of the models in the current chapter is corresponding to the façade's fenestration for the double glazed window alone. Firstly, the SHGC-based glazing model is investigated as it considers the heat transfer through the window by using total heat transfer coefficient.

It is followed by the glazing detail model which considers glazing's panes separately. Panes angular properties are simulated according to [26] and explained in this chapter.

These approaches allow to evaluate incident angle dependency by simplifying the input parameters of the model so it can be run with basic information about used materials properties. For each glazing model analysed there is apprehended a validation with the experimental data.

7.1 SHGC-based glazing model

Implementation of angle dependency in this model is desired to be done in a simple way so few input parameters are required while accuracy is maintained. In order to calculate the SHGC of the glazing, empirical model described in [27] proposes an equation where only angle of incidence and g-value at normal incidence angle for the whole glazing are needed. Equation given for the current model is:

$$g = g(0)[A\cos^{x}(\frac{\theta_i}{6}) + B\cos^{y}(\theta_i)] \tag{7.1}$$

Where:

g	total solar energy transmittance [−]
$g(0)$	total solar energy transmittance at normal incidence [−]
A, B	multipliers [−]
p	number of panes
θ_i	incidence angle [°]
	if $\theta_i \in [0°; 60°]$, $A = 1$ and $B = 0$
	if $\theta_i \in [60°; 90]$, $A = 0$ and $B = 1$
x, y	exponents [−]

Exponents x and y are depending on incidence angle and the number of panes.

$$x = (0,35 + \frac{p}{3})\frac{\theta_i}{10} \tag{7.2}$$

$$y = (0,103p + 0,06) + (\frac{\theta_i}{10} - 6)^m 0,078p^n \tag{7.3}$$

Where:

p	number of panes [−]
m,n	exponents [−]
	$m = (1,64)^{(1/0,75p)}$
	$n = \frac{1,72}{p}$

Results obtained from this equation are compared with angle dependency values of the window used in the experimental set up, and shown in Appendix F. The model is assumed to be good for the purpose of this simple approach, although small deviation exists from the real values.

Performance of this equation is also evaluated in a simple model as the one described in figure 7.1.

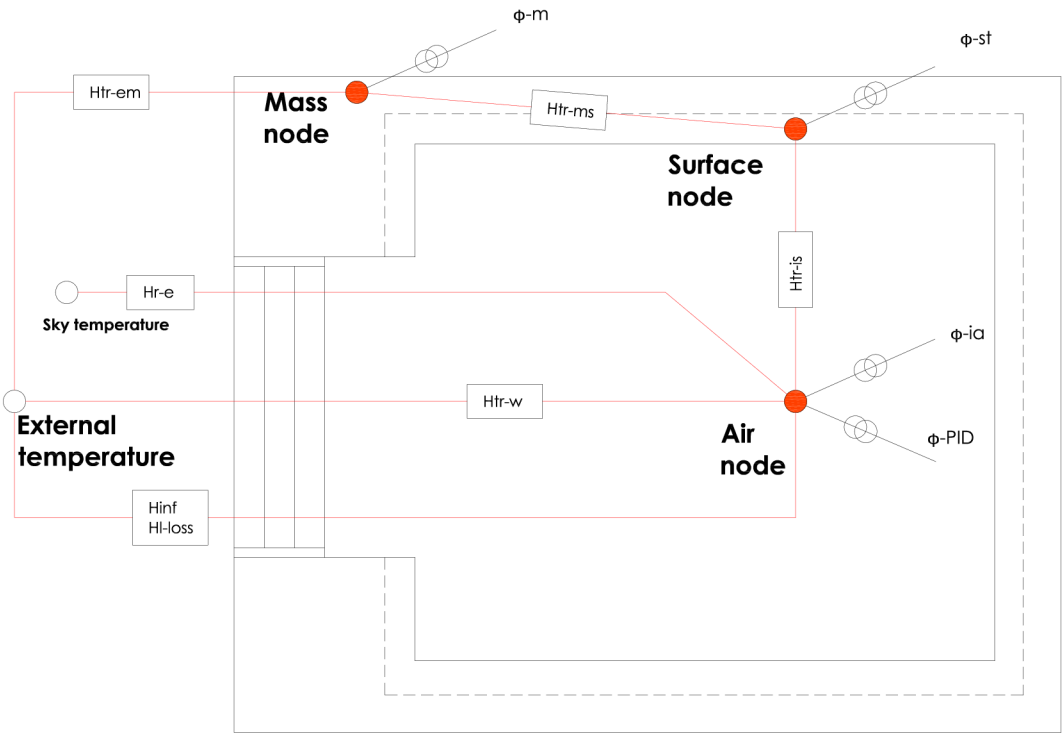

Figure 7.1. SHGC-based glazing model

This model considers transmission loss through the glazing, calculated according to standard EN 673 [21] for a double glazed window, where external and internal convective heat transfer coefficients are calculated according to Clarke [28] and explained in Appendix A.

It is also included uncontrolled cooling, considering infiltration losses with a constant infiltration flow of 0,0009 $\frac{m^3}{s}$,

$$H_{inf} = q_{inf}\rho_{air}C_p \tag{7.4}$$

and thermal bridge around the window with a linear loss of 0,3 $\frac{W}{mK}$,

$$H_{linearloss} = L_{line}\psi_{line} \tag{7.5}$$

Long-wave losses from external surface toward the sky are also considered and calculated according to:

$$H_{re} = 4\epsilon\sigma T_{out}^3 A_{faade} \tag{7.6}$$

Where ϵ refers to the emissivity of external surface of external pane and σ to the Stefan-Boltzmann constant.

7.1.1 Validation

A validation of the simple model approach which is considering the SHGC is done together with the measurements for the system taking into account the double glazing. In the following figures, there are presented temperatures of some nodes considered and compared with experiment. The power consumption and the significant parameters of the weather data file for $17th - 19th$ of May are introduced.

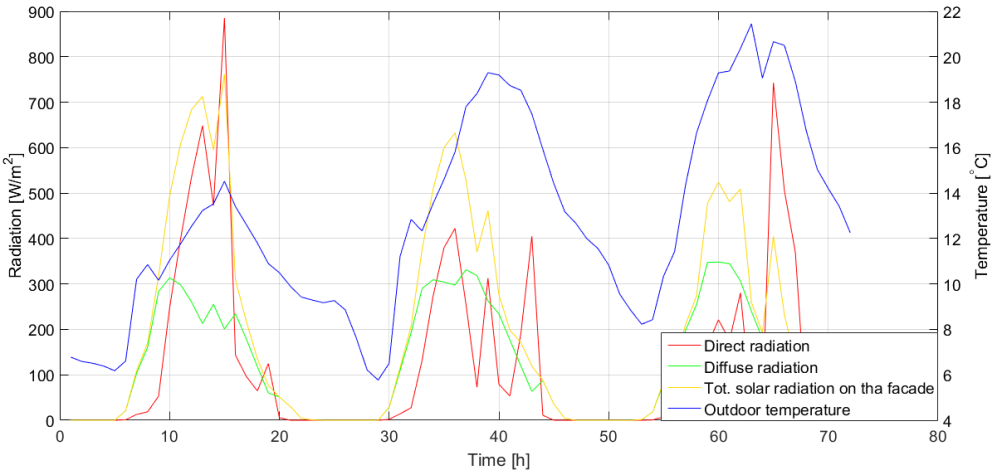

Figure 7.2. Weather conditions - Period 17^{th} to 19^{th} of May

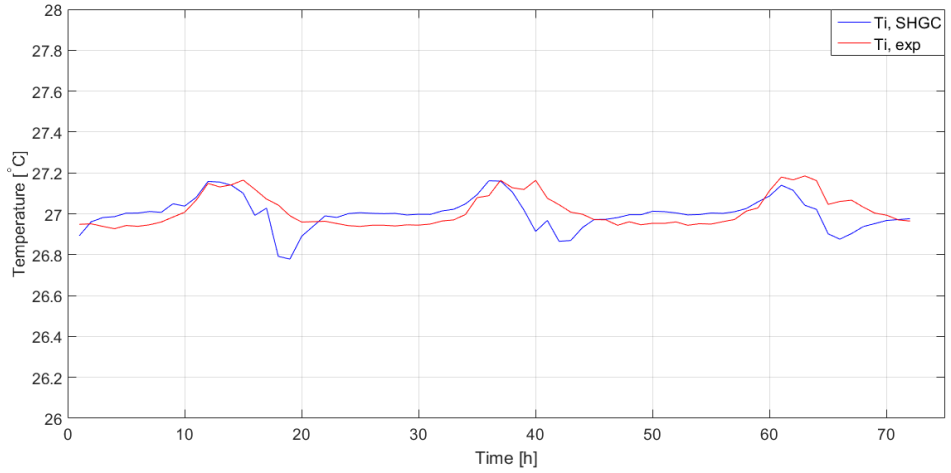

Figure 7.3. Room air temperature comparison between measurements and SHGC-based glazing model - Period $17thto19th$ of May

In figure 7.3 there is presented the internal air temperature and it can be observed that the temperature variation is rather small. The curve from experiment corresponds to the temperature measured by the sensor used for the control of the heating and cooling. Unlike the experiment, the air temperature has a faster response as it increases faster during the day and as quick it decreases when there is no solar radiation and this is a result of PI controller which is not tuned properly.

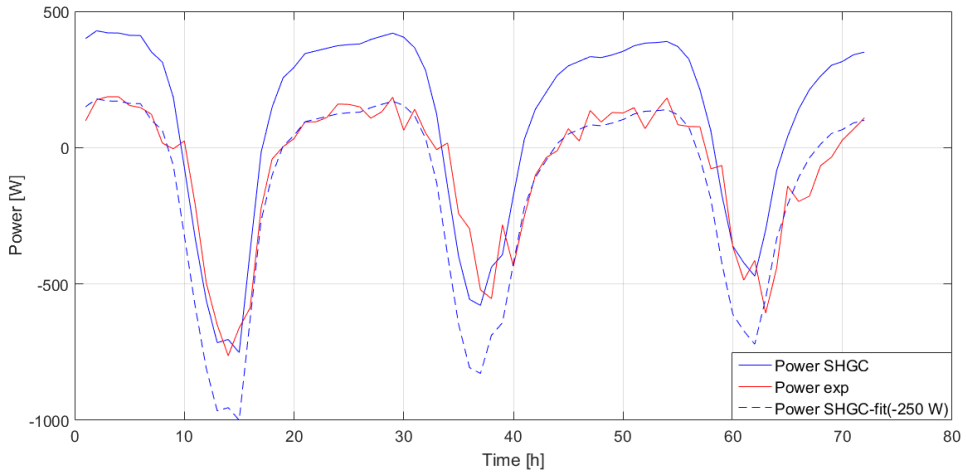

Figure 7.4. Energy consumption comparison between measurements and SHGC-based glazing model - Period 17^{th} to 19^{th} of May

Figure 7.4 relates to the power consumption of the simple model and the one from the measurements. Heating consumption is higher during the night so it can be assumed that the model overestimates heat losses. On the other hand cooling need during the day is 250 W overestimated as seen from the dashed line on figure above.

7.2 Glazing detail model

The present model consists of a series of five nodes having different thermal and spacial properties, where the main focus is on the window panes. A sketch of the model is shown on figure 7.6. The verification of the model for the window under steady state conditions is done in [16]. The model simplification has been determined by a grid sensitivity method from which, the most suitable one was that with just two nodes in the window panes. In this section the same grid sensitivity analysis is done under hourly dynamic conditions. Further, the content of the calculation method is explained and sets of different setups in the panes are done, followed by an overall analysis.

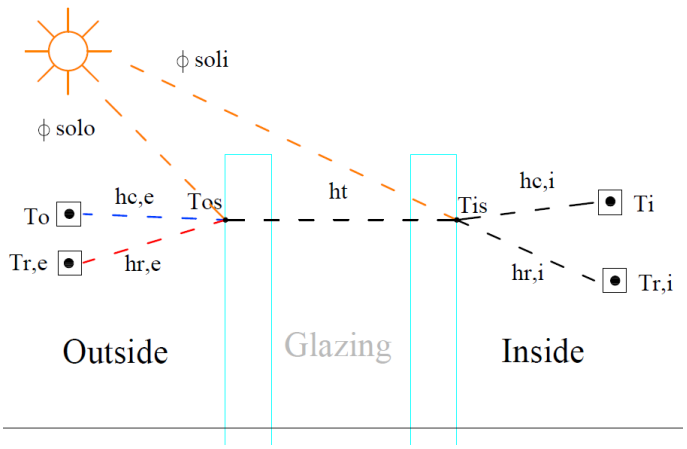

Figure 7.5. Heat balance of the window variables and thermal connexions. [16]

Figure 7.5 is illustrated by the modeling of the two nodes in the double glazed window, and its thermal connections with external and internal nodes. It is shown in this work that considering one node in the external surface of the external pane and one node in the internal surface of the internal pane give mainly accurate results when calculating the heat transfer through the window.

Description of the models

The models analysed are presented below having a specific name for each simulation as Mx, where x stands for the number of the nodes in the pane. There are also some distinct notations as the same model could have a different setting of the nodes in the pane thickness. Another exception is for the initial model where the x will be replaced with the notation 0, which has been presented before. Models are briefly enumerated as:

- M0 - Initial model
- M1 - Model 1 with the node in the center of the pane
- M1s - model 1 with the node in the surface
- M2s - model 2 with nodes in the surfaces
- M2m - model 2 with node in the surface and in the center of the pane
- M3 - model with nodes in the surfaces and in the center of the pane
- M4 - model with nodes in the surfaces and inside the pane

The main concept is to consider splitting formula presented in 4.2 on page 8 as having thermal conductances for different thicknesses between the nodes in the window. For the nodes in-between the glazing pane, the thermal conductance will be named H_j, where j will correspond to the pane number, and if it is the case for the next term, prime and secondary symbols (H_j',H_j") can be used. When the points are fixed on surface facing the gas space, the thermal conductance h_s is considered. When two of the nodes are inside the pane and in between gas space the thermal conductance of those is calculated later on as H_s.

Indoors, there are considered gains from internal and solar which are split between the air, mass and surface nodes. Equations representative for these thermal loads are given in section 6.1.

Initial model - M_0

In the initial script just a quarter of the total thermal mass of each pane is considered based on the assumption that in the glass volume the temperature is homogeneous. Nevertheless, the model takes into consideration the thermal mass of the glazing and the utilization of specific heat capacity of the glass leads to a realistic scenario [16]. Figure 7.6 is presenting the nodes' position in the system together with all the connection between them. Delimitation of the pane volume is done with the dashed magenta line. The scaled detail is determined as there is the need for the focus on the window nodes.

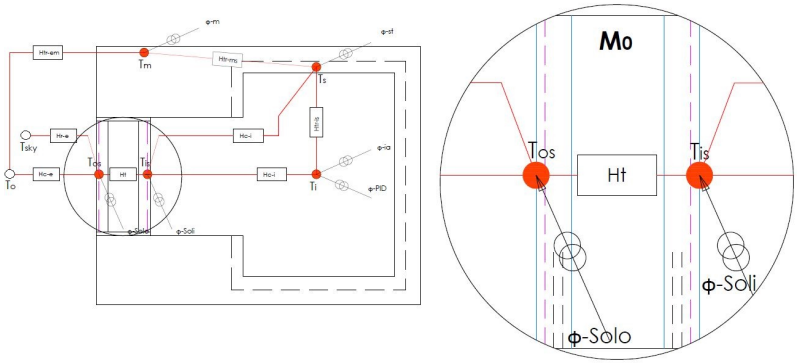

Figure 7.6. Nodal scheme for model M_0

An important consideration is given to the solar heat gains of the window that are divided into ϕ_{solo} and ϕ_{soli}, that are calculated from the external radiation by applying the different glazings' properties. Those parameters represent the absorbed radiation on the panes.

$$\phi_{solo} = 0,25(\phi_{dir}\alpha_{e1_{dir}} + \phi_{dif}\alpha_{e1_{dif}}) \tag{7.7}$$

$$\phi_{soli} = 0,25(\phi_{dir}\alpha_{e2_{dir}} + \phi_{dif}\alpha_{e2_{dif}}) \tag{7.8}$$

Where:

ϕ_{solo} and ϕ_{soli}	absorbed radiation in the external and internal nodes $[\frac{W}{m^2}]$
ϕ_{dir} and ϕ_{dif}	direct and diffuse radiation on the façade $[\frac{W}{m^2}]$
$\alpha_{e1,dir}$ and $\alpha_{e1,dif}$	direct and diffuse solar absorptance coefficients for the external pane [−]
$\alpha_{e2,dir}$ and $\alpha_{e2,dif}$	direct and diffuse solar absorptance coefficients for the internal pane [−]
0.25	factor due to division of each pane on 4 nodes, although only the external node in the external pane, and internal node in the internal pane are considered [−]

According to EN 410:1998 the total solar energy transmittance is calculated through the formula 4.7. For a double glazing, equations for transmittance and is as follow.

$$\tau = \frac{\tau_1 \tau_2}{1 - \rho_1' \rho_2} \tag{7.9}$$

Where:

τ_1 and τ_2	spectral transmittance of the outer and inner pane, [−]
ρ_1'	spectral reflectance of the outer pane, measured in the direction opposite to the incident radiation, [−]
ρ_2	spectral reflectance of the second pane, measured in the direction of the incident radiation, [−]

However solar transmittance through glazings is highly influenced by the radiation incident angle. Therefore many researches are done to model this angle dependency [26] [29], and a simplified method is performed in [16].

Transmittance, reflectance and absorptance are calculated with incident angles between 0° and 90°. Based on experimental researches conducted by J. Karlsson and A. Roos [26], a polynomial function is proposed to calculate the direct solar transmittance of a glazing.

$$g_{gzg}[\alpha_{in}] = g_{gzg}[0°](1 - a_{roos}(\frac{\alpha_{in}}{90})^{\alpha_{roos}} - b_{roos}(\frac{\alpha_{in}}{90})^{\beta_{roos}} - c_{roos}(\frac{\alpha_{in}}{90})^{\gamma_{roos}}) \tag{7.10}$$

Where:

$g_{gzg}[0°]$	direct solar transmittance at normal incidence angle, [−]
α_{in}	radiation incident angle, [−]
p	number of panes in the window, [−]
q	category parameter [1,10] depending on window's properties, [−]
	$a_{roos} = 8$, $b_{roos} = \frac{0,25}{q}$, $c_{roos} = (1 - a - b)$
	$\alpha_{roos} = 5,2 + 0,7q$
	$\beta_{roos} = 2$
	$\gamma_{roos} = (5,26 + 0,06p) + (0,73 + 0,04p)q$

Further research is make by Tilmann E. Kuhn [29] in order to calculate angle dependent window properties based on [26]

$$\tau_{gzg}[\alpha_{in}] \approx \tau_{gzg}[0°](1 - a_{roos}(\frac{\alpha_{in}}{90})^{\alpha_{roos}} - b_{roos}(\frac{\alpha_{in}}{90})^{\beta_{roos}} - c_{roos}(\frac{\alpha_{in}}{90})^{\gamma_{roos}}) \tag{7.11}$$

$$q_{i,gzg}[\alpha_{in}] = g_{gzg}[\alpha_{in}] - \tau_{gzg}[\alpha_{in}] \tag{7.12}$$

$$\rho^{x}_{gzg}[\alpha_{in}] \approx 1 - \tau_{gzg}[\alpha_{in}] - [1 - \rho^{x}_{gzg}[0°] - \tau_{gzg}[0°]],\ for\ \alpha_{in} \leq 75° \tag{7.13}$$

$$\rho^{x}_{gzg}[\alpha_{in}] \approx 1 - \tau_{gzg}[\alpha_{in}] - \alpha^{x}[0°]\frac{\alpha_{in} - 90°}{15°},\ for\ \alpha_{in} > 75° \tag{7.14}$$

Where x superscript can be either ' or nothing, referring to internal or external pane.

From the energy balance, the temperatures of the internal and external nodes T_{is} and, respectively T_{os} are calculated.

Model M_{1s}

The model is initiated by the case where the number of nodes in the pane is the same as the initial case, as in figure 7.7, but the whole thermal mass of the pane is considered in the calculation. This suggests as an important influence over the surface temperatures of the panes. All the other coefficients are equivalent as in the initial case.

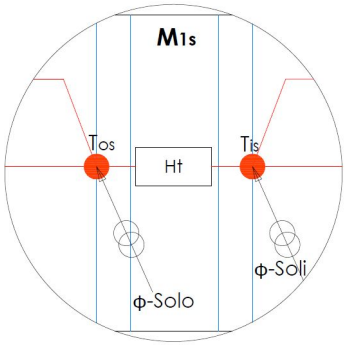

Figure 7.7. Nodal scheme for window detail for model M_{1s}

Model M_{1m}

The next model is done by moving the node from the external and internal surfaces in the center of the pane. The formula used for the thermal conductance of the window is presented in 7.15 on the facing page. The thicknesses of the panes are taken from the central points towards the gas spaces and correspond to half of the glazing thicknesses.

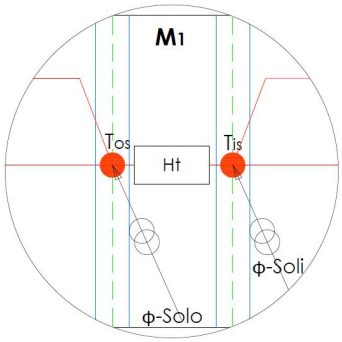

Figure 7.8. Nodal scheme for window detail for model M_{1m}

$$H_s = \frac{1}{\frac{1}{h_s} + 0.5d_1r_j + 0.5d_2r_j} \tag{7.15}$$

From the central position of the node towards outdoors for the external pane, the thermal conductance is calculated with half of the thickness and it is added to the external convective heat transfer coefficient $h_{c,e}$. The same procedure is done for the internal convective heat transfer coefficient $h_{c,i}$.

$$H_{c,e} = h_{c,e} + \frac{1}{0.5d_1r_j} \tag{7.16}$$

$$H_{c,i} = h_{c,i} + \frac{1}{0.5d_2r_j} \tag{7.17}$$

Model M_{2s}

This case regards two nodes in each of the panes, where they are situated on each of the pane surfaces, as shown in figure 7.9. The thermal conductances for each of the panes is calculated with the complete thicknesses of the glazing panes. The gas conductance h_s remains unchanged as well as the external and internal heat transfer coefficients.

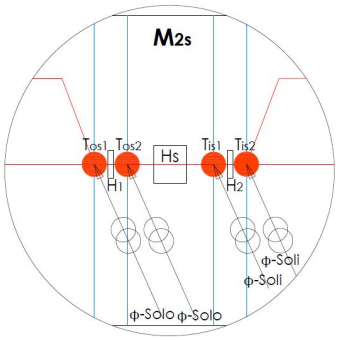

Figure 7.9. Nodal scheme for window detail for model M_{2s}

$$H_1 = \frac{1}{d_1 r_j} \tag{7.18}$$

$$H_2 = \frac{1}{d_2 r_j} \tag{7.19}$$

Model M_{2m}

The next simulation model is done for two nodes in the pane where one is in the surface and the other is in the central spot of the pane. From the model we obtain two temperatures in the external pane and two on the internal one. The thicknesses of the panes are taken from the central points (T_{os2} and T_{is1}) towards the gas spaces and introduced in the equation along with h_s as in formula 7.15 on the preceding page. The other halves are used to calculate the thermal conductances H_1 and H_2.

$$H_1 = \frac{1}{0.5 d_1 r_j} \tag{7.20}$$

$$H_2 = \frac{1}{0.5 d_2 r_j} \tag{7.21}$$

Figure 7.10 is shown with a different drawing for the nodes as it is more convenient and easier to use for further representations.

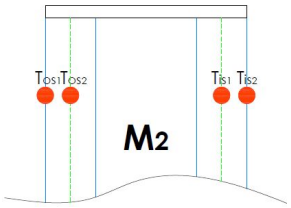

Figure 7.10. Nodal scheme for window detail for model M_{2m}

Model M_3

The next case is changed by including an extra node which is shown in figure 7.11 on the facing page. This model is fitting well in terms of positioning as two of the nodes are in the surfaces and the other one is placed centrally in the pane. In this case there is no change in external and internal heat transfer coefficients and the same goes for the gas space conductance of the window. There is added a new thermal conductance in each pane as the number of nodes increased to three.

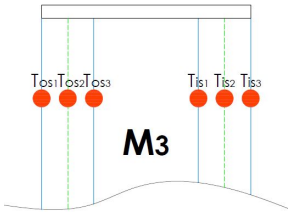

Figure 7.11. Nodal scheme for window detail for model M_3

$$H_1 = H_1' = \frac{1}{0.5 d_1 r_j} \tag{7.22}$$

$$H_2 = H_2' = \frac{1}{0.5 d_2 r_j} \tag{7.23}$$

Model M_4

The last model is corresponding with a number of four nodes in each of the panes represented in figure 7.12. The convective terms and gas space conductance remain the same as two of the nodes are positioned on the surfaces. The other two are equidistant from the surfaces and in this case there is added a new thermal conductance corresponding to a smaller thickness.

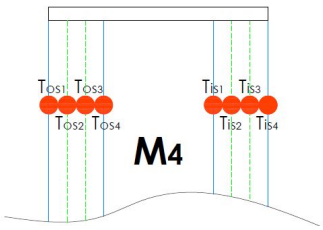

Figure 7.12. Nodal scheme for window detail for model M_4

$$H_1 = H_1' = H_1\text{"} = \frac{1}{0.33 d_1 r_j} \tag{7.24}$$

$$H_2 = H_2' = H_2\text{"} = \frac{1}{0.33 d_2 r_j} \tag{7.25}$$

7.2.1 Validation

In this section it is made a comparison between models with a different number of nodes in the glazing pane together with the experimental setup, from which the best solution is selected. The graphs are showing data for a period of three complete days $17th - 19th$

of May. The external conditions are represented by the external temperature of the air, the total solar radiation and direct and diffuse radiation. The overall power consumption from the models and the measurements and the temperatures of the glazing nodes have been also included.

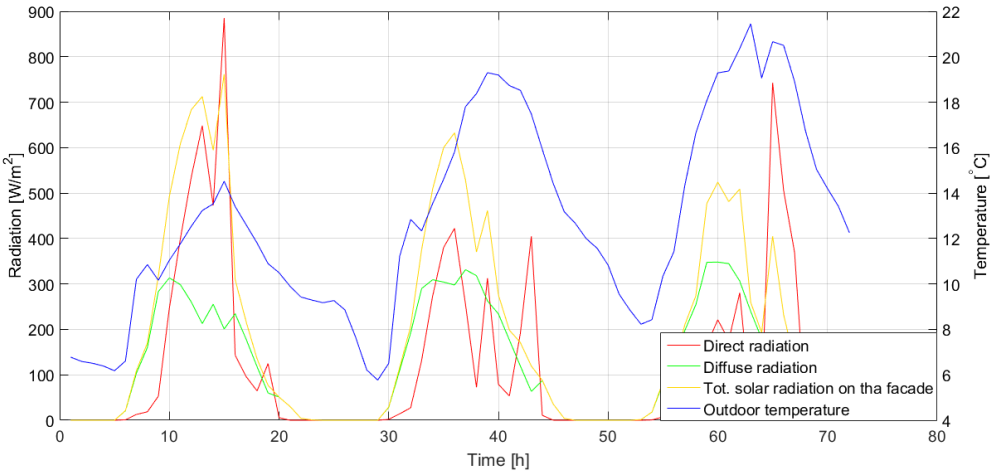

Figure 7.13. Weather conditions - Period 17^{th} to 19^{th} of May

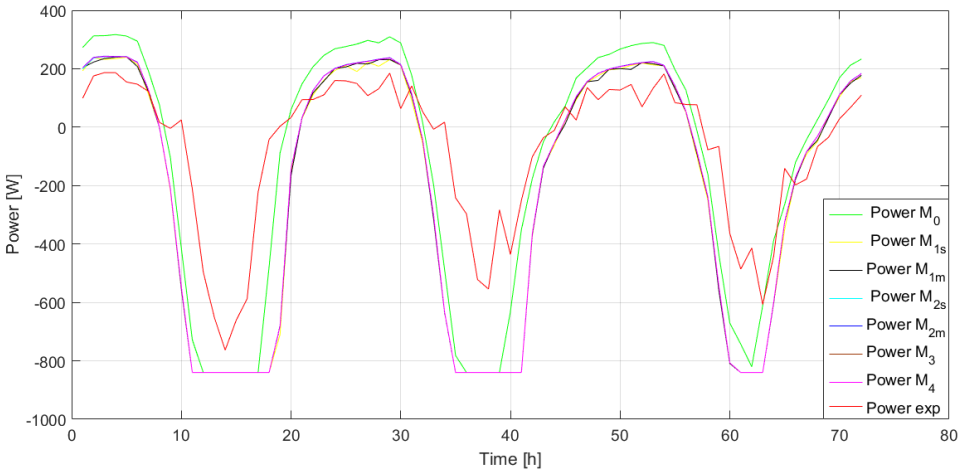

Figure 7.14. Energy consumption comparison between measurements and detail glazing models - Period 17^{th} to 19^{th} of May

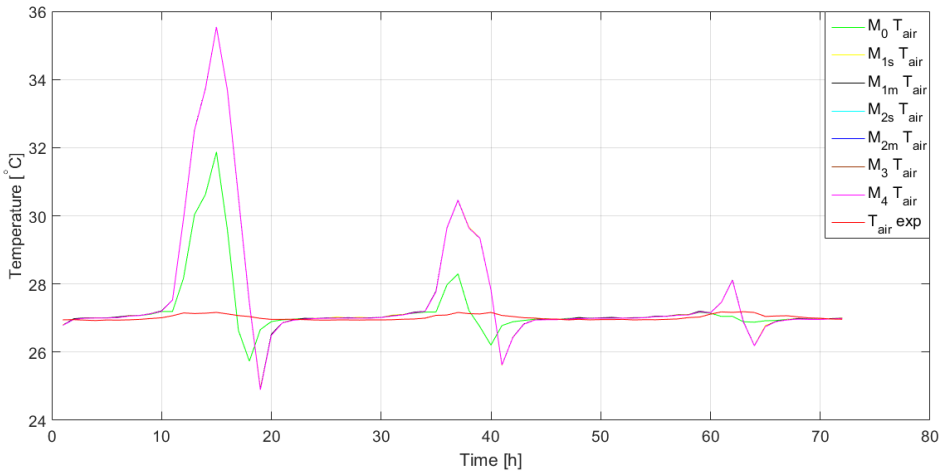

Figure 7.15. Room air temperature comparison between measurements and detail glazing models - Period 17^{th} to 19^{th} of May

The power consumption for heating and cooling is shown in figure 7.14. It can be seen that for the simulation models, a constant cooling load has been introduced in order to fit with the measurements. The simulation models have an overestimated cooling load during the day and it is closer for the heating need aside M_0. The model is known to have a smaller thermal mass considered. When the maximum cooling power is reached during the intense solar radiation , internal air temperature increases as shown in figure 7.15. This is due to the fact that the constant cooling is not powerful enough to cool down the room. When increasing the cooling power this matter is solved and results for this case are shown in Appendix H

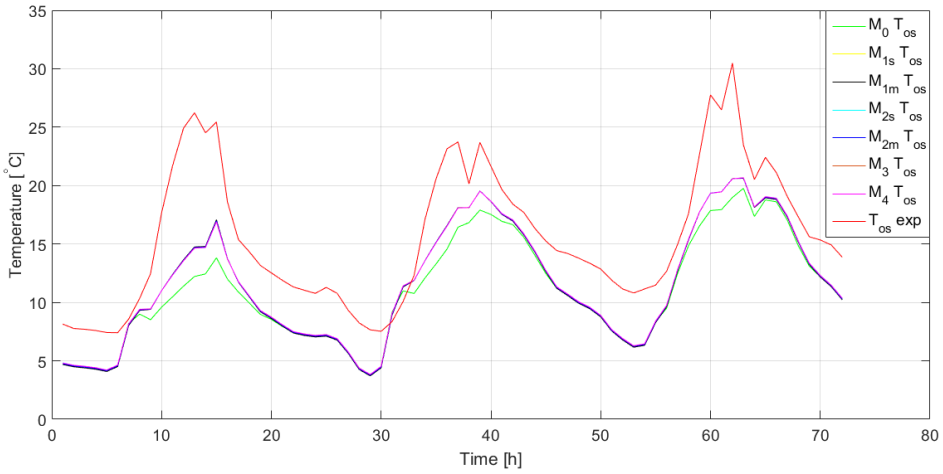

Figure 7.16. Glazing's external pane surface temperature comparison between measurements and detail glazing models having the node in the surface and in the central pane - Period 17^{th} to 19^{th} of May

Figure 7.16 shows the temperature on the external pane of the window. The only visible

difference emerges between the initial model and the others. With a reduced thermal mass, solar gains considered are also smaller, what results in decreased temperatures. Nevertheless, the influence in the increase of the nodes in the pane is not visible in the graph as the temperature distribution is similar. From model M_1 to M_4 the curves are similar and overlapping each other and just the initial model M_0 changes path when the solar radiation is present.

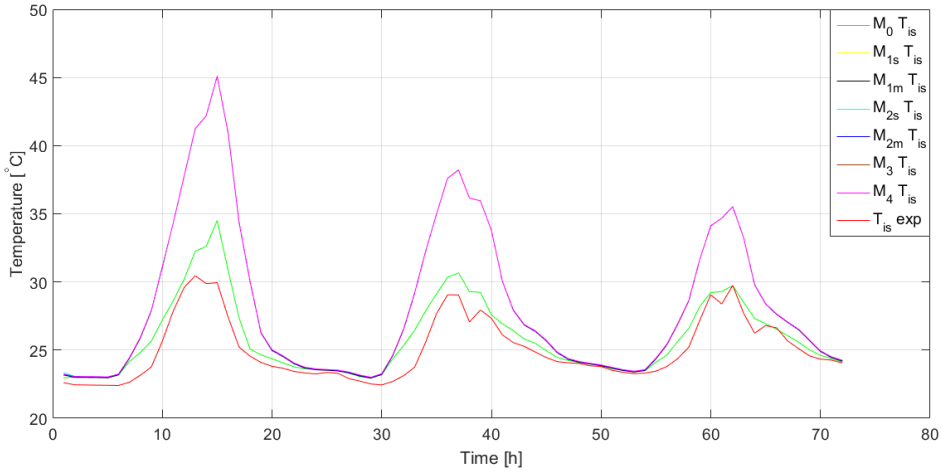

Figure 7.17. Glazing's internal pane surface temperature comparison between measurements and detail glazing models having the node in the surface and in the central pane - Period 17^{th} to 19^{th} of May

For the temperatures of the internal pane of the window the results are similar as the biggest difference occurs between the M_0 and the other models. It seems that there is a significant overestimation in the description of the solar gains in the model. Model M_0 which considers a quarter of the thermal mass on the window panes is used further in the detail approach for the shading model. This decision is done based on the fact that this model is the most accurate relating with the real measurements on the pane.

Shading 8

In this chapter shading is introduced in the model, where two approaches are considered depending on how in detail this implementation is performed. First section of the chapter refers to the simplest approach where blind properties and solar gains are considered by using solar heat gain coefficient. Second section is considering angular properties of each of the panes of the glazing and also of the shading also cavity in between shading and glazing is modelled.

8.1 SHGC-based shading model

From the basis for the model development explained in 6.1, where the room is represented by three nodes (air, internal surface and mass), it is intended to implement the glazing and blind in the simplest possible way so also good accuracy is achieved. Solar incident angle dependency is considered by using same approach as explained in 7.1.

Several options have been analysed by considering different nodes and links between them, although only the chosen model is presented in detail further. Conclusions obtained from disregarded options are explained in the following, and their models are briefly explained in Appendix I.

It is initially tried a model according to standard EN-13363-1 [5] that proposes a total solar heat gain coefficient in the room, considering both glazing and blind properties. This solution does not need to add more nodes than the three defining the room, however it leads to high cooling demand results due to a high heat gain estimation on the surfaces of the room. In case of adding an extra node in the glazing, obtained results are very similar as in previous model. Only advantage from this model would be to calculate glazing internal surface's temperature, although in terms of thermal comfort it is rather blind's surface temperature the one to be considered. Last analysed model considers an extra node in the air cavity between the glazing and the blind. Treating this cavity as a different thermal zone from the air in the room is found to be the best approach and therefore is the chosen solution.

With this extra node, SHGC-based shading model has four nodes in total; three nodes representing the room plus one extra node placed in the air cavity between the glazing and the blind. Model is represented in figure 8.1.

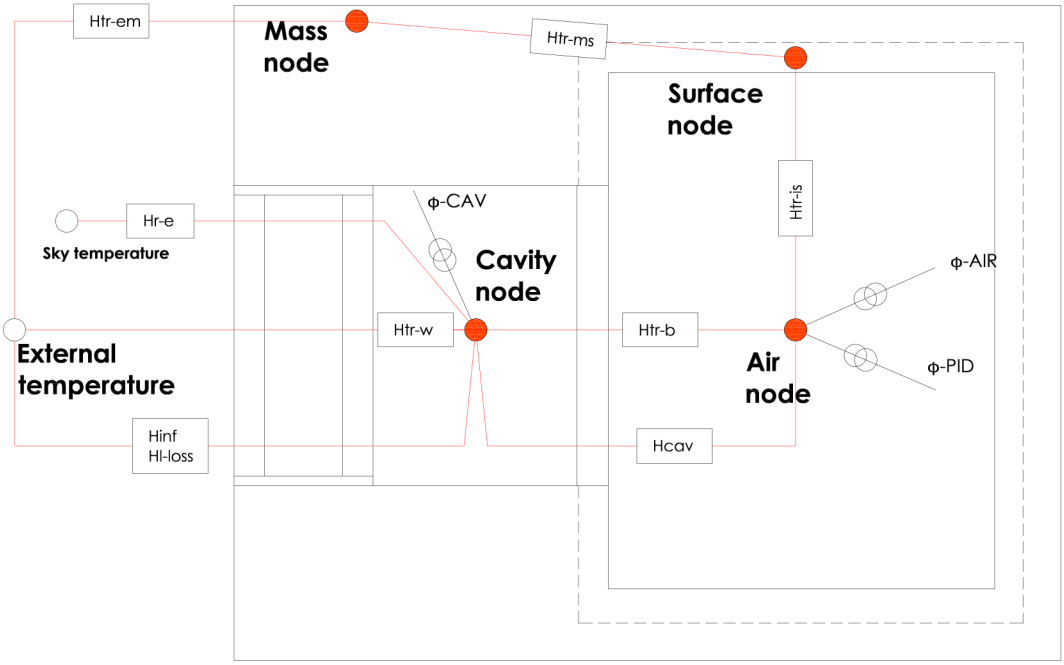

Figure 8.1. SHGC-based shading model

Heat transfer coefficient from cavity towards outdoor H_{tr-w} is calculated according to EN 673 [21] for a double pane window, and external and internal convective heat transfer coefficients according to Clarke [28]. Blind thermal resistance is neglected.

Long wave losses towards sky are calculated by using H_{r-e} heat transfer coefficient, which is considering convective resistance of the glazing and radiative coefficient from surface towards sky as explained in

Infiltration between cavity and room is estimated as a constant value, H_{cav}. It is calculated in the same way as ventilation into the room with equation 6.5 by considering a constant volume flow of 0,00114 $\frac{m^3}{s}$.

Thermal properties of the blind are estimated as 0,3 $\frac{W}{m^2K}$, having a thickness of 0,55 mm. Thermal resistance H_{tr-b} is calculated by considering internal convective heat transfer coefficient in both sides.

Solar gains are calculated by following proposed method in standard DIN-18599 [18] for sun-spaces in buildings, where solar gains are considered in the air of the internal room and unheated space. In this model, cavity between glazing and blind can be treated as unheated sun-space, and the blind as the internal window between the sun-space and room. However in terms of heat transfer blind's energy resistance has been neglected.

Proposed gains in the standard are according to the following equations:

$$\phi_{AIR} = I\tau_w g_B \tag{8.1}$$

$$\phi_{CAV} = Ig_w - I\tau_w g_B \tag{8.2}$$

Where g_B refers to the total heat transfer coefficient of the blind, which is estimated as the sum of its transitivity and half of its absorptivity ($g_B = \tau_B + 0,5\alpha_B$), and $I = \phi_{dir} + \phi_{dif}$;

8.2 Shading detail model

In this section of model development, shading device is implemented in a detail manner, following the standard ISO 15099. Model is complemented by additional descriptions of solar optical properties for a blinds, found in the work of [8]. In a final stage here, the cavity model is implemented.

Blind implementation

First approach is handled by consideration of the blind as additional pane for the window. Figure 8.2 gives visual explanation of presented system.

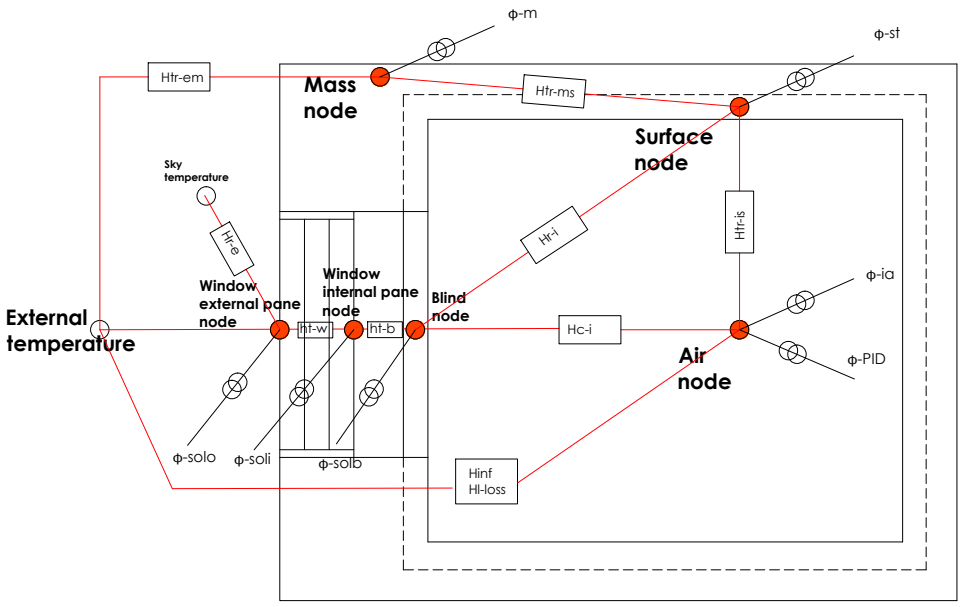

Figure 8.2. System with node for the shading device.

Calculations for the heat flows from heat sources to the nodes in the room (air, surface and mass nodes) is done according to the procedure followed in section 6.1 on page 35.

Nodes in the system of window with internal blind are treated as a triple glazing system. All the solar gains in the model are assumed in the façade and are split into the three nodes representing it:

- For window external pane ϕ_{solo} follows equation 7.7
- For window internal pane ϕ_{soli} follows equation 7.8
- For blind node ϕ_{solb} equation is:

$$\phi_{solb} = \phi_{dir}\alpha_{e3_{dir}} + \phi_{diff}\alpha_{e3_{dir}} \tag{8.3}$$

Above mentioned formulas consider the absorbed radiation on panes which is represented by direct absorbtance coefficients α_{e1}, α_{e2}, α_{e3}. These are calculated according to norm EN 410 [23] for a triple glazing.

$$\alpha_{e1} = \alpha_1 + \frac{\tau_1\alpha_1'\rho_2(1-\rho_2'\rho_3) + \tau_1\tau_2^2\alpha_1'\rho_3}{(1-\rho_1'\rho_2)\cdot(1-\rho_2'\rho_3) - \tau_2^2\rho_1'\rho_3} \tag{8.4}$$

$$\alpha_{e2} = \frac{\tau_1\alpha_2(1-\rho_2'\rho_3) + \tau_1\tau_2\alpha_2'\rho_3}{(1-\rho_1'\rho_2)\cdot(1-\rho_2'\rho_3) - \tau_2^2\rho_1'\rho_3} \tag{8.5}$$

$$\alpha_{e3} = \frac{\tau_1\tau_2\alpha_3}{(1-\rho_1'\rho_2)\cdot(1-\rho_2'\rho_3) - \tau_2^2\rho_1'\rho_3} \tag{8.6}$$

Indexes 1, 2 and 3 for the solar optical parameters α, τ, ρ corresponds to the each pane properties separately. For two first window panes, the properties depend on incident angle of a solar radiation and are calculated as presented in section 7.2.

Solar-optical angular properties of a blind

Semi-empirical method developed by[8] can be used to calculate the corresponding off-normal properties for a given solar optical properties of any fabric (shading device) at normal incidence. They measured the spectral direct-direct transmittance, direct-diffuse transmittance and direct-diffuse reflectance at the range of incident angle from 0 ° to 60 ° and then calculated corresponding solar properties (ASTM 1996). Then for the measured properties at different incident angle a cosine power function has been fitted. Cosine correlation was used due to the symmetrical and adjustable shape of the function. Details of the semi-empirical model implemented in the model are as follow.

Direct-direct transmittance model

Equation 8.7 calculates normalized direct-direct transmittance.

$$^{norm}\tau_{dir,dir} = \frac{\tau_{dir,dir}(\theta)}{\tau_{dir,dir}(\theta=0)} = cos^b(\frac{\theta}{\theta_{cutoff}}\frac{\pi}{2}) \qquad \theta \leq \theta_{cutoff} \tag{8.7}$$

Parameters θ_{cutoff} and b are used to characterise off-normal direct-direct transmission through all roller blinds. Following equations 8.8 and 8.9 are proposed.

$$b = 0.6cos^{0.3}(A_0\frac{\pi}{2}) \tag{8.8}$$

$$\theta_{cutoff} = 65^\circ + (90^\circ - 65^\circ) \cdot (1 - cos(A_0\frac{\pi}{2})) \tag{8.9}$$

Where the cut-off angle θ_{cutoff} denotes that the transmittance reduces to zero beyond a certain angle. And parameter A_0 is the openness factor.

Direct-hemispherical total transmittance model

Equation 8.10 represents normalized direct-hemispherical transmittance.

$$^{norm}\tau_{dir,h} = \frac{\tau_{dir,h}(\theta)}{\tau_{dir,h}(\theta = 0)} = cos^b(\theta) \qquad \theta \leq \theta_{cutoff} \tag{8.10}$$

In the presented formula the cut-off angle is not as straightforward as for direct-direct transmittance. Its application here is restricted only for a dark-color samples due to limited scattered reflection or transmission. Criterion for classification of light- and dark-color fabrics is not clear therefore in the model, presented description is followed for all types of fabrics.

Apparent transmittance of the roller blind 8.11 structure is defined, by noting that the portion of incident radiation intercepted by the structure is $1 - A_0 = 1 - \tau_{dir,dir}(\theta = 0)$ and that the structure only produces diffuse transmission:

$$\tau^{str} = \frac{\tau_{dir,dif}(\theta = 0)}{A_0} = \frac{\tau_{dir,h}(\theta = 0) - \tau_{dir,dir}(\theta = 0)}{1 - \tau_{dir,dir}(\theta = 0)} \tag{8.11}$$

Expressions for exponent b in equation 8.10 were developed in a way that for values of τ^{str} corresponding to the dark-color samples $b \approx 2$ was chosen while for τ^{str} corresponding to the light-color samples $b \approx 0.4$ was selected. Thus:

$$b = 0.133(\tau^{str} + 0.003)^{-0.467} \qquad 0 \leq \tau^{str} \leq 0.33 \tag{8.12}$$

$$b = 0.33(1 - \tau^{str}) \qquad 0.33 \leq \tau^{str} \leq 1 \tag{8.13}$$

Direct-diffuse transmittance model

For any given θ incidence angle, direct-diffuse transmittance is calculated according to the equation 8.14.

$$\tau_{dir,dif}(\theta) = \tau_{dir,h}(\theta) - \tau_{dir,dir}(\theta) \tag{8.14}$$

Diffuse-diffuse transmittance and reflectance model

Diffuse-diffuse solar optical properties are obtained by integration of direct-hemispherical properties over hemisphere.

$$\tau_{dif,dif} = 2\int_0^{\frac{\pi}{2}} \tau_{dir,h}(\theta)cos(\theta)sin(\theta)d\theta \tag{8.15}$$

$$\rho_{dif,dif} = 2\int_0^{\frac{\pi}{2}} \rho_{dir,h}(\theta)cos(\theta)sin(\theta)d\theta \tag{8.16}$$

However, [8] observed that plot of $\rho_{dif,dif}$ versus θ has no significant variation of $\rho_{dir,h}$ in respect to θ, therefore direct-hemispherical reflectance is considered to be constant. Thus, equation 8.16 reduces to:

$$\rho_{dif,dif} = \rho_{dir,h}(\theta = 0) \tag{8.17}$$

Cavity implementation

Next, cavity node is included and figure 8.3 presents this implementation.

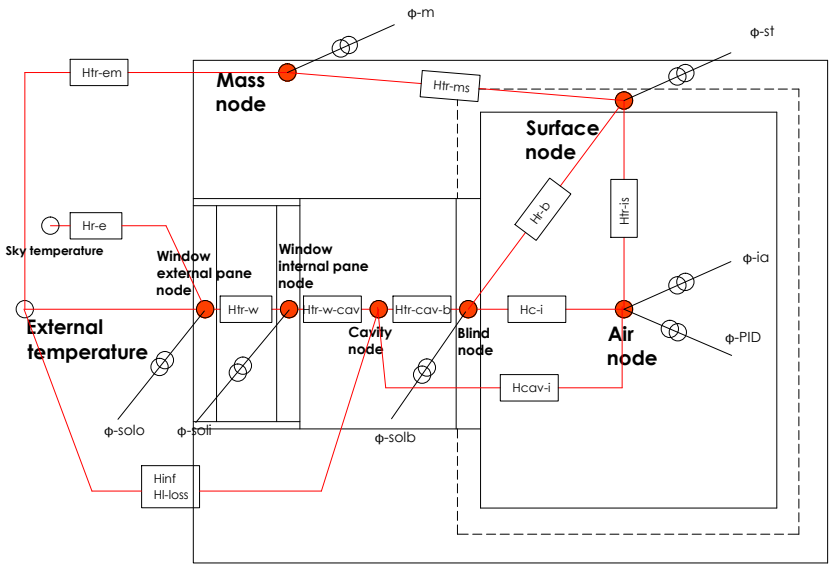

Figure 8.3. System with node for the shading device and cavity node.

Heat balance in the gap, considering it as ventilated requires an extra term, the amount of heat supplied to or extracted from the gap air by ventilation.

Extra term added to the heat balance, called heat transfer to the gap by ventilation is presented below.

$$q_{vl} = \frac{\rho \cdot C_p \cdot \phi_{vl}(T_{gap,inl} - T_{gap,out})}{(H \cdot L)} \tag{8.18}$$

Where:

ρ	density of the air in the cavity at temperature T_{gap}, $[\frac{\text{kg}}{\text{m}^3}]$
C_p	specific heat capacity of air, $[\frac{\text{J}}{\text{kgK}}]$
ϕ_{vl}	air flow rate in cavity $[[\frac{\text{m}^3}{\text{s}}]$
$T_{gap,inl}$	temperature at the inlet of the gap, [K]
$T_{gap,out}$	temperature at the outlet of the gap, [K]
L	length of cavity, [m]
H	height of cavity, [m]

Additionally, due to air movement in a ventilative gap, convective heat exchange is increased and this increased coefficient is written as:

$$h_{cv} = 2 \cdot h_g + 4 \cdot V \tag{8.19}$$

Where:

h_g	convection heat transfer coefficient for non-ventilated cavities $[\frac{\mathrm{W}}{\mathrm{Km}^2}]$
V	mean air velocity in the cavity, $[\frac{\mathrm{m}}{\mathrm{s}}]$

Air flow rate in the cavity and therefore a velocity of the air in a space is caused by the stack effect which depends on a driving pressure difference and resistance of the air flow of the openings of shading device and space itself. In order to obtain the air velocity in the cavity, the equation representing that the total pressure loss is equal to the driving pressure difference, should be solved.

$$\Delta P_{T,i,k} = \Delta P_{B,i} + \Delta P_{HP,i} + \Delta P_{Z,i} + \Delta P_{Z,k} + \Delta P_{B,k} + \Delta P_{HP,k} \tag{8.20}$$

Where:

$\Delta P_{T,i,k}$	driving pressure difference between space i and space k, [Pa]
$\Delta P_{B,i}$	Bernoulli pressure loss in space i, [Pa]
$\Delta P_{HP,i}$	Hagen-Poiseuille pressure loss in space i, [Pa]
$\Delta P_{Z,i}$	pressure loss Z at the inlet and outlet of space i, [Pa]
$\Delta P_{Z,k}$	pressure loss Z at the inlet and outlet of space k, [Pa]
$\Delta P_{B,k}$	Bernoulli pressure loss in space k, [Pa]
$\Delta P_{HP,k}$	Hagen-Poiseuille pressure loss in space k, [Pa]

In the investigated case of internal shading device,the space i is the cavity and the space k is the interior, thus according to the standard air velocity in this space is assumed $V_k = 0$. In that case the pressure loss terms for a space k in equation 8.20 are zero.

By rearranging above equation, the mean air velocity in the cavity is calculated in presented manner:

$$V = \frac{C_1}{C_2 \cdot V_{const} + C_3 + C_4 \cdot V_{const}} \tag{8.21}$$

Where:

$C_1, C_2, C_3 and C_4$	constants, $[-]$
V_{const}	constant air velocity in the cavity, $[\frac{\mathrm{m}}{\mathrm{s}}]$

$$C_1 = \rho T_0 g H \frac{|(T_{cav} - T_i)|}{T_{cav} \cdot T_i} \tag{8.22}$$

Where:

ρ_{air}	air density, $[\frac{\text{kg}}{\text{m}^3}]$
T_0	outdoor air temperature, [°C]
g	gravitational acceleration, $[\frac{\text{m}}{\text{s}^2}]$
H	height of the cavity, [m]
T_{cav}	air temperature in the cavity, [°C]
T_i	air temperature in the room, [°C]

$$C_2 = 0.5\rho \tag{8.23}$$

$$C_3 = 12 \cdot \mu \frac{H}{d} \tag{8.24}$$

$$C_4 = 0.5\rho(Z_{inl} - Z_{out}) \tag{8.25}$$

Where:

μ	dynamic viscosity of air , [Pas]
d	width of the cavity, [m]
Z	pressure loss factors of cavity, calculated according to the standard ISO 15099 [6] , [Pa]

Parameter V_{const} appears in equation 8.21 to avoid quadratic form of it and initial constant air velocity is assumed. This way the computational process is faster and equation is linearized.

Sum up

All presented in this section models are summed up in table 8.1

Table 8.1. Sum up of shading detail models

	SOLAR GAINS	
MODEL B+CAV		
Mass node	ϕ_m	zero, all gains are assumed in the façade
Air node	ϕ_{ia}	zero, all gains are assumed in the façade
Surface node	ϕ_{st}	zero, all gains are assumed in the façade
Glazing node paneI	ϕ_{solo}	$\phi_{solo} = \phi_{dir}\alpha_{e1_{dir}} + \phi_{diff}\alpha_{e1_{dir}}$
Glazing node paneII	ϕ_{soli}	$\phi_{soli} = \phi_{dir}\alpha_{e2_{dir}} + \phi_{diff}\alpha_{e2_{dir}}$
Cavity node	-	-
Blind node	ϕ_{solb}	$\phi_{solb} = \phi_{dir}\alpha_{e3_{dir}} + \phi_{diff}\alpha_{e3_{dir}}$
	UNCONTROLLED	**COOLING**
MODEL B+CAV		
Mass node	transmission loss	through the walls
Air node	infiltration	thermally driven air cavity (between air node and cavity)
Surface node	-	
Glazing node paneI	transmission loss	through glazing
	long-wave radiation	towards the sky
Glazing node paneII	-	
Cavity node	infiltration	thermally driven air cavity (between air node and cavity)
	infiltrations	towards outside
	thermal bridge	through the glazing frame
Blind node	-	

8.3 Validation

Here are presented results obtained from the models defined in sections 8.1 and 8.2 which are validated through the measurements described in chapter 5.

Experiments were performed in four periods as it is stated in table 5.4 on page 25. Here is presented the validation of only one period, 25-26 May 2016, when the Charcoal Grey blind was used for the measurements. It has been selected due to the most representative visualization of results. The conditions corresponds to overcast and clear day. The validations for other periods can be found in Appendix J.

First figure shows the weather conditions during experimental period. Here is displayed outdoor air temperature, measured total solar radiation on a façade and calculated values for direct and diffuse solar radiation [41].

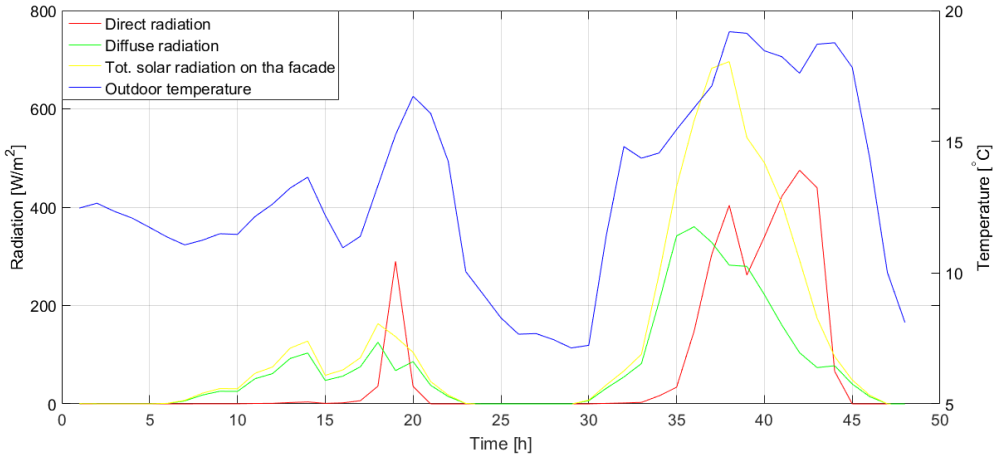

Figure 8.4. Weather conditions - Period 25^{th} to 26^{th} of May - Charcoal Grey blind

For the energy consumption, the curve fitting is done for both simulation results and this is represented by the dashed lines on the graph. In the legend is shown the constant value in watts added to the simulation results, in order to illustrate better the differences.

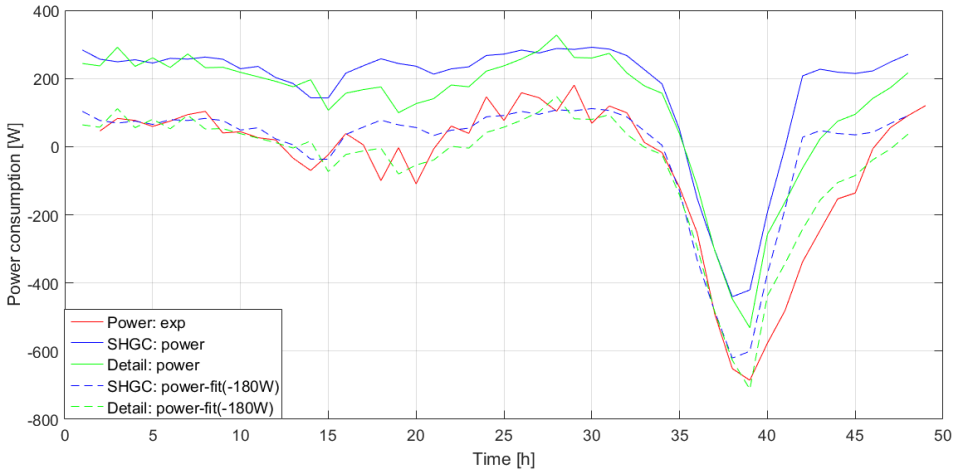

Figure 8.5. Energy consumption comparison between measurements, SHGC-based and detail models - Period 25^{th} to 26^{th} of May - Charcoal Grey blind

The heating need in both shading models is overestimated compared with the measurements. The reason is due to assumed too higher losses in the simulation than they are in the experimental set up. Since this value has not been checked experimentally its estimation was needed for the simulation purposes. The cooling demand is simulated properly for overcast and clear day. It responds to external conditions in the same way as in the experiment, although variation for SHGC model is steeper. The same situation is observed for another simulation period with Charcoal Grey blind (7-8 May) but other behaviour is observed in measurement case with White Pearl blind (10-15 May) for the detail model simulation.

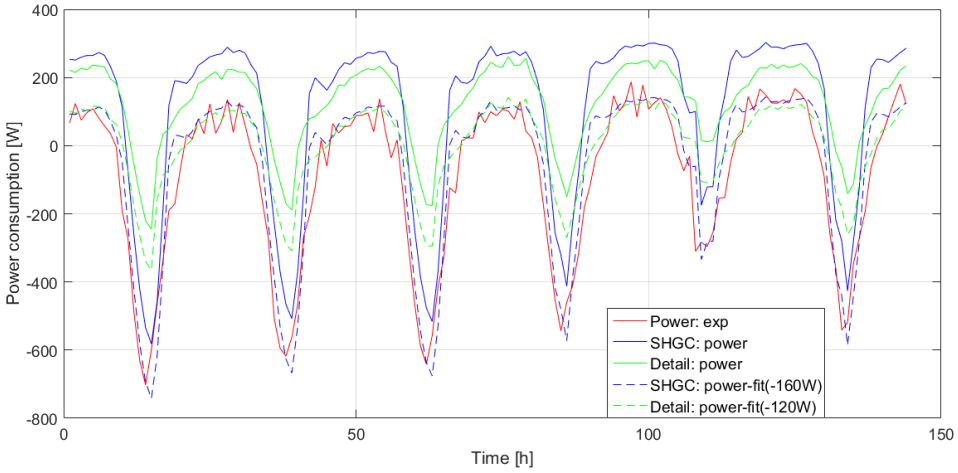

Figure 8.6. Energy consumption comparison between measurements, SHGC-based and detail models - Period 10^{th} to 15^{th} of May - White Pearl blind

Cooling consumption is underestimated while SHGC model predicts it well similarly to cases with Charcoal Grey blind. This difference arises due to the definition of solar gains in both models. Those, for SGHC model are assigned to the air in the cavity and in the room, while detail model defines them in the surfaces of panes and blind. It can be seen that while considering the solar gains in the surfaces and using the highly reflective blind (White Pearl), detail model underestimates the cooling need. This is due to underestimation of reflected radiation trapped in between window pane and blind. For its verification a comparison is done, where the higher and lower values of reflectance are applied to the blind in detail model. Figure 8.7 presents this variation.

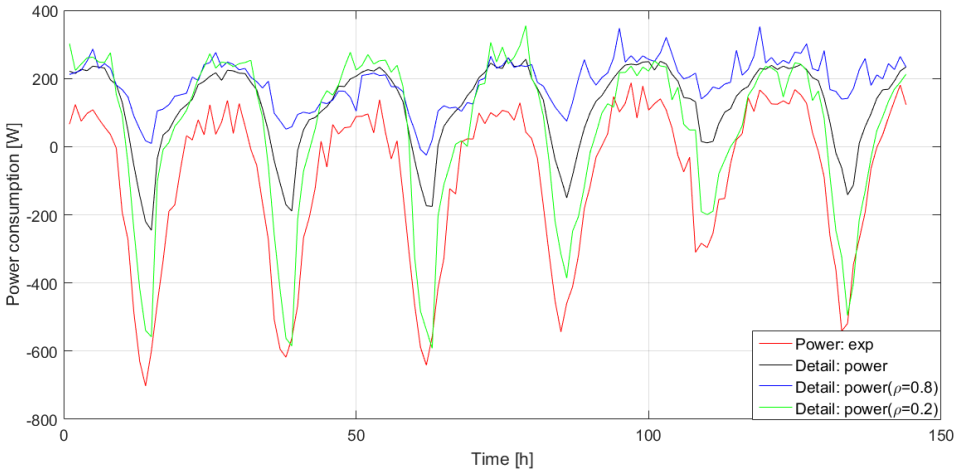

Figure 8.7. Energy consumption variation for different blind's reflective properties - Period 10^{th} to 15^{th} of May

It can be seen that reflected radiation has a great impact on the power consumption in detail model. It is concluded that the model underestimates it in a way that neglects this

trapped radiation in simulation process. Therefore, another and more detail definition of reflected radiation in between the cavity and blind should be applied in the model.

Next figure represents the air temperature in the room. Simulation results are compared to the temperature obtained from sensor instead of the one measured from thermocouples.

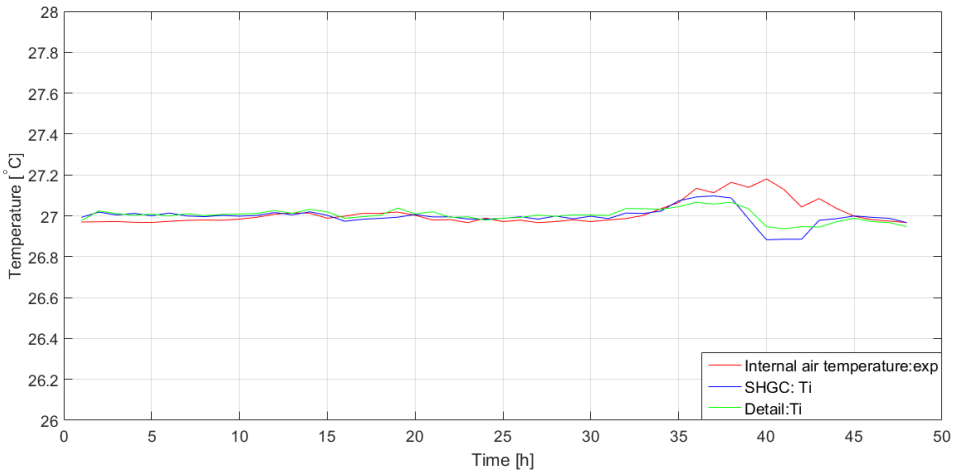

Figure 8.8. Room air temperature comparison between measurements, SHGC-based and detail models - Period 25^{th} to 26^{th} of May - Charcoal Grey blind

For both models the night temperature is simulated properly as well as during the overcast day. During the sunny day the little variation of $\pm$ 0.2 ° C is observed in comparison to the measured temperatures. Same behaviour is visible for other period of measurements, what can be seen in Appendix J. For sunny days, models simulate a temperature drop in the afternoon when solar radiation starts to decrease. This situation is related to the PI controller constants set in the simulations where its response time is fast. The influence of the PI controller constants is checked and evaluated in the next part of the report.

Evaluation of the air temperature in the cavity is done. Results are presented on figure 8.9

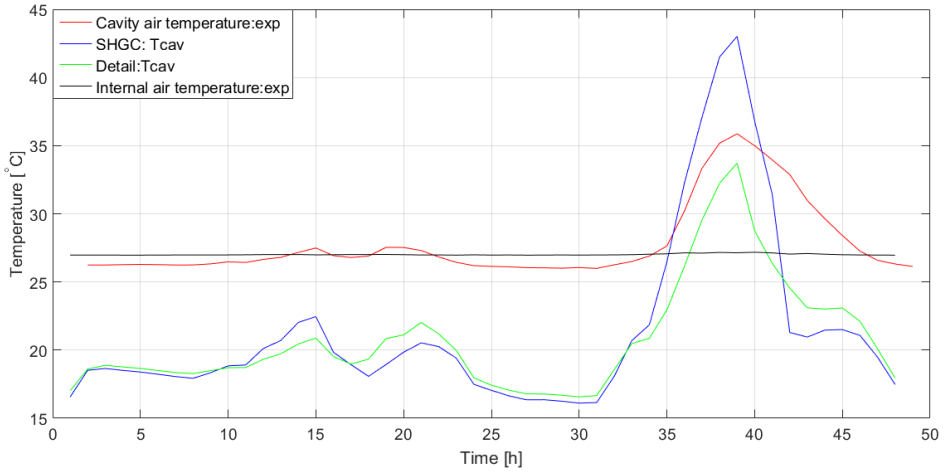

Figure 8.9. Cavity air temperature comparison between measurements, SHGC-based and detail models - Period 25^{th} to 26^{th} of May - Charcoal Grey blind

Both simulation models show underestimation of the temperatures during the night time. The same situation is observed during the overcast day when the direct solar radiation is very low. During sunny days, SHGC model highly overestimates the temperatures in the cavity whereas detail model still underestimates them. These variations are considered to be related to the description of infiltration losses from the cavity to the room air and air velocity movement in the cavity. This parameters are analysed later in the sensitivity analysis performed in chapter 9. The same behaviour is observed in other measurement cases and it can be seen in Appendix J.

The analysis of blind surface temperature is additionally made, however only one of analysed models simulates this parameter. Therefore, the comparison of the measurement values together with simulated ones for the blind surface temperatures, are presented together with the air cavity temperature for the detail model.

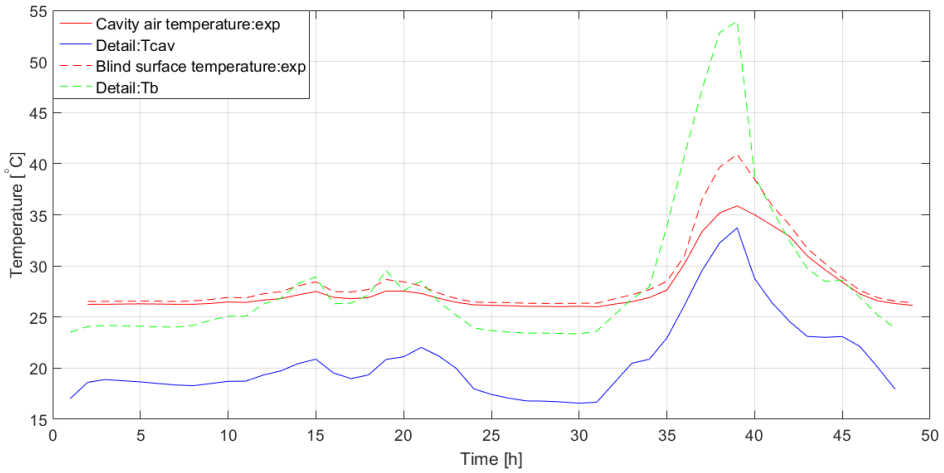

Figure 8.10. Blind surface and cavity air temperature comparison between measurements and detail models - Period 25^{th} to 26^{th} of May - Charcoal Grey blind

Blind surface temperatures during the night are underestimated but to a lower extent in comparison to the underestimation for the cavity temperature. Overestimation during sunny days is visible while for overcast case the simulation predicts temperatures more accurate. Reason for such a behaviour is considered to be due to the underestimated value of convective heat transfer coefficient from the blind to the surrounding air. That is checked and evaluated in the next part of this report.

Sum up

This paper aims to develop simplified calculation tool for the evaluation of the energy consumption for the buildings with double glazing façade and internal shading devices. Two paths of the model development were followed in this paper as described in sections 8.1 and 8.2. For each approach the same inputs have been implemented in the models in order to properly compare the outcomes of simulations. Even though, SHGC model performs better in terms of energy consumption, detail model allows more specific analysis due to its complexity. Additionally, detail model allows as well the analysis of the temperatures of the blind surfaces giving an advantage in terms of evaluation of local thermal comfort in the building. However, the fact that more parameters are defined makes it to be more uncertain by having higher range of error. Finally, the computational time for both of the models is similar, therefore this speaks for the choice of the detail model. Its sensitivity analysis is performed chapter 9 and possibilities for improvements are discussed.

Sensitivity analysis 9

When models are validated in previous chapters some conclusions are drawn by analysing the different results from studied parameters. This chapter analyses some of the input data that has an influence over those parameters, by performing a sensitivity analysis. Three main type of input values are considered: ones related to uncontrolled cooling, the PI controller, and the blind and cavity treatment.

9.1 Uncontrolled cooling parameters

Some parameters related to uncontrolled cooling are infiltration losses, linear losses, wind influence over convective loss in the façade.

For the linear loss a constant value of 0,3 $\frac{W}{mK}$ is taken from previous works in the Cube [4]. By using a thermographic camera this value was calculated as explained in Appendix K and obtained result are used for the sensitivity analysis. Heat balance presented in section 5.5 show realistic values for the used linear loss value, therefore the result from the calculation obtained from thermographic camera are neglected.

Same applies for used value for infiltration loss, of 0,0009 $\frac{m^3}{s}$. Standard [30] proposes a maximum infiltration rate of 27 $\frac{m^3}{hm^2}$ through openings which results in 0,032 $\frac{m^3}{s}$; this value is used to see the influence of the infiltration loss in the developed model.

Regarding the wind velocity a constant value of 5,5 $\frac{m}{s}$ is used, while in this part variable wind velocity and direction obtained from DMI weather data [31] are implemented.

Influence of these three parameters is shown in the next figures. In all cases temperature in the room is stable with little variation in the energy consumption, where the most influencing parameter is the infiltration rate.

Graphs present the experimental results together with the detail model results and simulation results after implementation of three mentioned changes.

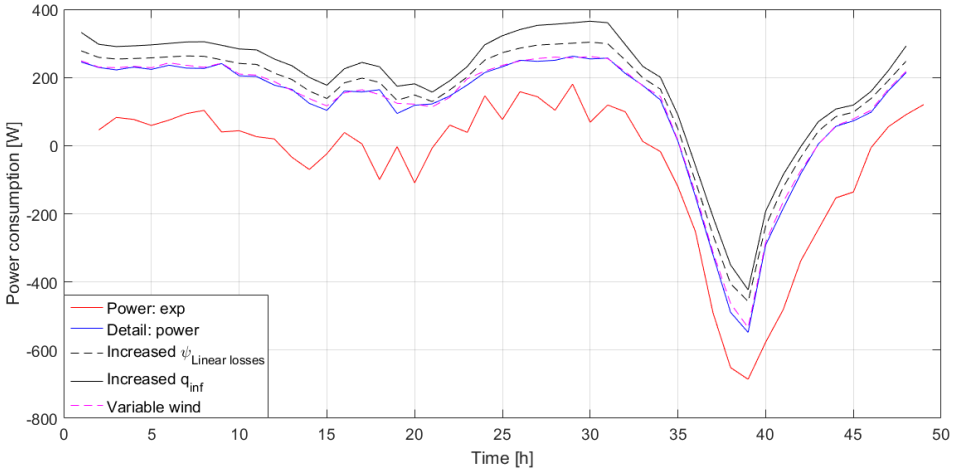

Figure 9.1. Uncontrolled parameters influence over energy consumption

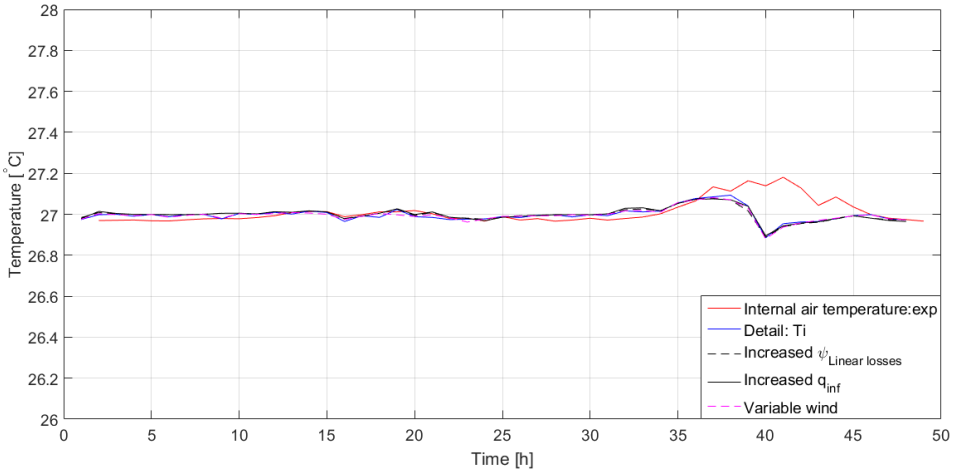

Figure 9.2. Uncontrolled parameters influence over room air temperature

Temperatures in the nodes directly linked to those parameters are being more affected. Air temperature in the cavity is decreased when increasing the linear loss or infiltration rate terms as seen on figure 9.3, and glazing external surface is decreased when considering variable wind velocity, as shown on figure 9.5.

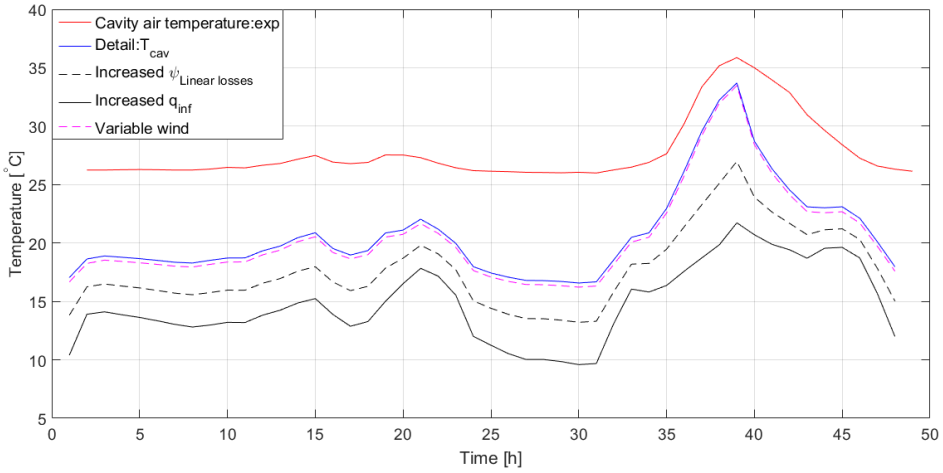

Figure 9.3. Uncontrolled parameters influence over cavity air temperature

In 8.3 is mentioned that the model has greater heat losses than in the measurements. Here it is analysed external and internal glazing surface's temperature variation when performing sensitivity analysis.

When infiltration loss is increased, air temperature in the cavity drops and causes a temperature decrease in the glazing's internal surface of 4°C, and external glazing temperature is not varying what can be seen on figures 9.4 and 9.5. From those results can be seen that conductive and convective heat transfer coefficients are performing well and extra heat losses does not occur through the window. Otherwise, this internal surface temperature drop, would have influenced external surface temperature.

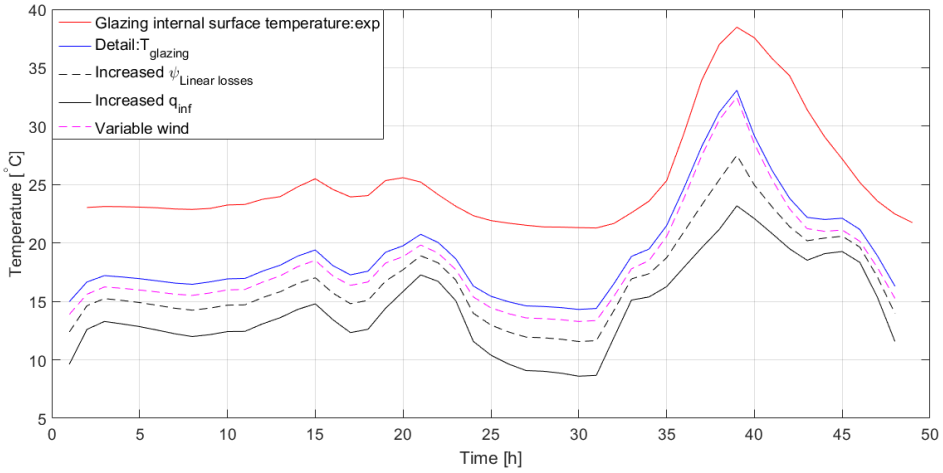

Figure 9.4. Uncontrolled parameters influence over glazing internal surface temperature

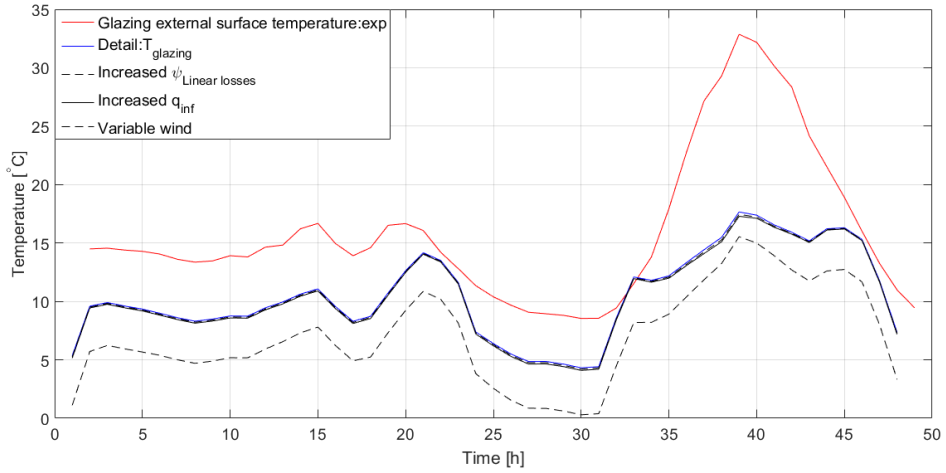

Figure 9.5. Uncontrolled parameters influence over glazing external surface temperature

Finally when variable wind velocity and direction are performed, glazing's external surface is decreased. Convective heat transfer coefficient is decreased from 27 $\frac{W}{m^2K}$ to 7,8 $\frac{W}{m^2K}$ due to wind northern direction though. This can be explained due to higher influence of long wave losses towards the sky.

9.2 PI controller

In 8.3 room air temperature results from the simulation are described, where strange behaviour occurs in the afternoon. This is related to bad tuning of the controller, however by running simulations with tuned controller, simulation time increases. Difference between the energy consumption is neglected for practical issues.

In order to see the influence of the tuning over the results several cases are performed. Tuning used in reference model corresponds to case 0, and case 1 corresponds to the tuning performed by MATLAB. Cases 2 and 3 are random variations to ilustrate simulation sensitivity.

Parameter	Case 0	Case 1	Case 2	Case 3
P	0,5	6,9	10	4
I	1	0,6	0,6	0,6

Table 9.1. Parameters variation for PI-controller in the simulation

Figures 9.7 and 9.8 show results for room air temperature and energy consumption. Strange behaviour from the air in the room corresponds to external radiation decrease in weather conditions. This phenomena disappears when proportional gain of the controller is increased. Regarding energy consumption higher fluctuations appear but as an overall its average is close to reference case energy consumption.

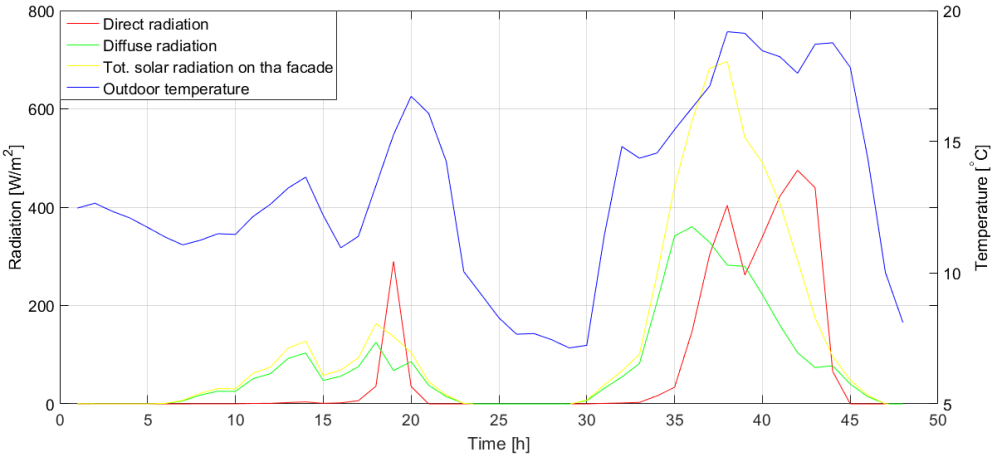

Figure 9.6. Weather conditions - Period 25*thto*26*th* of May - Charcoal Grey blind

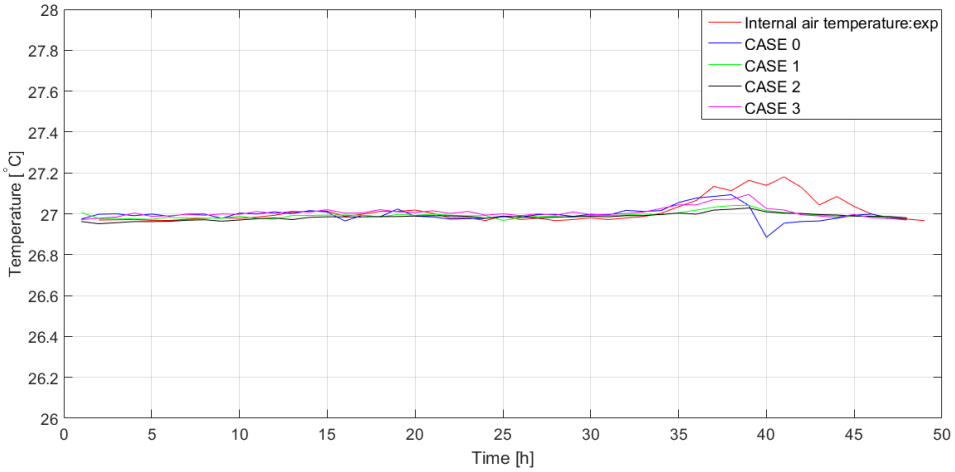

Figure 9.7. PI controller constants influence over room air temperature

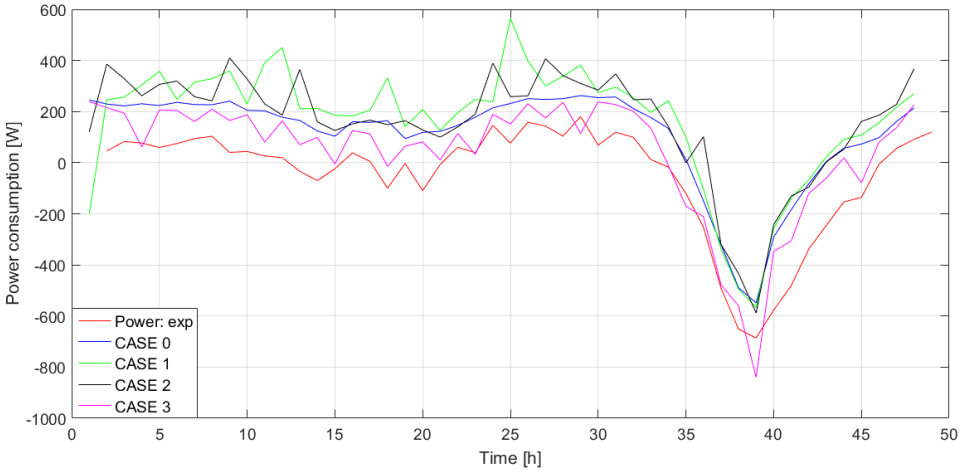

Figure 9.8. PI controller constants influence over energy consumption

9.3 Blind and cavity ventilation

As explained in 8.3 calculated temperature in the cavity during the night is much lower than the measured one and this could be due to overestimated heat transfer resistance from cavity to the room.

Blind

Blind thermal properties are not a given value from manufacturers and due to its porous composition it is difficult to calculate how heat transfer phenomena occurs through it. In the model, a thermal conductivity for the blind is estimated as $0,5\frac{W}{m^2K}$.

However in order to have an order of magnitude of this value, simple approach is done as follows. From the measurements it can be seen that during the night time, external temperature, cavity temperature and room temperature are constant, and consequently heat flux can be assumed to be constant.

It can be assumed that the cavity is tight and no infiltration occurs towards the room, so heat flux from the room through the cavity towards outside can be estimated from the following known values:

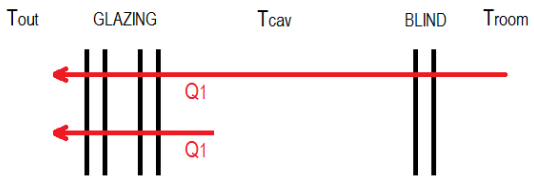

Figure 9.9. Heat flux - non ventilated cavity

$$Q_1 = h_{win}A_{win}(T_{cav} - T_{out}) = 1,06 \cdot 4,26 \cdot (25 - 10) = 67,57W$$

In the same way $h_{win+blind}$ can be guessed as,

$$h_{win+blind} = \frac{Q_1}{A_{win}(T_{room}-T_{out})} = \frac{67{,}57}{4{,}26(27-10)} = 0,93\frac{W}{m^2K}$$

and from thermal transmittance values, proportional part of the blind can be estimated as:

$$\frac{1}{h_{win+blind}} = \frac{1}{h_{win}} + \frac{1}{h_{blind}}$$

Where influence of the air in the cavity is neglected. This way is obtained $h_{blind} = 7,93\frac{W}{K}$ and thermal conductivity $\lambda_{blind} = 1,86\frac{W}{m^2K}$. Implementing this value do not change at all any of the temperature results in the simulation and only an average of 8 W for the energy consumption.

Cavity ventilation

Regarding the air flow between the cavity and the room, its calculation is explained in 8.2 and analysis of the results is done in 8.3, where problems of followed methodology were explained. So as to see its influence, similar approach as for blind's thermal conductivity is followed but considering a heat transfer between the cavity and the room.

Assuming an infiltration from the room towards the cavity, heat transfer through the glazing is considered as the sum of the heat transfer through the blind plus the infiltration. Here it is proposed the worst case scenario, where no return airflow is considered towards the room and all its energy is transmitted through the glazing, and blind's thermal conductance is the previously obtained value of $\lambda_{blind} = 1,86\frac{W}{m^2K}$.

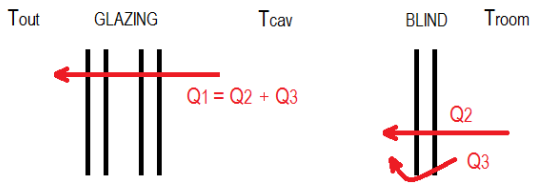

Figure 9.10. Heat flux - ventilated cavity

Thermal resistance of the blind can be calculated as:

$$\frac{1}{h_{blind}} = \frac{1}{h_{conv}} + \frac{d_{blind}}{\lambda_{blind}} + \frac{1}{h_{conv}} = \frac{1}{8} + \frac{0{,}00055}{1{,}86} + \frac{1}{8} = 0,2503\frac{m^2K}{W}$$

and heat transfer through the blind is:

$$Q_2 = h_{blind}A_{win}(T_{cav} - T_{out}) = 3,99 \cdot 4,26 \cdot (27-25) = 34,06W$$

Then heat transfer due to infiltration from room to the cavity Q_3 is:

$$Q_3 = Q_1 - Q_2 = 67,57 - 34,06 = 33,51W$$

Knowing this value it is possible to estimate a volume flow from the following equation:

$$Q_3 = \rho_{air}q_{air}c_{p_{air}}\Delta T$$

where,

$$q_{air} = \frac{Q_3}{\rho_{air}c_{p_{air}}\Delta T} = \frac{33{,}51}{1{,}189 \cdot 1008(27-25)} = 0,014\frac{m^3}{s}$$

From assumed opening area between cavity and room, $A_{ve} = 0,0875m^2$, air velocity in the cavity is obtained. The value is implemented in the model, assuming constant velocity in the cavity, and temperature results for the air in the cavity and blind's surface are shown on figures 9.11 and 9.12.

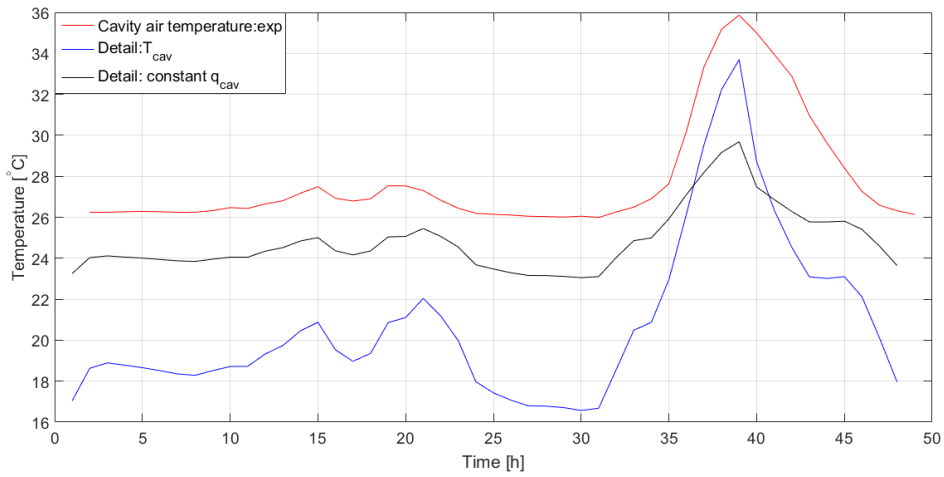

Figure 9.11. Air volume flow between cavity and room influence, over cavity air temperature

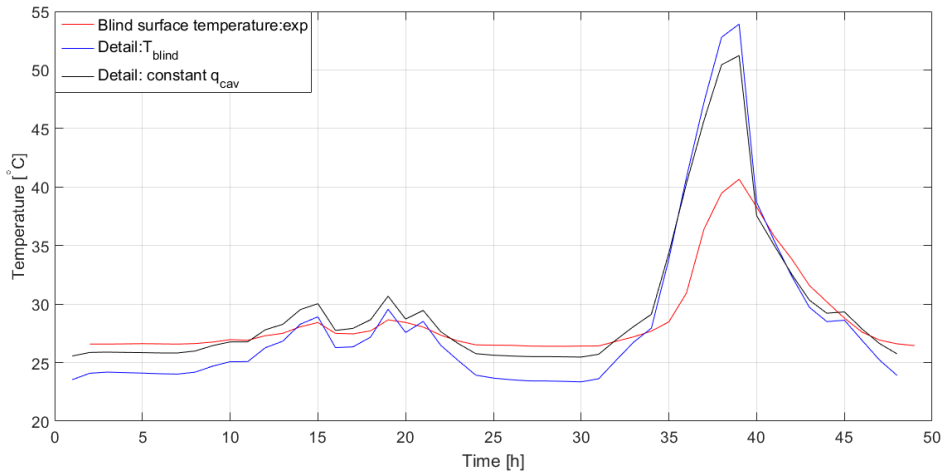

Figure 9.12. Air volume flow between cavity and room influence, over blind surface temperature

Energy consumption is not shown since there was no relevant result. Most significant variation is in air cavity temperature, where during the night time and overcast day calculated temperature is close to experiment, due to incoming warm air from the room. However during the day temperature increase is small. This can be related to the fact that blind's surface temperature reaches very high values, compared to measurements, and does not release the energy to its surroundings. This phenomena is related to its convective heat transfer coefficient.

Convective heat transfer coefficient from blind to air in the model is in the range of 3 $\frac{W}{m^2K}$.

In figure 9.13 is shown blind's surface temperature variation when considering convective heat transfer from blind to air of 7 $\frac{W}{m^2K}$, and keeping constant air velocity from cavity to room of $0,16\frac{m}{s}$.

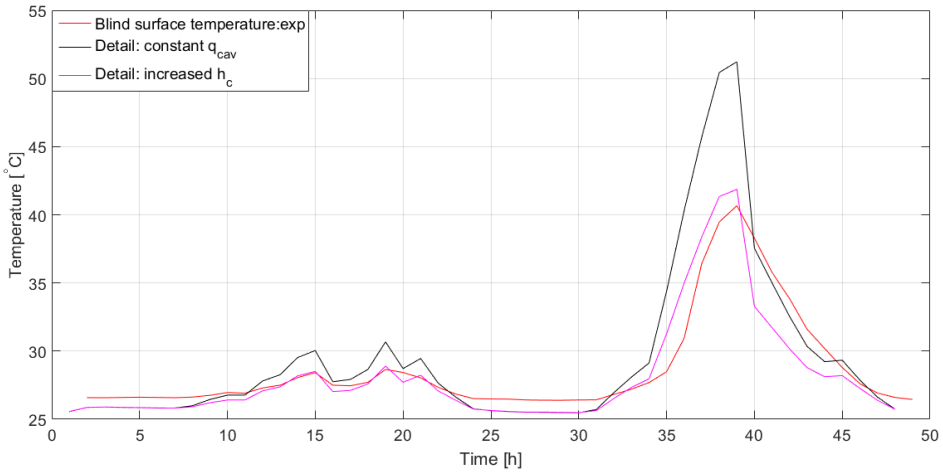

Figure 9.13. Blind's convective heat transfer coefficient influence over blind surface temperature

This higher heat release from surface to air does not cause a temperature increase in the cavity. One reason can be low thermal mass of the blind where little amount of energy is stored, and once it is realised by increasing convective heat transfer coefficient it has no effect over air temperatures in the room and the cavity. However this change influences energy consumption resulting in even higher cooling underestimation as seen in figure 9.14.

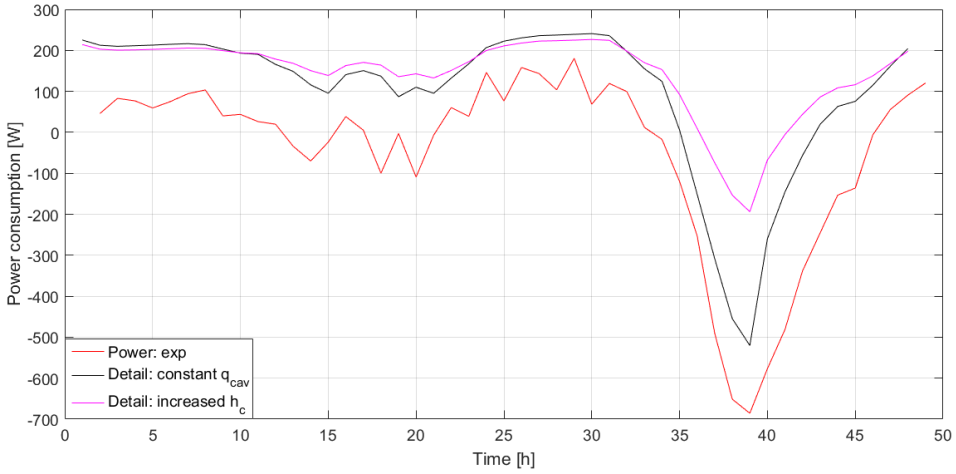

Figure 9.14. Blind's convective heat transfer coefficient influence over energy consumption

This means that blind's surface temperature exchanges more energy through radiation than convection. Figure 9.15 shows the radiative energy transfer for both cases where convective coefficient is varied. When the convective transfer is increased temperature of

the blind decreases without influencing air temperatures in the surroundings. However this blind's surface temperature drop, leads to a decrease of the radiative energy transfer towards the room, influencing this way the energy consumption.

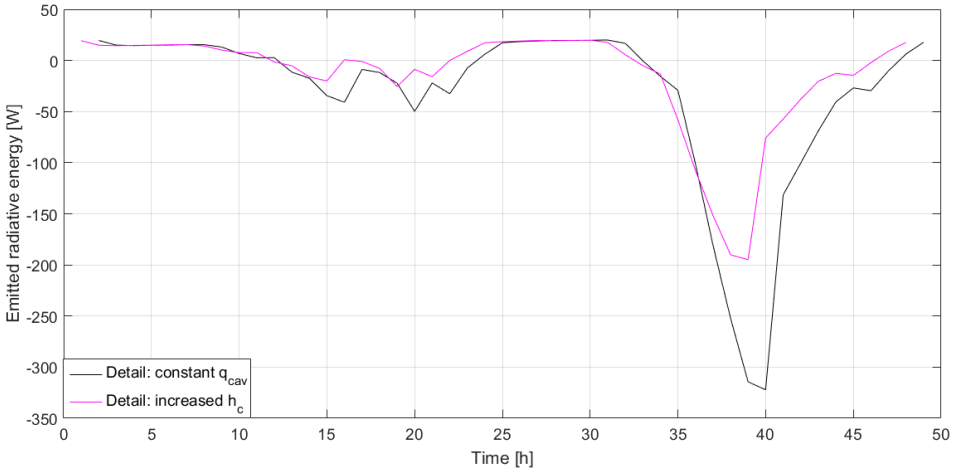

Figure 9.15. Blind's convective heat transfer coefficient influence over emitted radiative energy from blind to internal surface

9.4 Sum up

After performing this sensitivity analysis over some of the most influencing parameters of the model, their influence is analysed and in some way it is justified for some of the weak points or weird behaviour in the model or differences between the experiment. Uncontrolled losses are possible to be measured today and simulated accurately. However, there is bigger uncertainty related to the cavity and blind. Air velocity in the cavity needs very detailed treatment in order to analyse different infiltrations towards the room. Convective heat transfer coefficient of the blind also needs special definition as it does not have same properties as homogeneous surfaces.

Part IV

Recapitulation

Discussion 10

This project develops two energy simulation models of a room with glazed façade and internal shading device. Models calculate in an hourly based period, heating and cooling energy consumption besides temperatures in surfaces and air, allowing an evaluation of thermal comfort. Two mentioned approaches have been chosen based on the literature review performed at the beginning of the study.

First approach called SHGC-based model, considers the total heat transfer coefficient including blind properties. Second approach called detail model, includes the shading device by treating the system with the glazing as a triple glazed window where the angular properties of the blind are assigned. Additionally, the cavity is treated as a ventilated space and the air movement is performed.

First concern for models development is solar gains definition in the system. SHGC-based model have the gains assigned to the air of the room and the cavity. These are calculated considering angular dependency of the glazing and blind. Detail model assigns the gains in the surfaces of the façade. The results of the power consumption show the good agreement with experimental data for both approaches. However, there is a deviation of the results suggesting higher heat losses in the models. From the sensitivity analysis, where some uncontrolled cooling parameters are analysed, the reason for obtained shifted values has not been found. Long-wave losses towards the sky which are not included in the sensitivity analysis do not seem to be the reason for this problem. From obtained results, for the overcast day, the deviation is similar as for a clear day. Additionally, from the results of the grid sensitivity analysis of the glazing itself, similar deviation can be seen. This way for the models with implemented blind, its surface temperature does not have any influence over the problem with deviated power consumption.

There is also a problem when considering the gains in the surfaces. On one hand it leads to an overestimation of solar heat gains. From glazing model analysis is assumed only 25 % of the thermal mass of each pane, and also for the detail model solar gains inside the room are neglected. On the other hand the way solar gains are considered depends on the type of shading used in terms of its reflective properties. As observed in the validation part where the reflectivity of the blind is varied, the higher is the reflectivity the higher is the underestimation of the energy cooling consumption.

Regarding thermal comfort, SHGC-model cannot be used to calculate local thermal

discomfort since it does not simulate blind's surface temperature. Only detail model simulates it and that is one of the reasons why this model is considered for the sensitivity analysis. Although there is an overestimation of the temperatures in the model, its reason is examined in the sensitivity analysis. As a result, infiltration between cavity and room, and convective heat transfer coefficient of the blind are some of the influencing parameters over the temperature calculations. Cavity air temperature during the night time is close to room air temperature so it indicates that both zones are more connected than in the model, suggesting a higher air infiltration rate in between them. As well simulated blind temperature is much more higher than the measured one. This suggests a higher convective heat transfer coefficient from the blind surface to the surroundings and it is considered as a realistic conclusion due to the porous structure of the blind.

When blind's surface temperature is decreased, cooling energy consumption in the simulation is lower. This is due to fact that emitted radiative energy from the blind towards the inside of the room is decreased. This leads to consideration of additional gains in the model and invalidation of the assumptions done about the reduction of the thermal mass of the glazing and omission of the internal heat gains in the room.

So far, simulation results are validated with measurements, but those also should be questioned. Measured temperatures in the surfaces might give some inaccuracies due to the experimental setup. Moreover, the PI controller of the Cube has not been tuned for this specific setup and the used values are similar to the ones from the previous works in the facility. The controller response is affecting the power consumption for the used heating system. Therefore, the difference in the results obtained from the experiment and the simulation might be also related to that.

Regarding the problems with the developed models it has been noticed that there is no significant difference in the results when varying the thermal mass of the room. Generally, that would influence the time response of the system therefore it should be implemented in a different way. The two models are developed for the specific size of the cavity, however the followed approach might not be valid for different geometries.

Finally, the direct and diffuse radiation used for the simulation is calculated according to empirical model from measured values of global radiation. Used values differ from the measured ones and that affects the simulation results.

Conclusion 11

This project develops a simplified calculation method for the room having double glazed window with internal shading devices.

Currently, there is need for the reduction of energy consumption in the buildings therefore the development of accurate models which can predict it from the design phase is crucial. Internal shading devices are commonly used solution in everyday life for the energy reduction and thermal comfort improvement. From the literature review it has been noticed that the current models are not accurate enough and more work needs to be done in this area.

Developed models in this thesis are based on the nodal approach where two different paths are followed. First approach called SHGC-based model, considers the total heat transfer coefficient including blind properties. Second approach called detail model, includes the shading device by treating the system with the glazing as a triple glazed window where the angular properties of the blind are assigned. Additionally, the cavity is treated as a ventilated space and the air movement is performed.

Both models require weather data conditions, material properties and room geometry definition as inputs. They need also to define the values for the solar-optical properties of the window and blind at normal incidence angle. SHGC-based model uses the g-value of the glazing while detail model requires the properties of the individual panes.

As a result, the outputs of the models are the heating and cooling energy consumption and room air temperature. Additionally, detail model provides the surface's temperature for the glazing and the blind allowing the evaluation of local thermal discomfort.

Both models calculate properly the energy consumption, however detail model requires more precise definition for the temperature calculations. By having more complex definition, detail model is not necessarily more accurate due to more possible uncertainties and errors.

The two models consider the air in the cavity as a different thermal zone from the air in the room. From the simulations it is seen that this approach is appropriate and the cavity and blind need to be treated more in detail.

Further work

From the results obtained in this work, further investigation related to solar heat gains consideration and cavity treatment can be suggested.

In this project gains are considered in two different ways for each of the models. Development of simulation models considering a combination between both of them can provide better outcomes.

Bibliography

[1] D. H. Meadows, D. L. Meadows, J. Randers, W. W. Behrens III, The Limits to Growth, Universe Books, 1972

[2] http://www.unep.org/sbci/AboutSBCI/Background.asp

[3] A. Kirimtat, B. K. Koyunbaba, I. Chatzikonstantinou, S. Sariyildiz, Review of simulation modeling for shading devices in buildings, 2015

[4] J. Hedegaard, T.D. Iversen, Performance Investigation of Glazing Systems in Combination with Internal Solar Shading, Master thesis project, Aalborg Univesity, 2015

[5] EN13363-1:2003 Solar protection devices combined with glazing - Calculation of solar and light transmittance - Part 1: Simplified method, 2007

[6] ISO 15099 Thermal performance of windows, doors and shading devices - Detailed calculation, 2003

[7] Y. Chan, A. Tzempelikos, B. Protzman, Solar optical properties of roller shades: Modeling approaches, measured results and impact on energy use and visual comfort, 3^{rd} International High Performance Building Conference at Purdue, July 14-17, 2014

[8] N.A. Kotey, J.L.Wright, M.R. Collins, Determining off-normal solar optical properties of roller blinds, ASHRAE 2009

[9] M. Bessoudo, A. Tzempelikos, A.K. Athienitis, R. Zmeureanu, Indoor thermal environmental conditions near glazed facades with shading devices - Part I: Experiments and building thermal model, 2010

[10] M. Bessoudo, A. Tzempelikos, A.K. Athienitis, R. Zmeureanu, Indoor thermal environmental conditions near glazed facades with shading devices - Part II: Thermal comfort simulation and impact of glazing and shading properties, 2010

[11] F. Frontinia, T. E. Kuhn, The influence of various internal blinds on thermal comfort: A new method for calculating the mean radiant temperature in office spaces, 2013

[12] A. R. Othman, A. A. M. Khalid, Comparative Performance of Internal Venetian Blind and Roller Blind with Respects to Indoor Illumination Levels, Malaysia, April 2013

[13] A. Tzempelikos, H. Shen, Comparative control strategies for roller shades with respect to daylight and energy performance, Building and Environment 67, 179-192, 2013

[14] I. Konstantzos, A. Tzempelikos, Y.-C. Chan, Experimental and simulation analysis of daylight glare probability in offices with dynamic window shades, USA, 2014

[15] Y. Ye, P. Xu, J. Mao, Y. Ji, Experimental study on the effectiveness of internal shading devices, China, 2016

[16] M. Liu, K.B. Wittchen,P. K. Heiselberg, F.V. Winther, Development and sensitivity study of a simplified and dynamic method for double glazing façade and verified by a ful-scale façade element, Energy and Buildings 68 (2014) 432-443

[17] DS/EN ISO 13790 Energy performance of buildings - Calculation of energy use for space heating and cooling, 2008

[18] DIN 18599 Energy efficiency of buildings - Calculation of the energy needs, delivered energy and primary energy for heating, cooling, ventilation, domestic hot water and lighting - Part 2: Energy needs for heating and coling of building zones, 2005

[19] Matlab Software

[20] D.R. Pitts, L.E. Sissom, Schaum's outline of theory and problems of Heat transfer-second edition.

[21] EN673 Glass in building - Determination of thermal transmittance (U-value)-Calculation method, 2002

[22] T.E. Khun, C. Buhler, W.J. Platzer, Evaluation of overheating protection with sun-shading systems, Germany, 2001

[23] EN410 Glass in building - Determination of luminous and solar characteristics of glazing, 1998

[24] O. Kalyanova, P. Heiselberg, Experimental Set-up and Full-scale measurements in 'The Cube', DCE, Technical Reports, nr. 034, Aalborg University, Department of Civil Engineering, Aalborg, 2008.

[25] National Instruments - modular hardware platform and system design software

[26] J. Karlsson, A. Roos, Modelling th Angular behaviour of the total solar energy transmittance of windows, Solar Energy Vol. 69, No. 4, pp.321-329, 2000

[27] M.C Singh, S.N. Garg, An empirical model for angle-dependent g-value of glazing, Energy and Buildings 42 (2010) 375-379

[28] J.A. Clarke, Energy simulation in building design, 2nd Edition, Great Britain, 2001

[29] T. E. Khun, Solar control: A general evaluation method for façades with venetian blinds or other solar control systems, Energy and Buildings 38 (2006) 648-660

[30] DB-HE Documento Basico, Ahorro de Energia - Codigo Tecnico de la Edificacion (CTE)

[31] $http://www.dmi.dk$

[32] Cambridge University press

[33] Lecture notes: "Radiation and convection in buildings", Jerome Le Dreau, 2015

[34] J. A. Duffie, W. A. Beckman, Solar Engineering of Thermal Processes, 4th Edition, 2013

[35] $https://en.wikipedia.org/wiki/Sunlight$

[36] N. Artmann, R. Vonbank, R. L. Jensen, Temperature measurements using type K thermocouples and the Fluke Helios Plus 2287 A data logger, October 2008

[37] Jerome thesis

[38] $https://spectrum.pilkington.com/Main.aspx?country=DK$

[39] $https://www.sunscreen-mermet.com$

[40] Window software

[41] H. Lund, Calculation of diffuse solar radiation, 2007-2008

Heat transfer A

Conduction

Conduction is the movement of heat from particle to particle through a substance. Hot particles move faster than cold particles. They collide with their cooler neighbours and pass on energy. [32] Conduction is described by the first Fourier's law and it is represented by following equation.

$$q = -\lambda A \frac{\partial T}{\partial n} \tag{A.1}$$

Where:

$\frac{\partial T}{\partial n}$	temperature gradient in the direction normal to the area A
λ	thermal conductivity of the material, $[\frac{\mathrm{W}}{\mathrm{mK}}]$

The minus sign in front of the right hand side is required by the second law of thermodynamics, stating that the thermal energy transfer resulting from a thermal gradient must be from a warmer to a colder region.

Convection

Convection is defined as heat transfer by fluids in motion. A temperature difference between the surface and the fluid is required. Convection may be classified by the driving force of the fluid motion[33]

- Forced convection: fluid motion is driven by an external force, i.e. a fan
- Natural (or free) convection: fluid motion is driven by buoyancy forces
- Mixed convection: a combination of the above

Convection may also be classified by the physical nature of the fluid motion:

- Laminar flow
- Transient flow
- Turbulent flow (most of the time in buildings)

Relationship for heat transfer by convection can be described by second Newton's law for cooling, which follows the equation.

$$Q_c = h_c A(T_a - T_b) \tag{A.2}$$

Where:

h_c	convective heat transfer coefficient, $[\frac{\mathrm{W}}{\mathrm{m^2K}}]$
A	surface area, $[\mathrm{m}^2]$
T_a	temperature of the solid surface, [K]
T_b	temperature of the gas, [K]

The convective heat transfer between a surface and the air is depending on many variables, as surface properties, nature of the flow of the air or temperature. It can be calculated [28], for natural or forced convection.

- Natural convection at internal surface

$$h_c = ([a(\frac{\Delta\theta}{d})^p]^m + [b(\Delta\theta)^q]^m)^{\frac{1}{m}} \tag{A.3}$$

Where:

a, b, p, q and m	empirical coefficients, [−]
A	surface area, $[\mathrm{m}^2]$
$\Delta\theta$	surface-to-air temperature difference, [K]
d	surface height, [m]

- Forced convection at external surface

$$h_c = 5,678[a + b(\frac{V}{0.3048})^n] \tag{A.4}$$

Where:

a, b and n	empirical coefficients depending on the flow velocity, [−]
V	parallel component of the flow velocity, $[\frac{\mathrm{m}}{\mathrm{s}}]$

V is obtained experimentally for a reference temperature of 21,1 °C. An adjustment for the velocity is needed so instead of V: $\frac{294.26V}{273.16+\theta_n}$; where θ_n is the non-reference temperature, [°C]

Additionally is given an approximation between the local velocity in the surface and the free stream velocity:

- Surface on the windward side:

  for $V_f > 2\frac{m}{s}$; $V = 0,25V_f$

  for $V_f < 2\frac{m}{s}$; $V = 0,5$
- Surface on the leeward side:

  $V = 0,3 + 0,05V_f$

Radiation

Electromagnetic waves are capable to carry energy from one location to another, even in vacuum (broadcast radio, microwaves, X-rays, cosmic rays, light,...). Thermal radiation is the electromagnetic phenomenon where radiation is emitted by a material substance solely due to its temperature. The rate of heat transfer depends on the surface temperature and properties. [33]

A blackbody represents a perfect absorber of radiation regardless of its wavelength and also an ideal emitter of thermal radiation. [34] All other surfaces emit less and the thermal emission from grey bodies can be well represented by equation following Stefan-Boltzmann's law.

$$q = \epsilon \sigma_s A T^4 \tag{A.5}$$

Where:

ϵ	emissivity of the body, [−]
σ_s	Stefan-Boltzmann constant, $5{,}67 \cdot 10^{-8}$ $[\frac{\mathrm{W}}{\mathrm{m^2K^4}}]$
T	temperature of the body, [K]

Solar radiation B

The sun has a primary influence over the climate and more specifically over building energy and thermal performance. Therefore it is imperative to describe it.

Radiation description

The total solar radiation outside our atmosphere has a value of 1367 W/m^2 and at zenith on the Earth's surface is nearly 1120 W/m^2, from which direct solar radiation is almost 1050 W/m^2.These values are presented for ideal condition case. As well the solar radiation is divided in two wavelength ranges as the shortwave and longwave radiation. In the first range there are included radiation types (x-ray and gamma), UV and visible light spectrum and for the second one are the infrared, microwave and radio wavelengths. A representation of solar radiation spectrum is done in figure B.1.

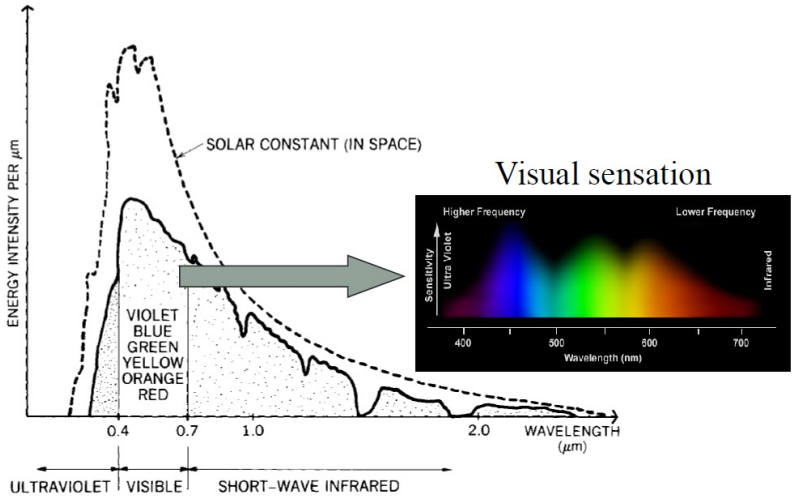

Figure B.1. Solar radiation intensity

The main radiation that has the property to be transmitted through glass is shortwave radiation. Ultraviolet wavelengths on the other hand, are mainly filtered and absorbed by the material. Longwave radiation can interact as a radiation between any surfaces for indoors or outdoors by having a temperature difference. It can be the case for the radiation between walls or the ground radiation towards sky or buildings. [34] [35]

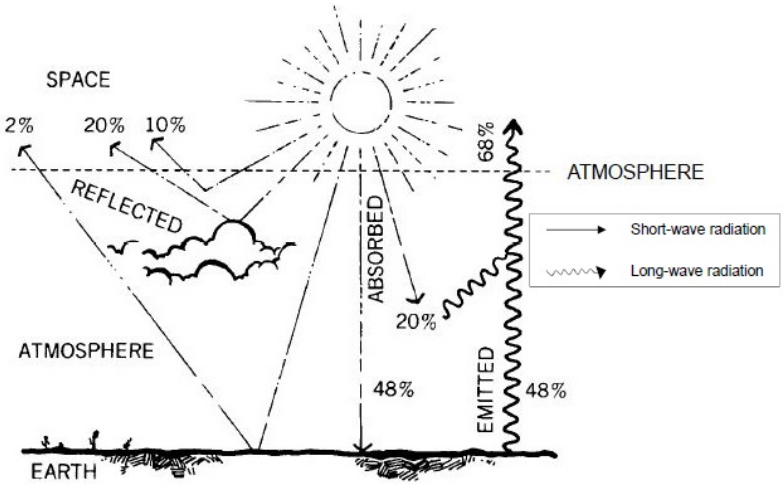

Figure B.2. Sun influence over atmosphere and Earth surfaces with long-wave and short-wave radiation

The radiation coming from the sun can be categorized such as:

- Direct solar radiation, which is also called 'beam radiation' describes the solar radiation that follows a straight line from the sun down to the earth's surface.

- Diffuse solar radiation is defined as the solar radiation that is scattered in every direction by the atmosphere or by particles and molecules. It can be also called sky or solar sky radiation.

- Total solar radiation is characterized as the combination of the direct and diffuse solar radiation. Depending on the weather conditions and the cloud coverage the percentage between

Sun path

Sun path refers to the hourly trajectory change of the sun caused by earth's axis rotation and also by orbiting around the sun. By having accurate knowledge about the position of the sun in the sky can influence greatly the design of buildings and its solar systems or equipments. This position is represented by the altitude and the azimuth angle as shown in figure B.3 on the following page.

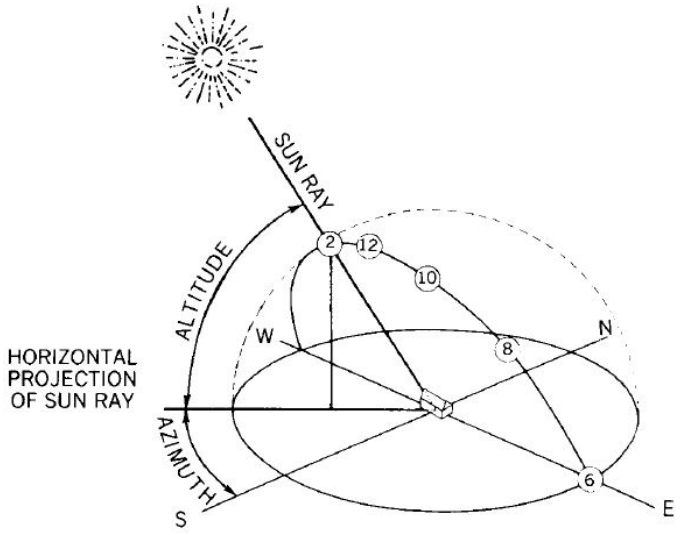

Figure B.3. Sun ray's azimuth and altitude angle

It is possible to generate a sun chart diagram that is displaying the position of the sun in the sky with the solar altitude and azimuth angle. Figure B.4 shows a sun chart diagram in the Cartesian coordinates for the position 57.01° latitude N and 10° longitude E.

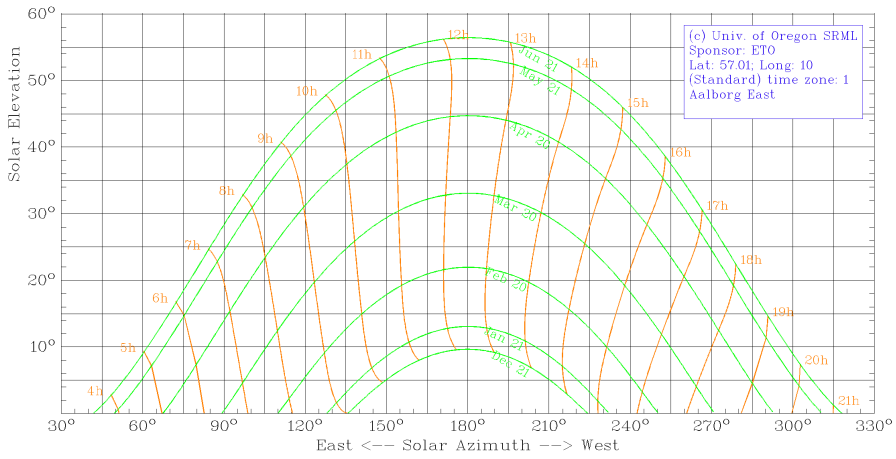

Figure B.4. Sun position reported to azimuth and altitude angle in Cartesian coordinates

The solar azimuth and altitude angles, that describes the position of the sun in a point, are also used in a set of relationships to calculate the angle of incidence. This term is defined as the angle between the direct solar radiation on a surface and the normal to that surface. If the angle of incidence is closer to 0° it means that the direct solar radiation is hitting nearly perpendicular on the analysed surface (window + blinds). A representation for the angle of incidence can be seen in figure B.5 on the facing page. [34]

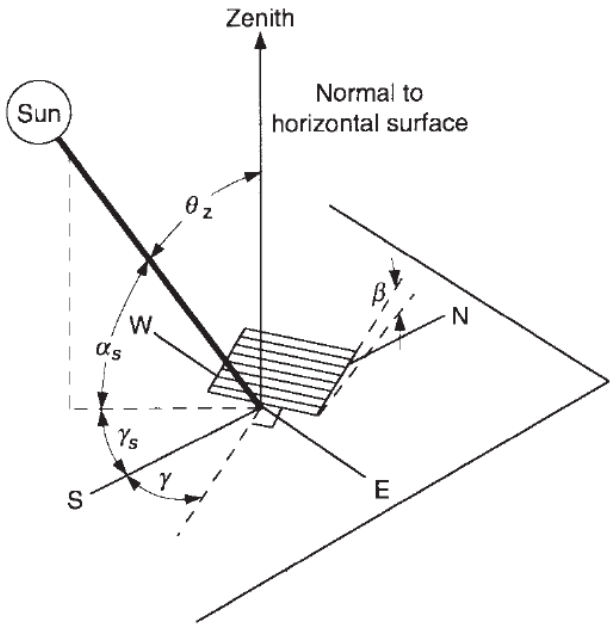

Figure B.5. Incidence angle

The angle of incidence calculation for vertical surfaces is calculated with the formula B.1.[34]

$$\cos(\theta_i) = \cos(\alpha_z) \cdot \cos(\beta) + \sin(\alpha_z) \cdot \sin(\beta) \cdot \cos(\gamma_{sun} - \gamma_{surf}) \tag{B.1}$$

Where:

θ_i	Angle of incidence [°]
α_z	Altitude angle of the sun [°]
β	Slope of the surface [°]
γ_{sun}	Azimuth angle of the sun [°]
γ_{surf}	Azimuth angle of the surface [°]

According to previous formula an analysis of incident angles is done, over different vertical surfaces orientations. Surfaces' position corresponds to Cube's location. Figure B.6 shows a cumulative distribution for the angles of incidence, only considering angles between zero and 90 degrees and day time hours. Higher angles correspond to incident radiation behind the surface. Day time hours have been selected according to information provided by the Danish Building Research Institute in DRY-file 2013.

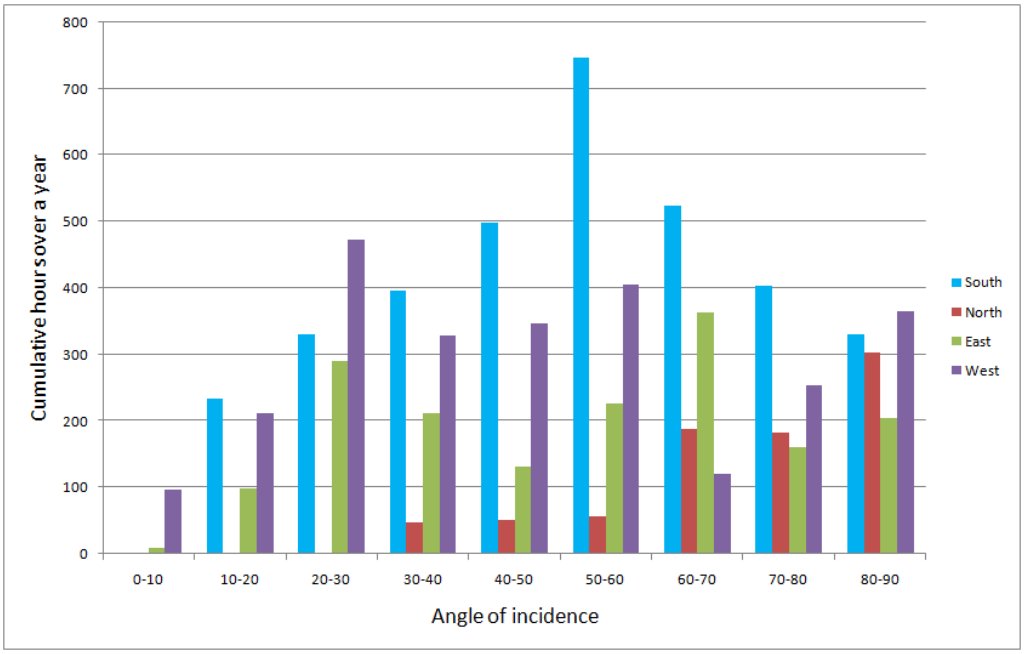

Figure B.6. Incidence angle

It can be seen how the southern façade is having the biggest amount of hours with incident radiation which maximum reaches the façade at incident angle 50 to 60°.

Calibration + Measuring equipment

C

Thermocouples

The temperature measurements are done with a series of type K thermocouples. This is formed of two different nickel alloys as Alumel, that gives the negative thermoelectric potential, and Chromel, which provides the positive one. They have a sensitivity of approx. 41 μV/K. A voltage is generated as there is a temperature gradient between two measuring points, thus the thermocouples do not measure the absolute temperature. Between the voltage and the temperature is a polynomial equation, which transforms the electrical output into heat measurements. Thermocouples measure just the temperature difference, so it has to be connected to an Ice Point Reference device [36].

Calibration of the thermocouples

In order for the temperature measurements to be accurate, a calibration of the thermocouples is indispensable. Three thick type K thermocouples are chosen as reference. The calibration process is illustrated on figure C.1 on the following page. The three thermocouples are connected with the cold end to the Ice Point Reference in order to get the reference junction at 0 °C. The hot end of the thermocouples are placed in the Isocal equipment, where there is a temperature change in six steps from 40 °C to 10 °C. The device is reaching steady state condition for each step and a precision thermometer is also placed in the Isocal and is measuring the actual temperature in all the steps. A computer is connected through Helios.vi Labview script to Isocal, precision thermometer and Helios data logger equipment. Helios is connected to the Ice point reference through copper wires. The script registers the voltage of thermocouples and then it converts it to a formula capable of calculating the temperatures at the hot ends. Figure C.1 on the next page shows the coupling of the equipment used for calibration of the three reference thermocouples.

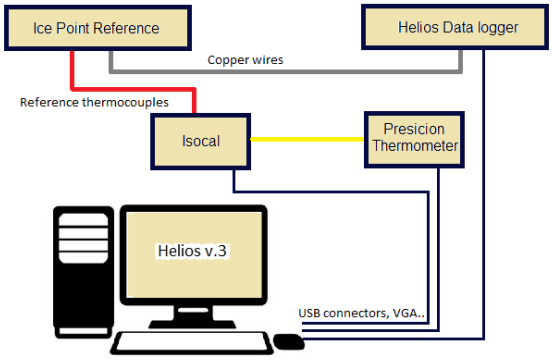

Figure C.1. Calibration scheme for reference thermocouples

The reference thermocouples are placed in a compensation box. The other thermocouples are connected through copper wires to the data logger and now the temperature difference is between the compensation box and the measuring point. The box is insulated to be shielded from disturbances of the ambient conditions. Then the thermocouples are calibrated with the same devices as before and shown on figure C.2.

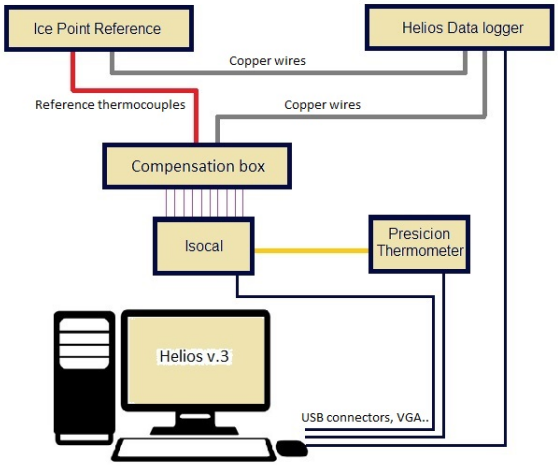

Figure C.2. Calibration scheme for thermocouples

The resulted equations from the calibration will be further used in the experimental measurements. The equation is the type with a second degree unknown. The calibration formulas can be found in appendix /vref.

$f = ax^2 + bx + c$

Solar radiation

Solar radiation measurements are crucial in order to complete the weather data as the boundary conditions. The solar radiation is calculated by a surface per unit area. There are used a series devices for irradiance measurements as pyranometers. They are placed on different locations of the Cube in order to get the most accurate data.

On the roof, there is placed horizontally a CMP21 pyranomenter which measures the global solar radiation as there is no influence from the ground reflected radiation. Another device of CMP type is used on the vertical surface on the South facade of the building. In order to evaluate the performance of the glazing system the last pyranometer is placed centrally in the gap between the window and the shading.

Figure C.3. Pyranometers: CMP21 on the roof, CMP21 on the South façade and CMP22 inside the room

All pyranometers are connected directly to the Helios Data logger in order to collect the irradiance data. Also, the calibration files were previously calculated for the equipment and they were included from the [37] thesis work.

Pressure transducers

The differential pressure transducers are used in order to ensure that the test zone is sealed tight from the guarding zone of the Cube. Also another pressure transducer is used for the fan between the test and the adjoining room, from which we can get the air flow going into the room. The pressure transducer is shown on figure C.4 and its range is $0 - 100$Pa.

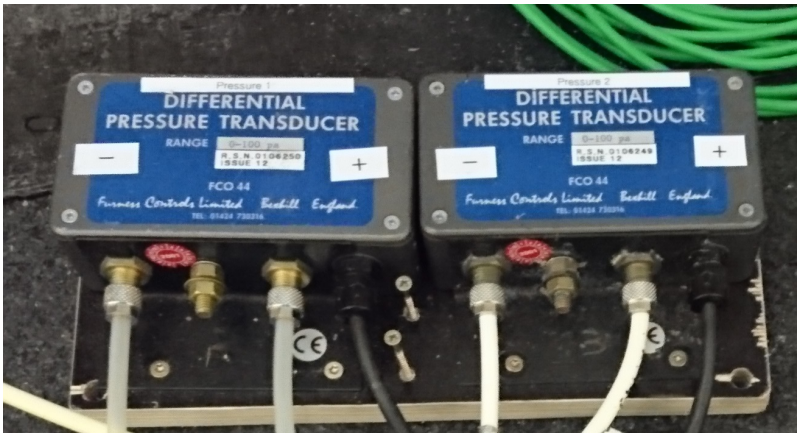

Figure C.4. Differential pressure transducer

Calibration of the differential pressure transducer

In order to calibrate the pressure transducers the scheme in figure C.5 has to be followed accordingly. The Debro micromanometer is connected through rubber tubes to pressure transducer to one end and for the other one there is a device that introduces pressure or

creates vacuum in the pipes. As well the pressure transducer is connected to the Helios data logger in order to get a voltage.

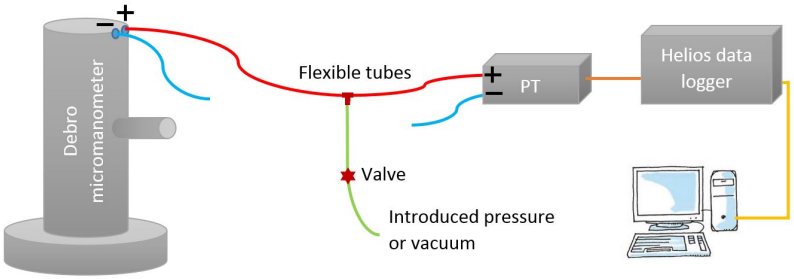

Figure C.5. Pressure transducer calibration scheme

From different measurements, a linear curve is obtained and calibration formula is found from the graph. Figures C.6 and C.7 represents the resultant curves with the calibration equations.

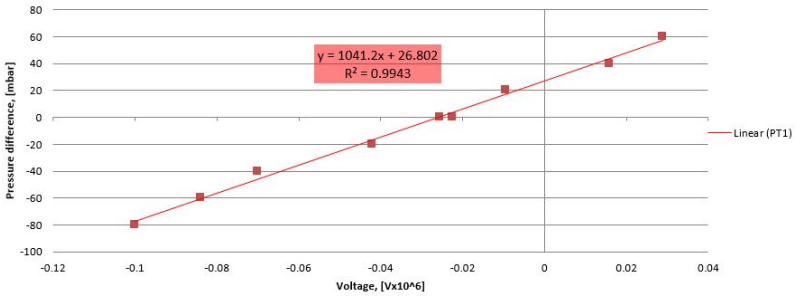

Figure C.6. Pressure transducer 1 curve

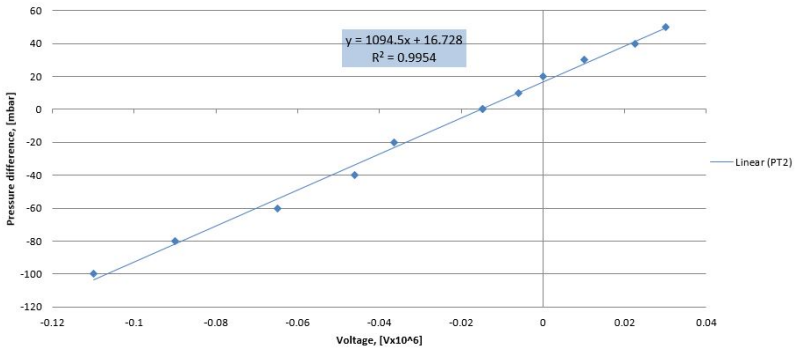

Figure C.7. Pressure transducer 2 curve

Window properties and shading data sheets D

This appendix presents the data sheets with the detailed properties for the window and for the shadings.

1. Data sheet for double glazed window from Pilkinton Spectrum On-line calculation program [38]
2. Data sheet for two different types of shading (White Pearl and Charcoal Grey) [39]

PILKINGTON
NSG Group Flat Glass Business

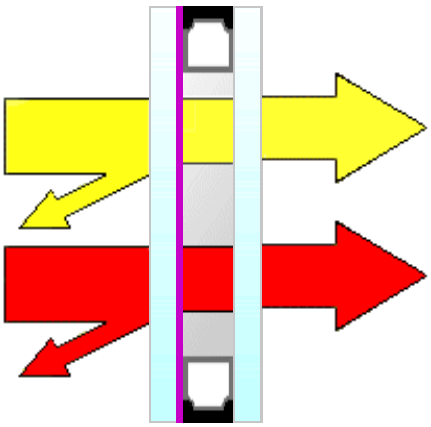

Description

Position	Product	Process	Thickness (nominal) mm	Weight kg/m^2
Glass 1	Pilkington Suncool 66/33	Annealed	6	15
Cavity 1	Argon (90%)		12	
Glass 2	Pilkington Optifloat Clear	Annealed	6	15
Product Code	6C(66)-12Ar-6		24	30

Performance

Light		
Transmittance	LT	65%
	UV %	11%
Reflectance Out	LR out	16%
Reflectance In	LR in	18%

Energy		
Direct Transmittance	ET	32%
Reflectance	ER	35%
Absorptance	EA	33%
Total Transmittance	g	36%
Shading Coefficient Total		0.41
Shading Coefficient Shortwave		0.37

Sound Reduction	R_w dB (C;C_{tr})	31 (-1; -4)
Thermal Transmittance	W/m^{2}K	1.2

Ra	93

Performance Code	
U-value/Light/Energy	1.2 / 65 / 36

The values of some of characteristics are displayed as NPD. This stands for No Performance Determined.

Pilkington Spectrum allows you to combine a wide range of products available from Pilkington and determine their key properties such as light transmittance, g value and U value. The program includes restrictions that prevent some combinations being selected that may be considered unwise or impractical. Even with these restrictions, it is still possible to create product combinations that may not be available from your supplier. Please check with your supplier that your chosen product combination is possible, available in the sizes required and in a timescale appropriate to your project. Furthermore, it is essential that you check that your product combination is appropriate for satisfying local, regional, national and other project-specific requirements.

Calculations are made according to EN standards 410 and 673/12898

Pilkington Spectrum Version 4.0.0 08/02/2016

MERMET E-screen. Internal blinds for solar protection

4 comfort factors to choose the right fabric for the function and colour required and ensure the success of your solar protection.

Level of incoming natural light:
For the same type of fabric, light colours let through more light than dark colours.

Glare control:
For the same type of fabric, dark colours provide better glare control than light.

Protection against the heat gain from sunlight:
External applications provide a more effective heat protection. For a better protection, dark colours should be used externally and light colours internally.

Quality of outward visibility:
The quality of the outside view is not only created by the fabric openness factor but also its light transmission which varies with colours. Darker colours will provide better outward visibility.

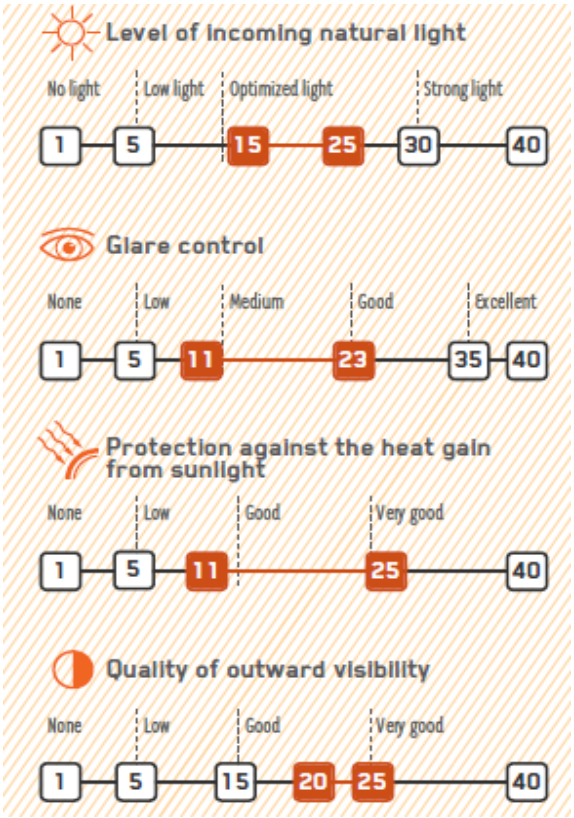

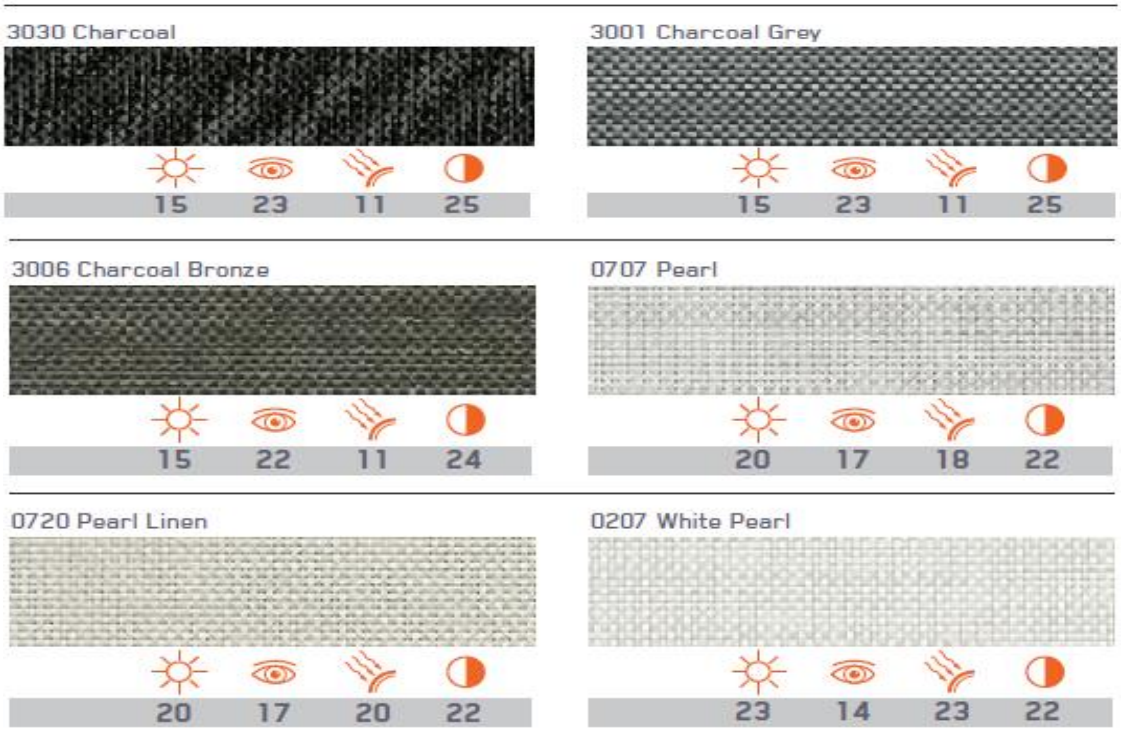

The technical data

E-Screen 7505

COMPOSITION	**36% Fibreglass / 64% PVC**		
FIRE, SMOKE CLASSIFICATION AND OTHER OFFICIAL TEST REPORTS	**M1 (F)** **F3 (F)** FR, AS, B1 (CN), C UNO, HHV *		NFP 92 503 NF F 16-101
HEALTH / SAFETY	**No chemicals harmful to health and safety of users** **Guarantee of indoor air quality (VOC)**		Oeko-tex Standard 100 class IV Greenguard®
OPENNESS FACTOR	**5%**		
UV SCREEN	**Up to 94%**		
WIDTHS	**200 - 250 - 310 cm / 89 - 127 mm**		
WEAVE	**Basket weave 2 x 2**		
YARN COUNT Warp: Weft:	 **22 yarns/cm ± 5%** **17 yarns/cm ± 5%**		 ISO 7211/2
WEIGHT/m²	**385 g ± 5%**		ISO 2286 - 2
THICKNESS	**0,47 mm ± 5%**		ISO 2286 - 3
MECHANICAL RESISTANCE Warp: Weft:	BREAKING **> 190 daN/5cm** **> 150 daN/5cm** ISO 1421	TEAR **≥ 5 daN** **≥ 4 daN** EN 1875-3	FOLDING **≥ 20 daN/5cm** **≥ 20 daN/5cm** ISO 1421**
ELONGATION Warp and Weft:	 **< 5%**		 ISO 1421
COLOUR FASTNESS TO LIGHT (Scale of 8)	**7/8** **White not graded**		ISO 105 B02

The data in this document is for information only and may not be considered as binding
* Reports available on request, please contact Mermet
** Internal procedure derived from ISO 1421 standard

The main thermal and optical factors

The regulations value the gtot factor for thermal comfort and Tv for visual comfort.

→Thermal factors

Ts Solar transmittance: proportion of solar energy transmitted through the fabric. A low percentage means the fabric performs well at reducing solar energy.

Rs Solar reflectance: proportion of solar radiation reflected by the fabric. A high percentage means the fabric performs well at reflecting solar energy.

As Solar absorptance: proportion of solar radiation absorbed by the fabric. A low percentage means the fabric absorbs little solar energy.
Solar radiation is always partially transmitted through, absorbed or reflected by the fabric. The sum of all 3 equals 100.
Ts + Rs + As = 100% of solar energy.

gtot Total solar factor: solar energy which actually penetrates into a room through the blind and glazing. A low value means good thermal performance.

→Optical factors

OF Openness Factor: relative area of the openings in the fabric (hole). It is considered as independent of the colour. For fabrics with the same weave, it should be measured using the darkest colour in the range.

Tv Visible light transmittance: total percentage of light radiated through the fabric over a wavelength of 380 to 780 nm (nanometers), called the visible spectrum (total illumination).

→Optical factors (cont'd)

Rv **Visible light reflectance:** proportion of light reflected by the fabric.

Tdif **Diffuse transmission factor:** correlation of the two factors above: Tdif = Tv – OF.
It is indicated as **Tvndif** for the aspects of glare and shape recognition (outward visibility / night privacy). A low figure shows a better visual comfort.

However, for natural light control, it is indicated as **Tvdifh**. It is used to ascertain a fabric's light diffusion capacity. A high figure means more natural light.

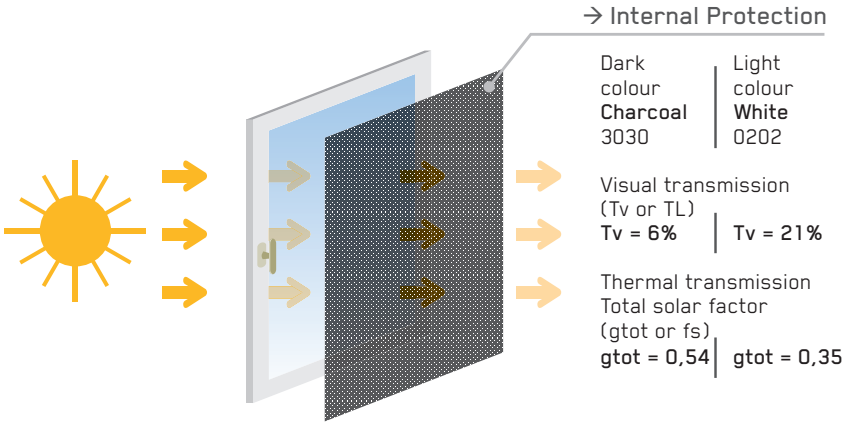

Thermal and optical factors in the European standard EN 14501

E-Screen 7505

Openness Factor OF 5% Colours	Thermal factors					Optical factors			
	Fabric			Fabric + glazing					
	Ts	Rs	As	gv=0,59 gtot internal blind	gv=0,32 gtot internal blind	Tv	Rv	Tvndif	Tvdifh
0202 White	22	67	11	0,35	0,25	21	75	14	17
0220 White Linen	18	62	20	0,37	0,25	16	68	10	13
0207 White Pearl	17	52	31	0,40	0,26	14	56	8	12
2020 Linen	23	51	26	0,40	0,26	19	56	14	16
2022 Linen Stone	20	54	26	0,39	0,26	17	58	11	14
0720 Pearl Linen	17	45	38	0,42	0,27	15	48	8	12
0707 Pearl	18	38	44	0,44	0,27	15	41	9	12
3001 Charcoal Grey	9	11	80	0,52	0,29	8	10	1	6
3006 Charcoal Bronze	8	6	86	0,54	0,30	8	6	1	6
3030 Charcoal	6	6	88	0,54	0,30	6	5	0	5

gv = 0,59: solar factor of standard glazing (C), low-emission 4/16/4 double glazing filled with Argon (U value thermal transmittance = 1,2 W/m²K).
gv = 0,32: solar factor of standard glazing (D), reflecting low-emission 4/16/4 double glazing filled with Argon (U value thermal transmittance = 1,1 W/m²K).

Samples tested according to EN 14500 standard defining the measurements and calculation methods as specified in the standard EN 13363-1 "Solar protection devices combined with glazing calculation of solar and light transmittance – Part 1: simplified method" and EN 410 "Glass in building – Determination of luminous and solar characteristics of glazing".

Data treatment E

As the amount of data from the experimental measurements is substantial, there is the necessity of data refinement for a straightforward use. The processes involved for the data treatment will be presented next. As the information is registered every six seconds, a regular hourly averaging is done for all channels.

There are five thermocouples that measure each of the surfaces' temperatures of the window and blind. For checking the surface temperature only the central ones are used.

Air temperature in the room is measured by thermocouples placed in three different poles, with three thermocouples at different highs each. Air temperature in the room is obtained by using an averaged mean calculated according to

$$T_{air} = \frac{\frac{1}{3}0{,}1(T_1+T_2+T_3)+\frac{1}{3}1{,}1(T_1+T_2+T_3)\frac{1}{3}2{,}1(T_1+T_2+T_3)}{0{,}1+1{,}1+2{,}1}$$

where T_i refers to the temperatures measured in poles 1, 2 and 3 at highs 0,1 m, 1,1 m and 2,1 m. Results from this calculation give a big variation, therefore for the comparison purposes the temperature obtained from the sensor in the PI controller is used.

Air temperature in the gap is calculated in the same way.

Power consumption from the heating is directly measured from the powermeter. Power consumption from the cooling is calculated from the measured values with brunatas, water flow and forward and return water temperatures. This is done according to:

$$Q_{cooling} = q\rho C_p \Delta T$$

Where:

q	is the water flow $[\frac{m^3}{s}]$
ρ	is the water density $[\frac{kg}{m^3}]$
C_p	is the specific heat capacity of the water $[\frac{J}{kgK}]$
ΔT	is the temperature difference in the forward and return water [K]

Solar radiation is measured in the external façade of the building in $\frac{W}{m^2}$ by CMP pyranometers. This measurement is including direct, diffuse and ground reflected radiation. Ground reflected radiation is estimated to be 20% of the global measured

radiation so this amount is discounted from measured values.

Direct and diffuse radiation are calculated according to work done by Hans Lund [41].

Glazing angle dependency equation validation

F

Angle dependency of the glazing is calculated in the SHGC-model according to [27] explained in chapter 7. In order to see if it is possible to use this method, results obtained by using it are compared with the ones obtained by using WINDOW software [40] for three different glazings. Figure F.1 presents the comparison between obtained results.

All windows analysed are double glazed with:

- external pane with internal coating
  - 11061 - COOL-LITE SKN from Saint-Gobain Glass, 6 mm
  - 4383 - Stopray Vision 60T on Clearvision from AGC Glass Europe, 5.8 mm
  - 11373 - PLANITHERM MAX from Saint-Gobain Glass, 6 mm
- gap filled with Argon, 12 mm
- internal pane Optifloat Clear from Pilkington, 6 mm

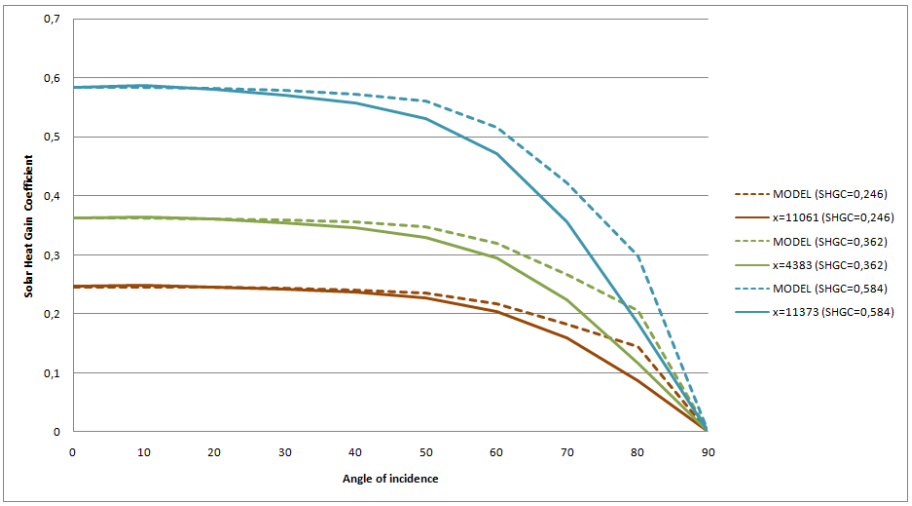

Figure F.1. Comparison of the model and results obtained from WINDOW

Additionally reflectivity, absorptivity and transitivity are calculated and compared. Absorptivity and transitivity are calculated by using the same equation, while reflectivity is obtained by knowing that the sum of the three parameters is one.

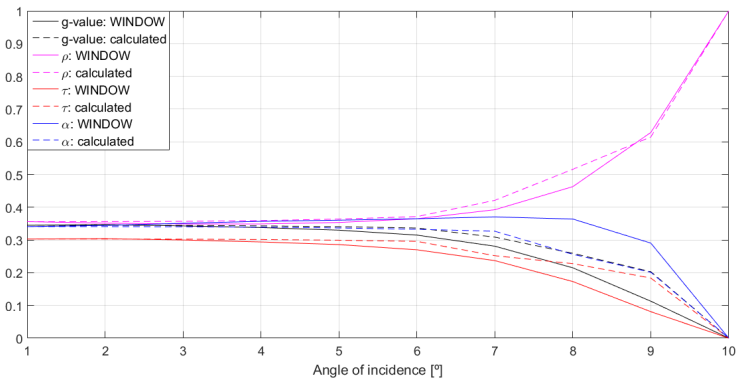

Figure F.2. Comparison of the model and results obtained from WINDOW

As it can be seen in the figures, model fits properly for low angles of incidence, while it has bigger deviation for higher angles of incidence. Deviation is also higher in windows with high SHGC; glazing used in experimental setup has low SHGC, therefore proposed equation is assumed to be good for the purpose of this simple approach.

Heat balance G

As presented in section 5.5 on page 25, the formulas have been used to get an accurate heat balance from the measurements. Further, there will be presented three different cases with different time periods. In all scenarios there will be presented the internal heat exchange in air, uncontrolled and controlled cooling and the controlled heat and solar gains resulted compared with the measured one.

Case 1 - Glazing measurement

The case takes place from 17^{th} to 19^{th} of May, where just the measurements for the glazing are performed. The weather presented for this case is with clear sky and solar radiation.

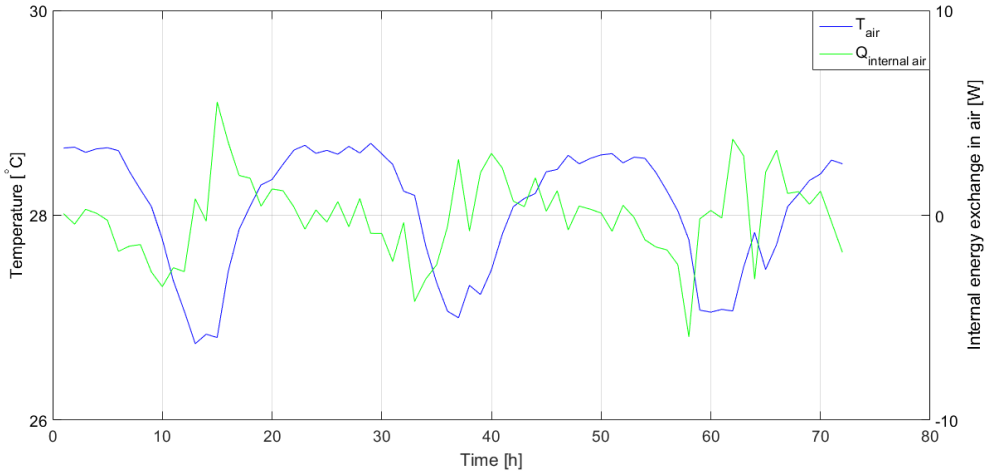

Figure G.1. Energy storage in the air of the room - Period 17^{th} to 19^{th} of May

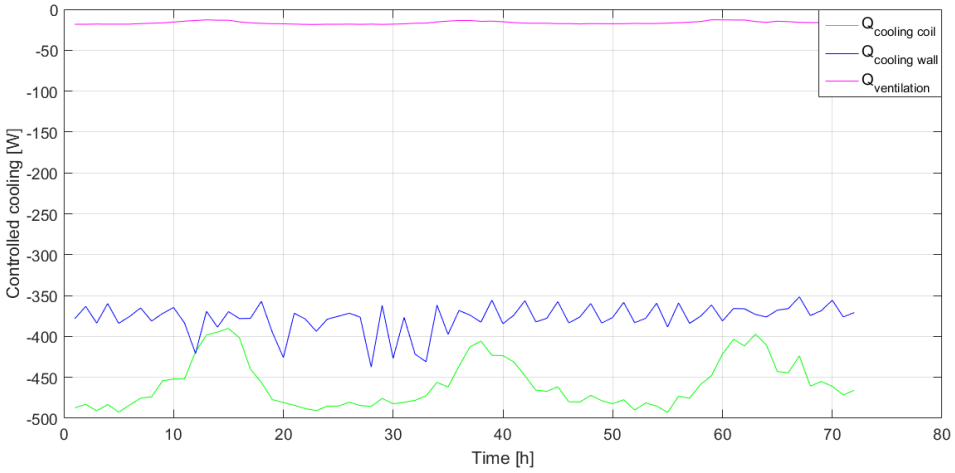

Figure G.2. Controlled cooling of the room - Period 17^{th} to 19^{th} of May

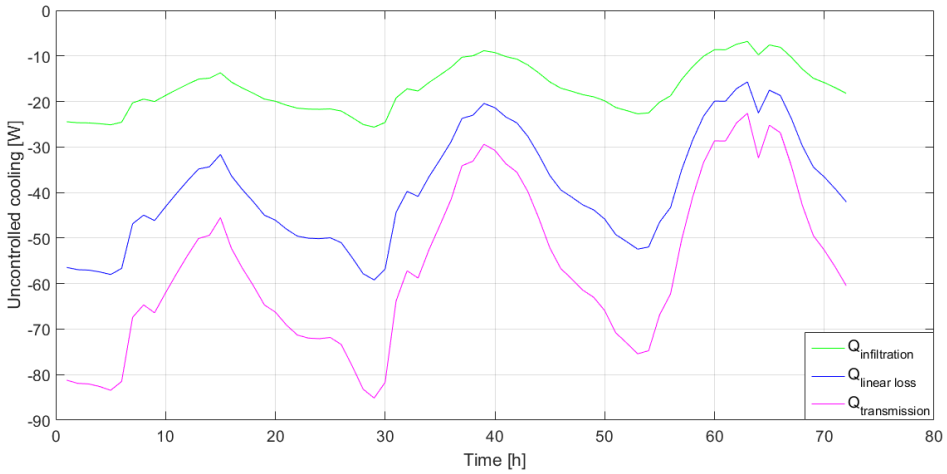

Figure G.3. Uncontrolled cooling of the room - Period 17^{th} to 19^{th} of May

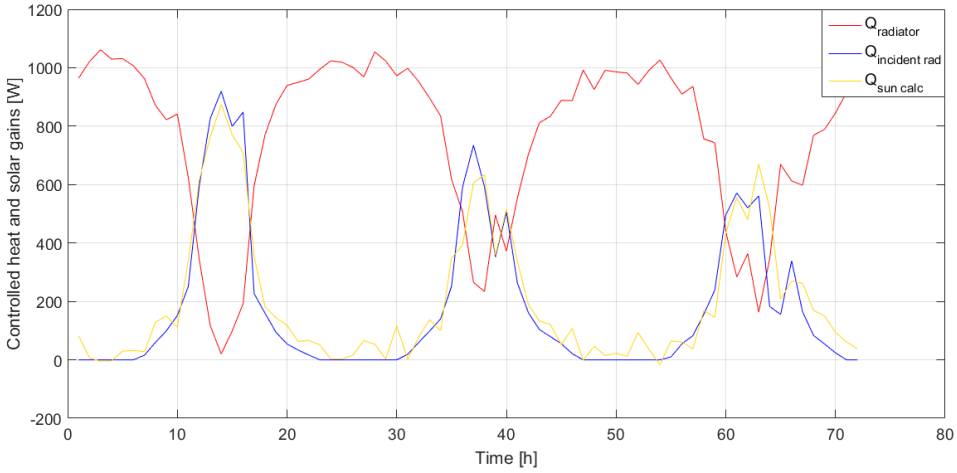

Figure G.4. Heat balance for 17^{th} to 19^{th} of May

Case 2 - Shading measurement - Charcoal Grey

The scenario is done from 25^{th} to 26^{th} of May, where charcoal grey shading is used for measurements. The weather presented for this case is overcast for the first day and a clear sky with solar radiation for the next one.

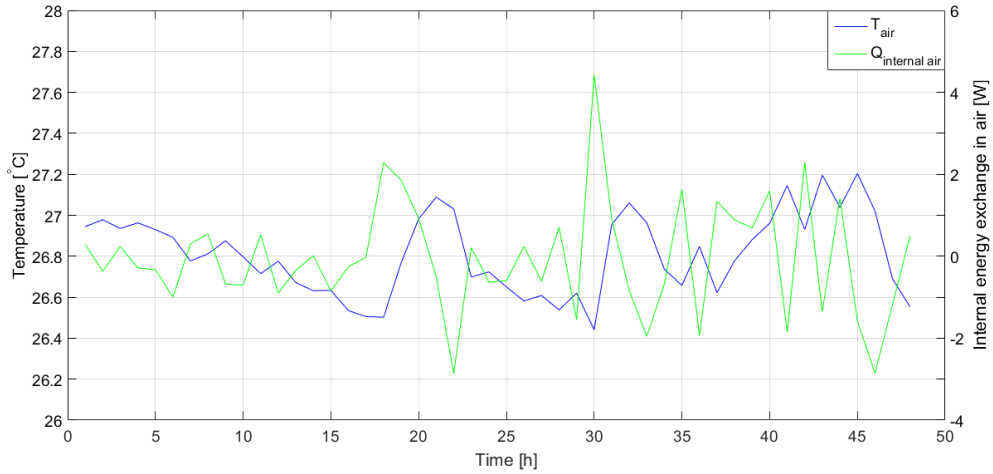

Figure G.5. Energy storage in the air of the room - Period 25^{th} to 26^{th} of May

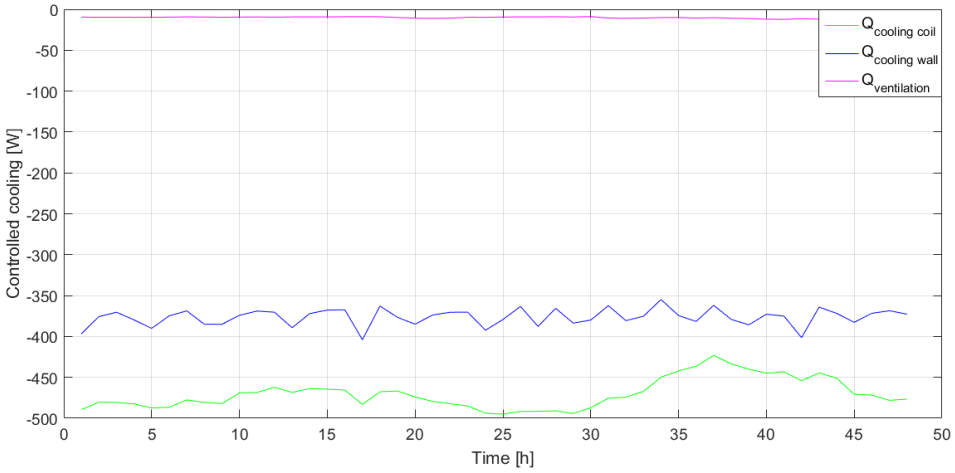

Figure G.6. Controlled cooling of the room - Period 25^{th} to 26^{th} of May

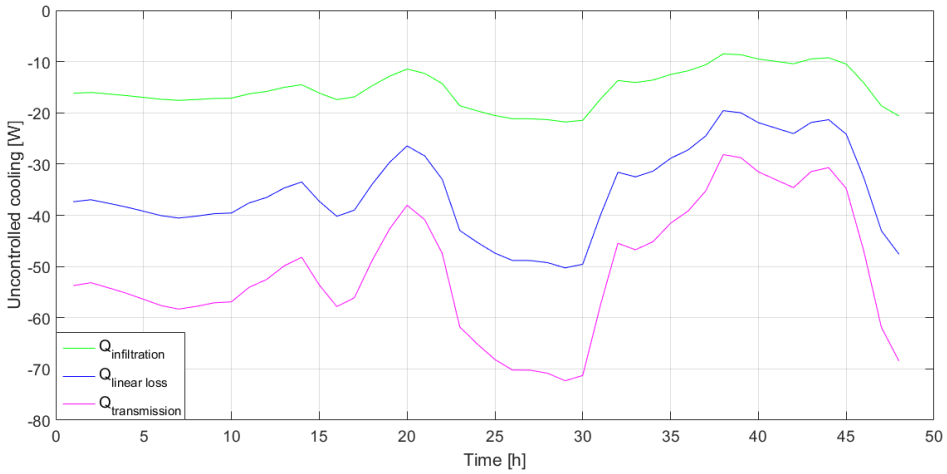

Figure G.7. Uncontrolled cooling of the room - Period 25^{th} to 26^{th} of May

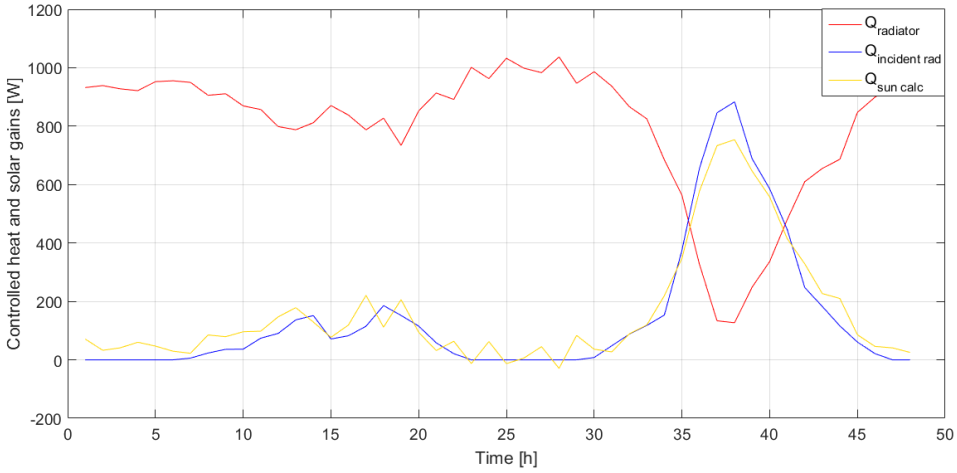

Figure G.8. Heat balance for 25^{th} to 26^{th} of May

Case 3 - Shading measurement - White pearl

The measurements are handled from 10^{th} to 15^{th} of May, where the shading white pearl is used. The weather data for this case is sunny for the first three days and for the following there are three with partial sun.

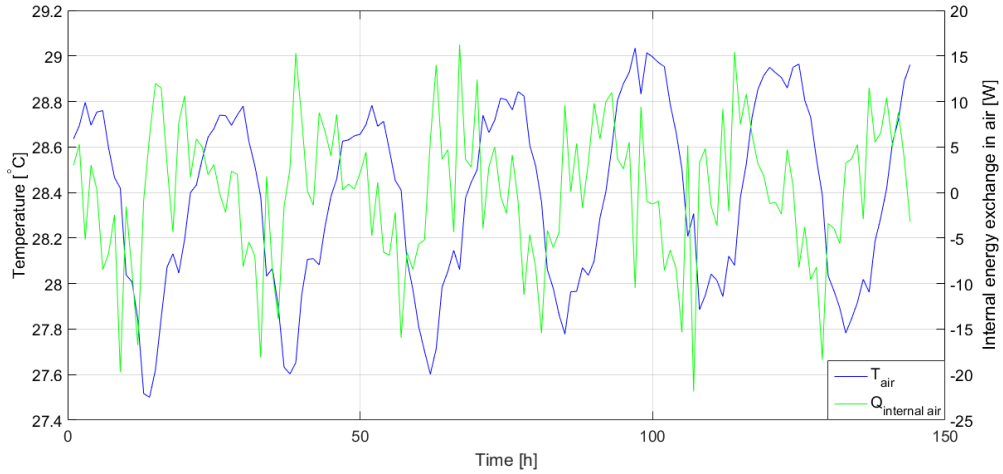

Figure G.9. Energy storage in the air of the room - Period 10^{th} to 15^{th} of May

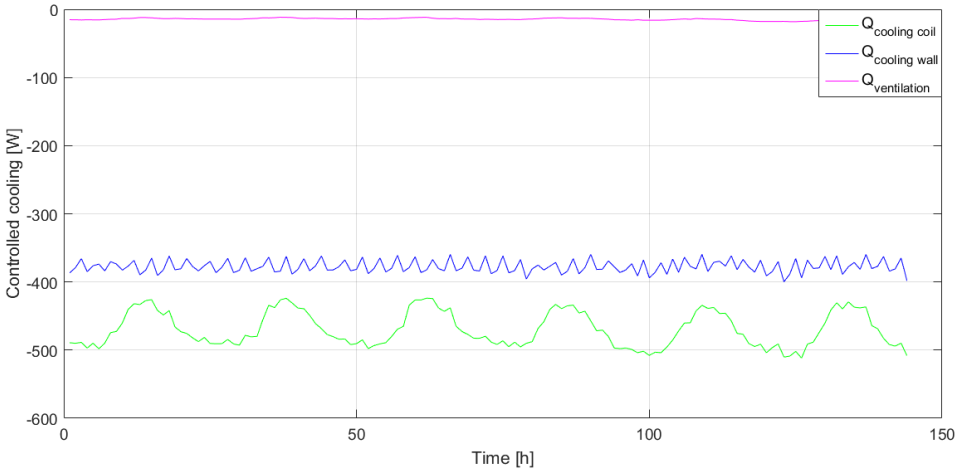

Figure G.10. Controlled cooling of the room - Period 10^{th} to 15^{th} of May

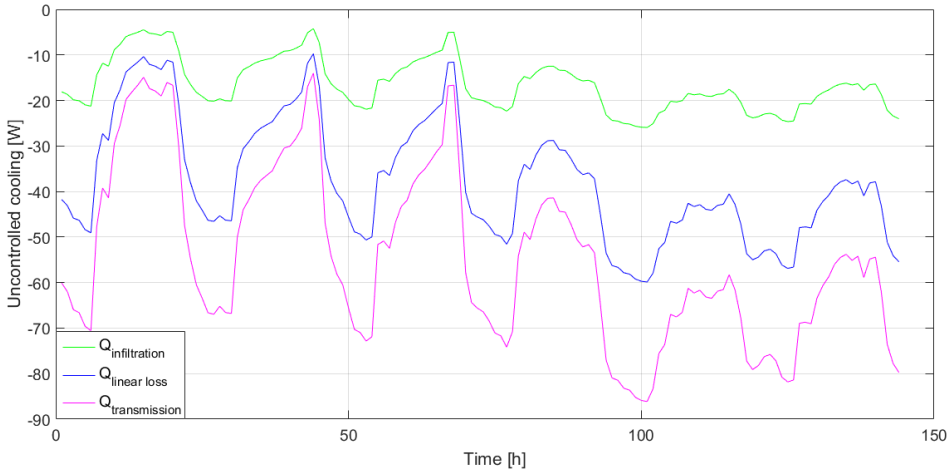

Figure G.11. Uncontrolled cooling of the room - Period 10^{th} to 15^{th} of May

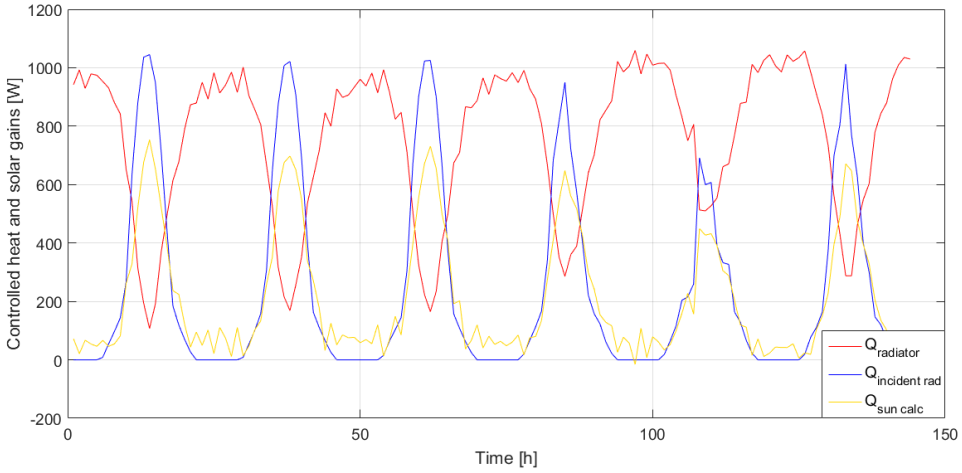

Figure G.12. Heat balance for 10^{th} to 15^{th} of May

Detail glazing model - Control cooling

H

In this appendix, it is included the simulation for the detail glazing model where the cooling is controlled with a PI controller, in the same way as heating. In section 7.2.1 on page 49, there is presented the case where the cooling is with a constant value which is functioning at all times. Figure H.2 on the following page shows the internal air temperature of the detail models used in the glazing simulation and the experimental data. It is visible that in this case the internal air temperature is stable.

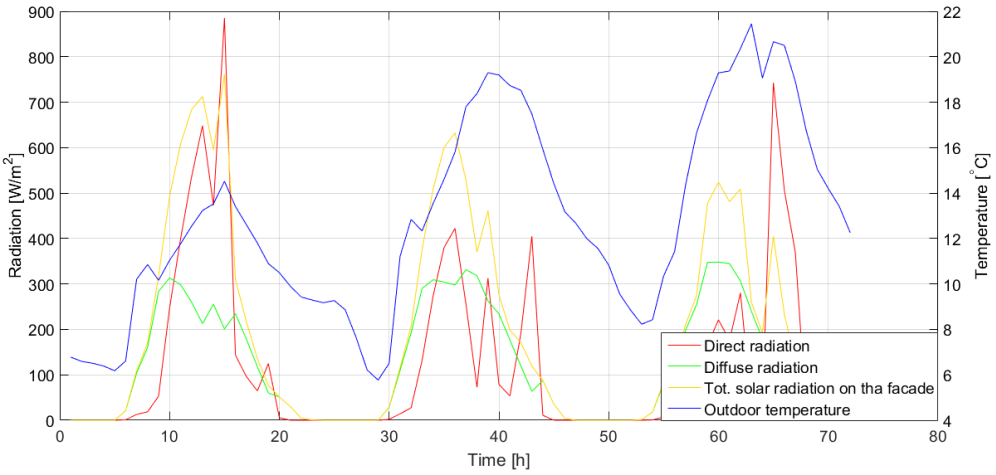

Figure H.1. Weather conditions - Period 17*th*to19*th* of May

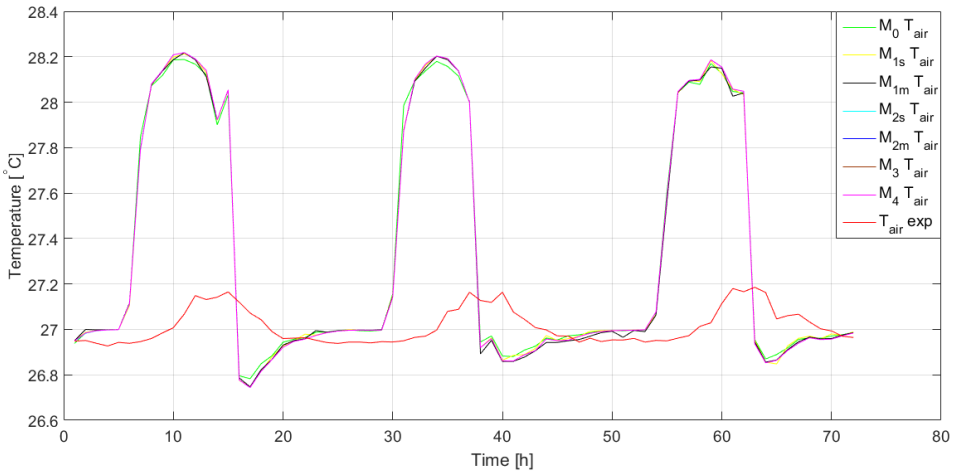

Figure H.2. Room air temperature comparison between measurements and detail glazing models - Period 17*th*to19*th* of May

Next figure, presents the external surface temperatures of the window pane. The models have the same trend and the only difference emerges between the model M_0 and the others.

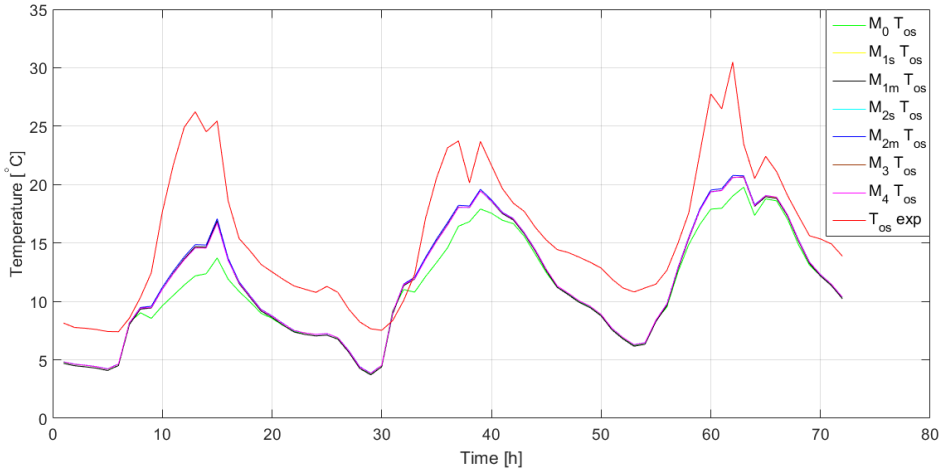

Figure H.3. Glazing's external pane surface temperature comparison between measurements and detail glazing models having the node in the surface and in the central pane - Period 17*th*to19*th* of May

Also the internal surface of the window is displayed in figure H.4 on the next page.

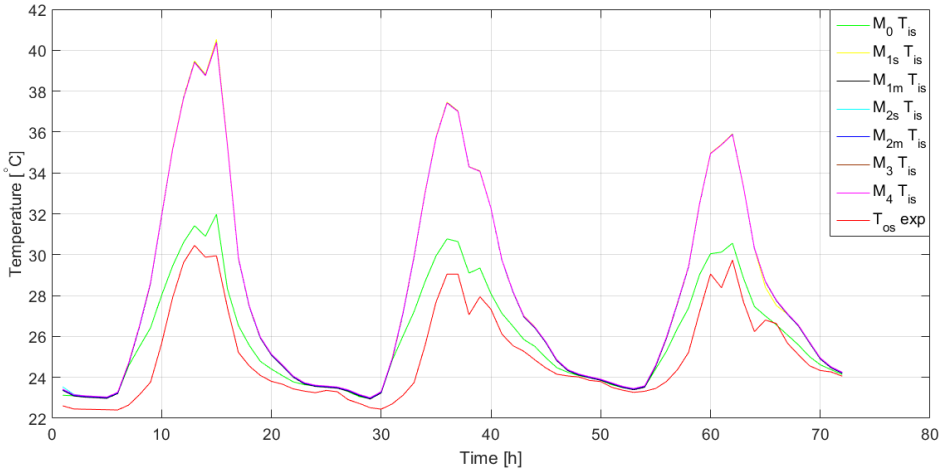

Figure H.4. Glazing's internal pane surface temperature comparison between measurements and detail glazing models having the node in the surface and in the central pane - Period 17*th*to19*th* of May

The power consumption for the simulation cases when there is a controller for both heating and cooling is shown in figure H.5. In this situation, the cooling need is high for most of the cases and the average value from the experimental cooling consumption is exceeded.

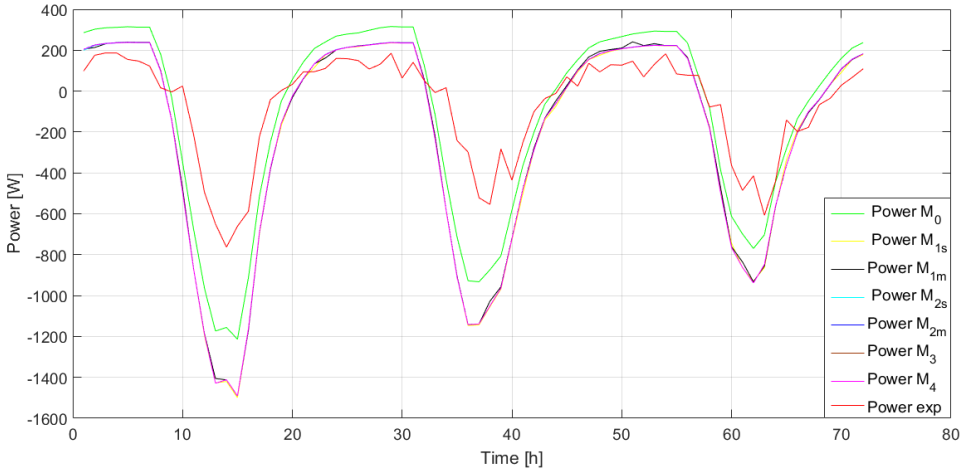

Figure H.5. Energy consumption comparison between measurements and detail glazing models - Period 17*th*to19*th* of May

SHGC-based disregarded models

I

In this appendix are briefly explained other guessed models that have been disregarded.

Three nodes model - 3N

This three nodes model is based on standard ISO-13790 [17]. Solar heat gains are considered in the internal surface of the room, and the blind is implemented by treating the double glazing and blind as a three layer window. Representation of the model is shown in figure I.1.

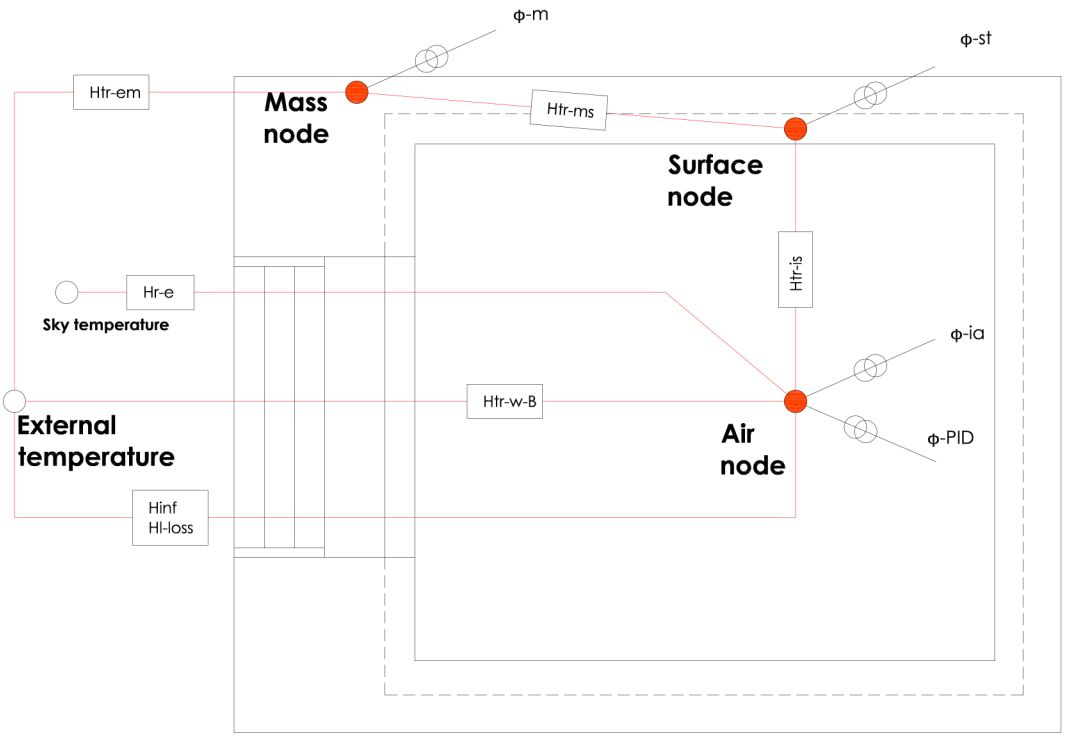

Figure I.1. 3 nodes model

Heat transfer between air node and outdoors H_{tr-w-B} is calculated according to standard EN 673 [21] where glazing and shading device are considered as a three layer window.

In order to calculate total energy transmittance when including internal shading device, standard EN-13363-1 [5] proposes the following equation:

$$g_t = g_w(1 - g_w\rho_B - \alpha_B\frac{G_{internal}}{G_2}) \tag{I.1}$$

Where:

g_t	is the total energy transmittance through window and shading
g_w	is the energy transmittance of the glazing
ρ_B	is the reflectance of the shading device
α_B	is the absorptance of the shading device
G_2	is the thermal conductance, $[\frac{W}{m^2K}]$
	$G_{internal} = (\frac{1}{U_e} + \frac{1}{G_2})^{-1}$
	where U_e is the U-value of the window, $[\frac{W}{m^2K}]$

Solar direct transmittance is calculated according to the following equation, which also considers the shading:

$$\tau_t = \frac{\tau_w\tau_B}{1 - \rho'_w\rho_B} \tag{I.2}$$

Where:

τ_w, τ_B	is the solar direct transmittance of the glazing and the blind
ρ'_w	is the solar direct reflectance of the side of the glazing away from the incident radiation
ρ_B	is the solar reflectance of the side of the blind facing the incident radiation

Then solar gain ϕ_{sol} is introduced in ϕ_{st} according to standard ISO-13790 [17] and is calculated as:

$$\phi_{sol} = (\phi_{dir} + \phi_{dif})\tau_t \tag{I.3}$$

Four nodes model - 4N-WIN

This model considers in the fourth node the internal surface of the internal pane of the glazing, and assumes the cavity to be part of the air in the room. Sketch of this model is shown in figure I.2.

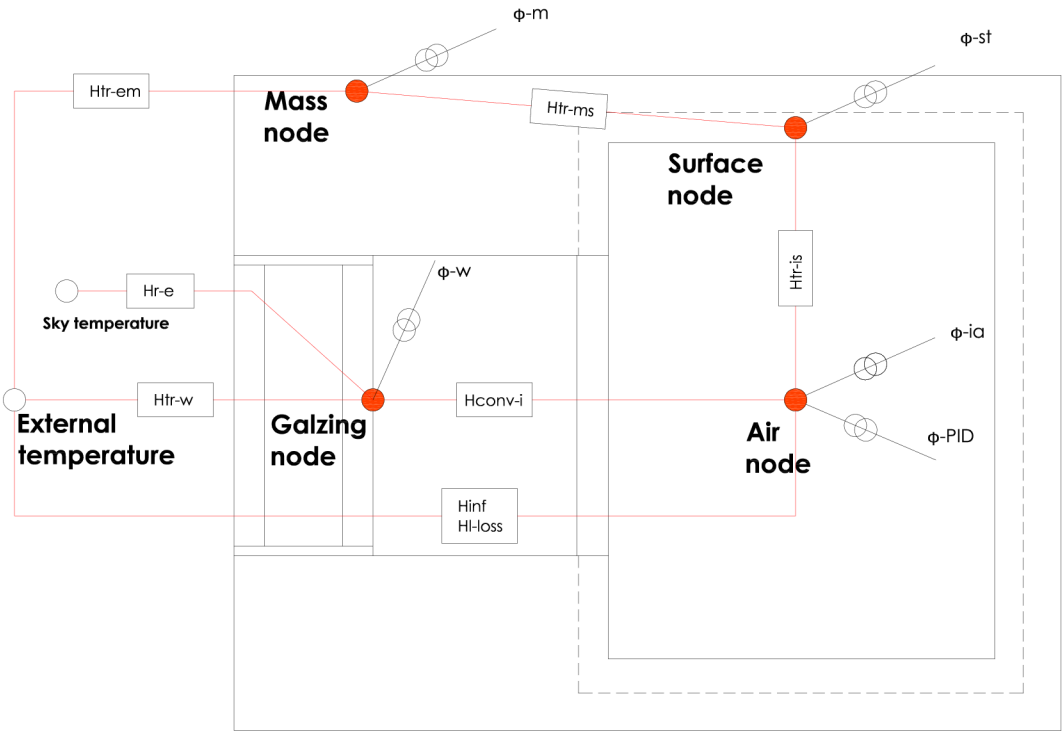

Figure I.2. 4 nodes model considering glazing's internal surface

Heat transfer coefficients H_{tr-w} is calculated according to standard EN 673 [21], and H_{tr-b} considers blind thermal conductivity and internal convective heat transfer coefficients in both sides of the shading.

Solar heat gains consider the same as in standard ISO-13790 [17] plus a gain in the glazing node according to glazing's absorptivity.

Comparison of the models

For this comparison only data from measurements with White Pearl blind are shown since conclusions are similar for the rest of experiment setup. External weather conditions for this case are shown in the next figure.

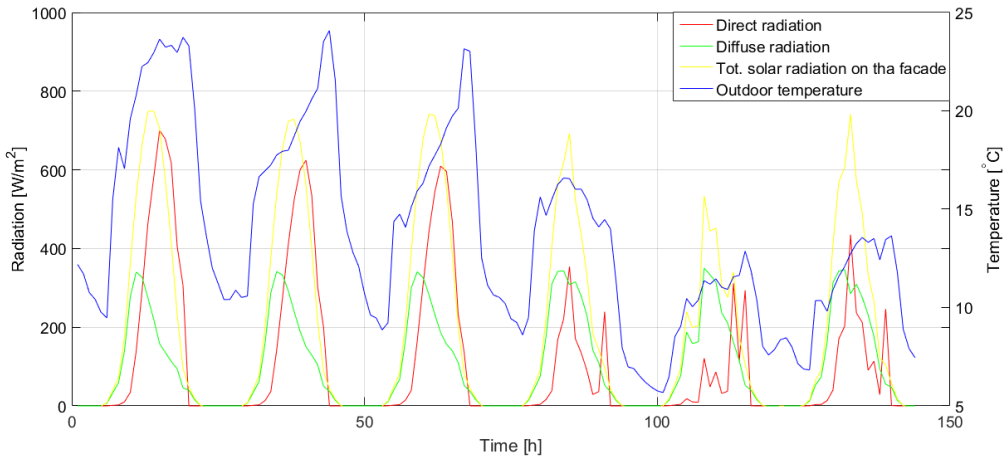

Figure I.3. External weather conditions. White Pearl blind

From the analysis of the energy consumption can be seen how models 3N and 4N-WIN have very similar results. Only advantage from model 4N-WIN would be glazing temperature calculation, but as seen in figure I.6 results are underestimated. All models calculate higher heating demand during the night time than the measured one. By fitting the curves to the value of heating demand from the experiment, it is seen that models 4N-WIN and 3N have a cooling overestimation, while model 4N-CAV is fitting well.

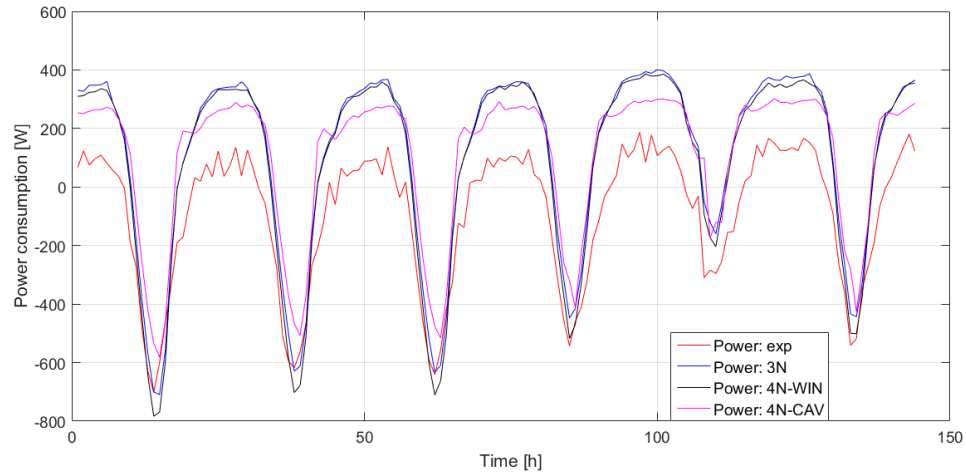

Figure I.4. Energy consumption. White Pearl blind

Regarding air temperature in the room, all models perform very similarly.

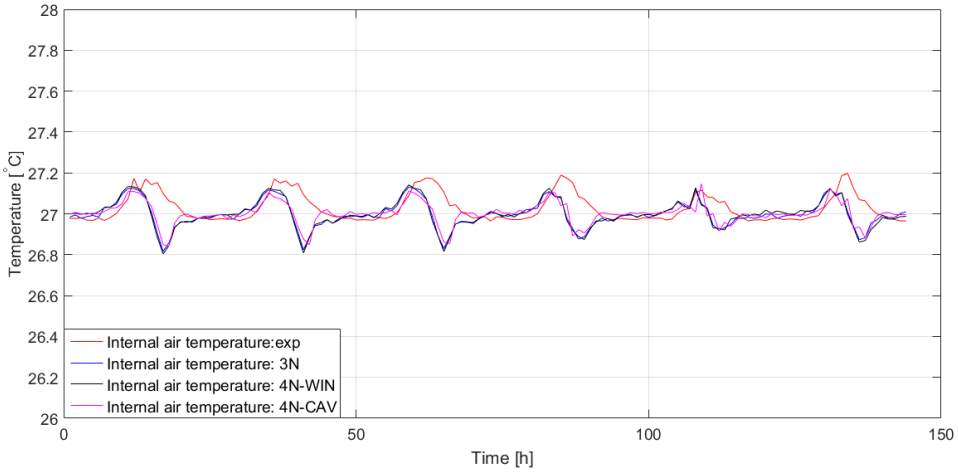

Figure I.5. Room air temperature. White Pearl blind

This final graph shows glazing internal surface temperature. Results seem underestimated from measurements although experiment values might be inaccurate and representing higher values than the reality.

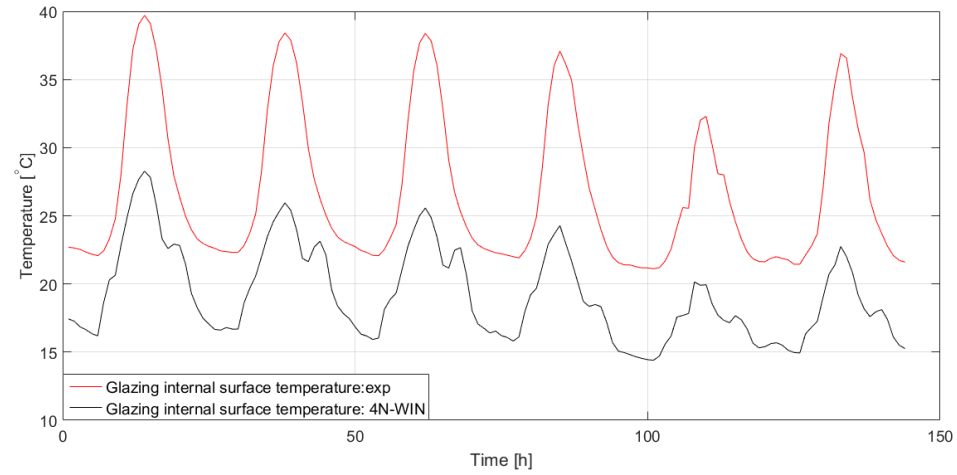

Figure I.6. Glazing internal surface temperature. White Pearl blind

All in all, based on energy consumption results model 4N-CAV is chosen, which is the one explained in the project.

Validation of shading models J

Here are stated validations of two developed models described in sections 8.1 and 8.2 for the remaining periods on measurements provided in the Cube with the shading devices (Table 5.4). Periods: 7-8 May 2016 and 10-15 May 2016 are presented.

Weather conditions for period with White Pearl blind are displayed below. Outdoor temperature and solar radiations are presented.

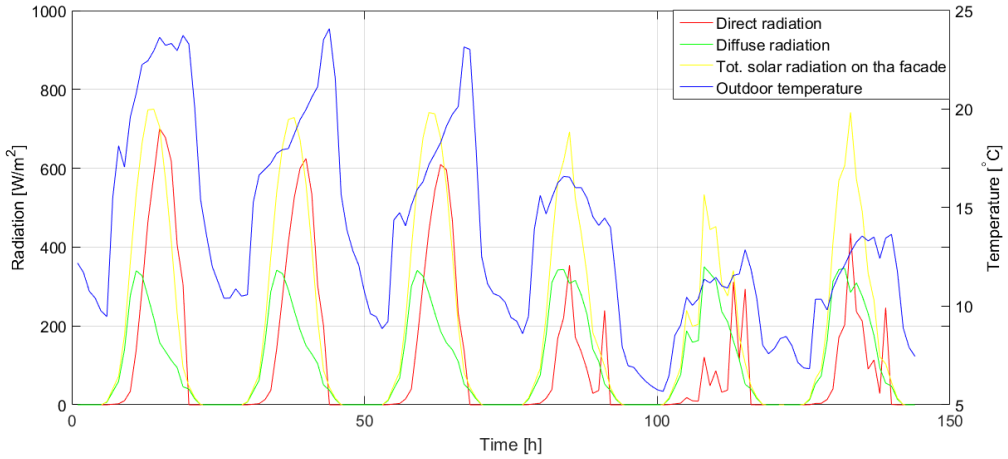

Figure J.1. External weather conditions for the measurement period 10-15 May with White Pearl blind.

Power consumption is plotted and additionally the curve fitting is done for the simulation models for a better representation of differences. In the legend are stated constant values in watts added to the simulation results.

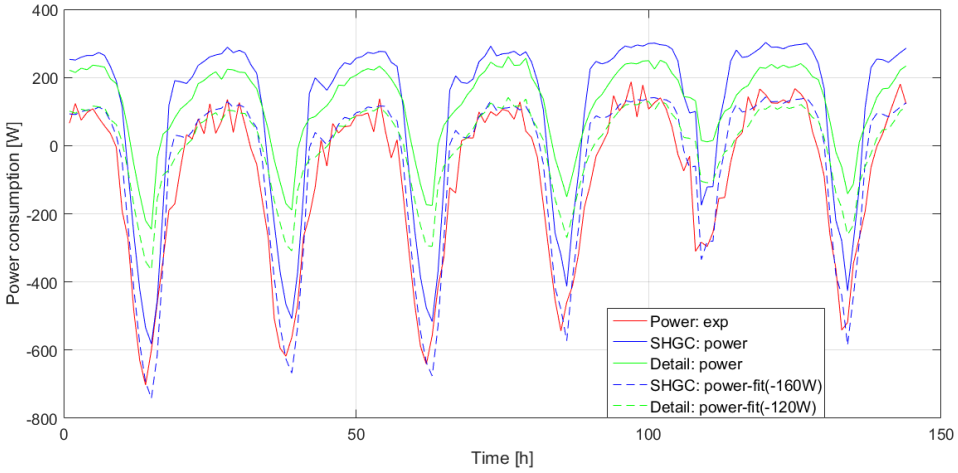

Figure J.2. Energy consumption for the measurement period 10-15 May with White Pearl blind.

Air room temperature and temperature of air in the cavity obtained from the simulations are compared with measured once. Results are presented below on figures J.3 and J.4.

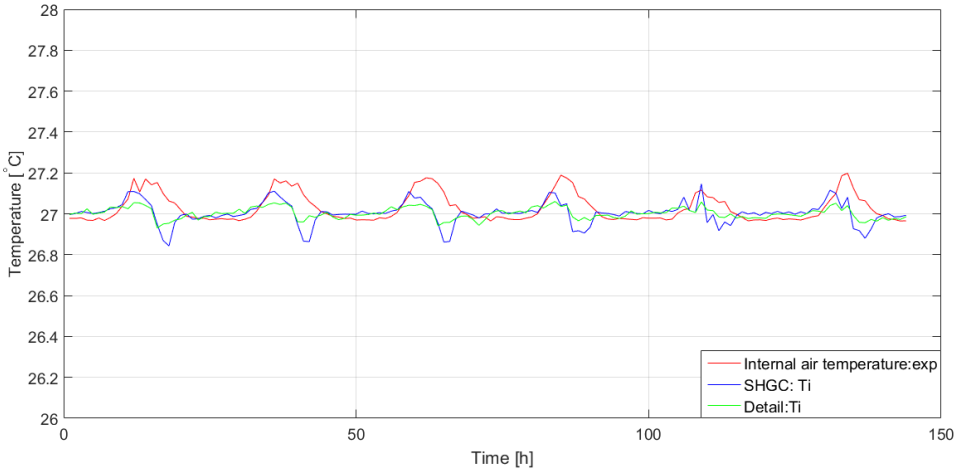

Figure J.3. Indoor air temperature for the measurement period 10-15 May with White Pearl blind.

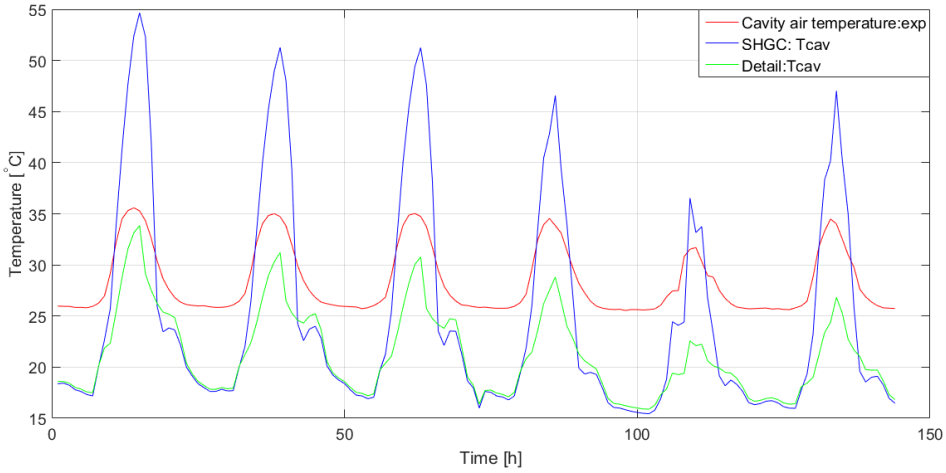

Figure J.4. Cavity air temperature for the measurement period 10-15 May with White Pearl blind.

Blind surface temperatures are validated with the measured once and the results are displayed together with cavity air temperatures obtained from simulation and measurements. Only detail model can simulate the blind surface temperatures therefore only the results from this model are presented.

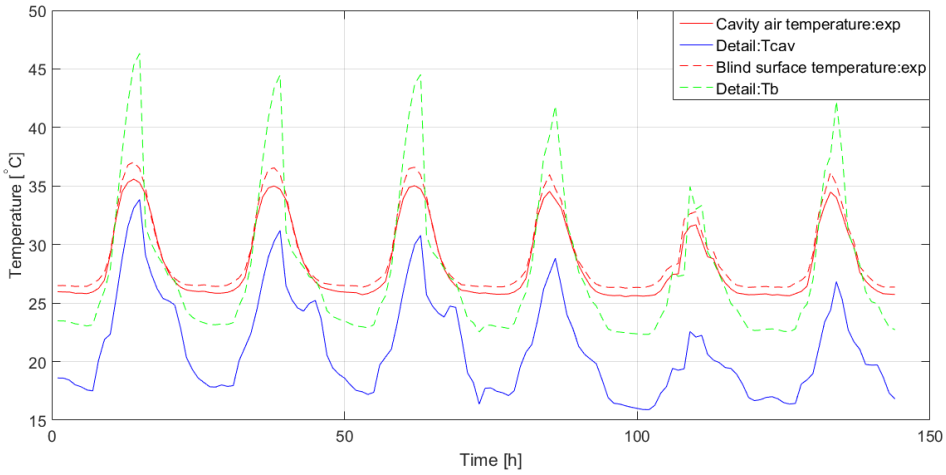

Figure J.5. Cavity air temperature for the measurement period 10-15 May with White Pearl blind.

The same set of figures is done for the measurement period 7-8 May 2016 where the Charcoal Grey blind was used. Experiment results are compared with simulations.

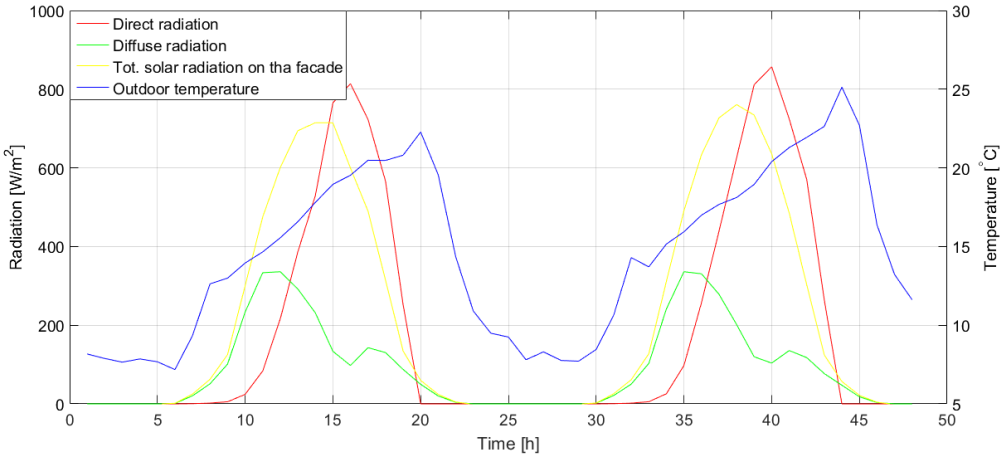

Figure J.6. External weather conditions for the measurement period 7-8 May with Charcoal Grey blind.

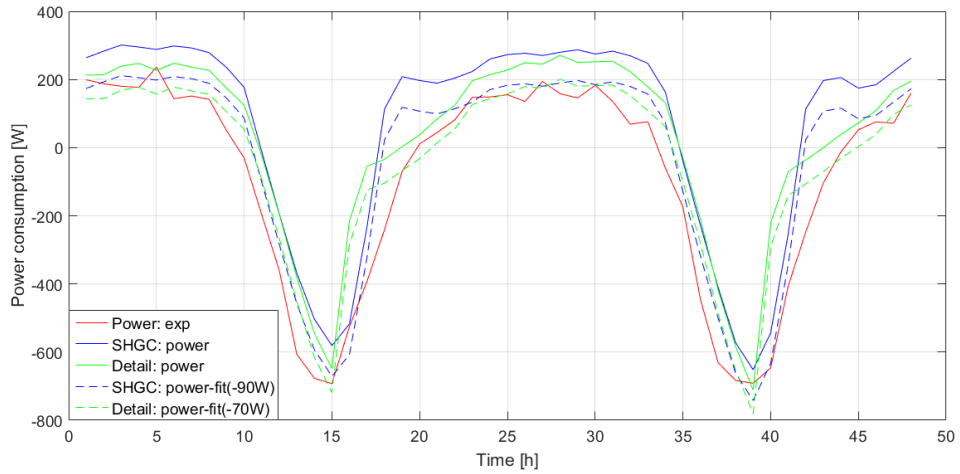

Figure J.7. Energy consumption for the measurement period 7-8 May with Charcoal Grey blind.

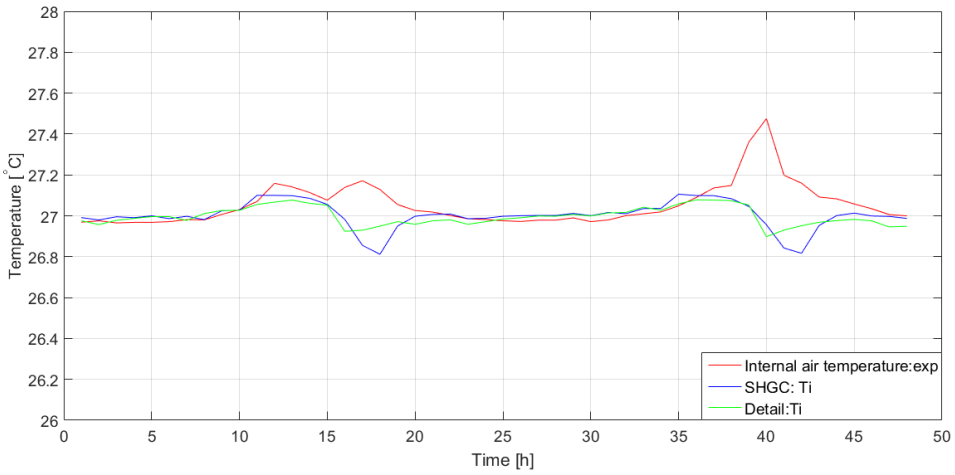

Figure J.8. Indoor air temperature for the measurement period 7-8 May with Charcoal Grey blind.

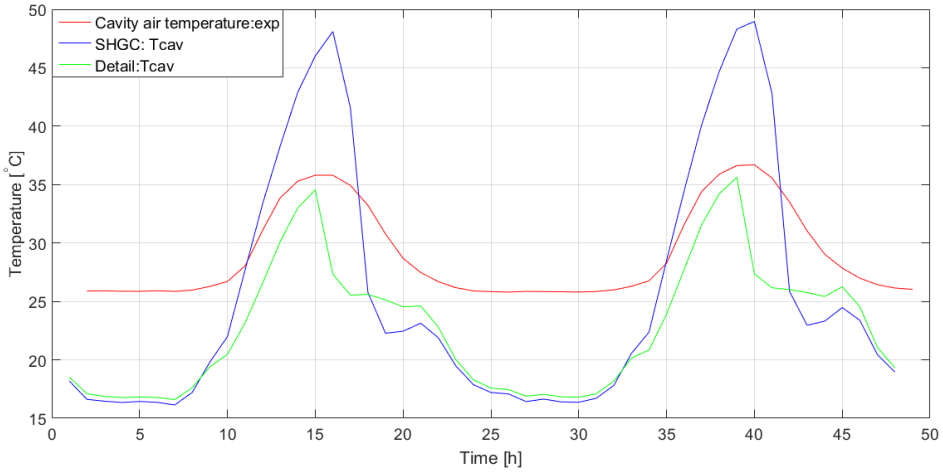

Figure J.9. Cavity air temperature for the measurement period 7-8 May with Charcoal Grey blind.

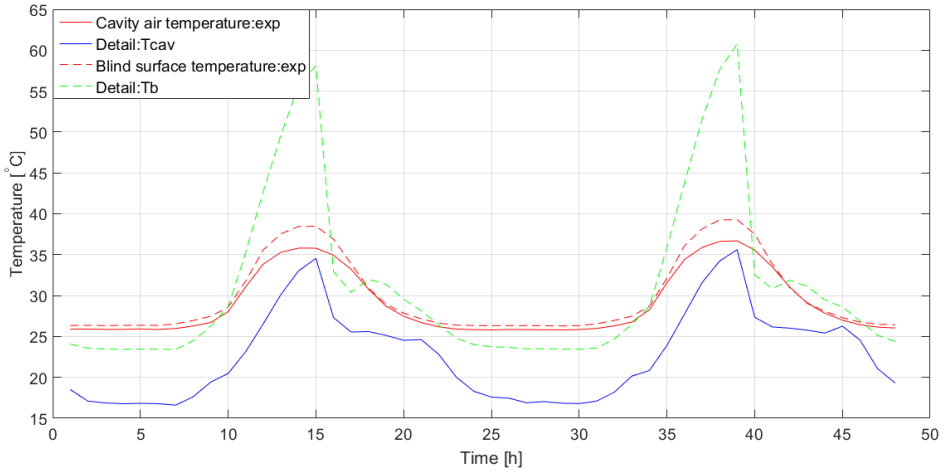

Figure J.10. Cavity air temperature for the measurement period 7-8 May with Charcoal Grey blind.

Window linear loss calculation

K

By using the thermographic camera, linear loss coefficient has been estimated for the window. Several pictures have been taken from different corners of the window and the left edge, and an average of those temperatures has been used for the calculation. Temperature set point for the air of the room is set to 28 degrees during 24 hours.

ZONE:	I	II	III	IV	V	AVERAGE:
TEMPERATURES:	20.6	20.9	19	17.4	21.6	19.9

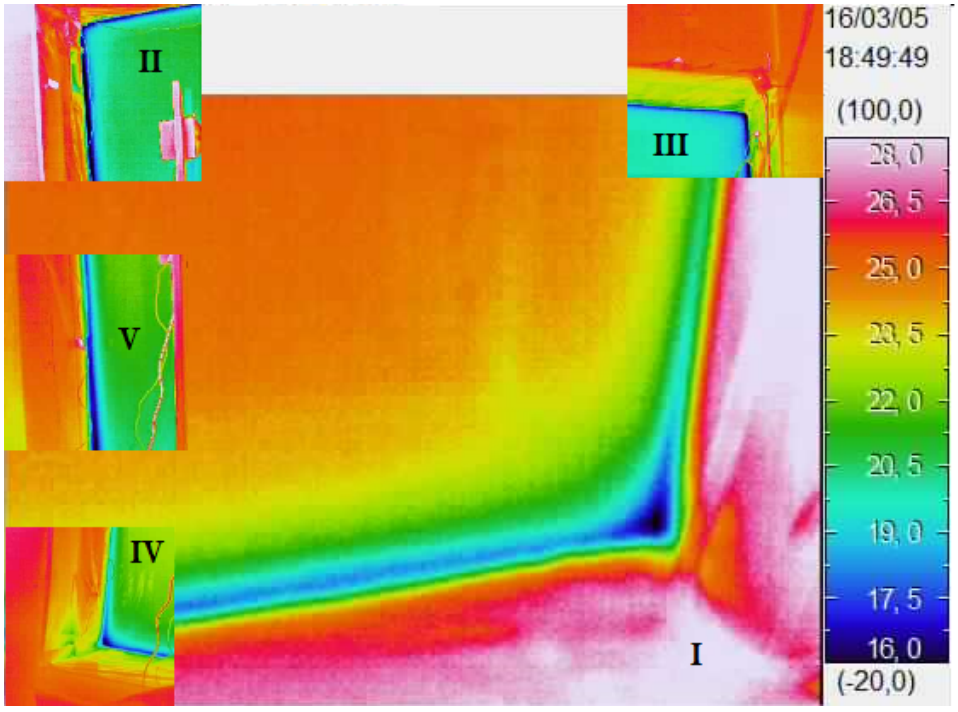

Figure K.1. Pictures obtained with thermographic camera from the window.

Heat transfer coefficient of the glazing is calculated considering external convective heat transfer and conductive heat transfer coefficients. Convective heat transfer coefficient for

the glazing is $0,866 \frac{W}{m^2 K}$, and external and internal convective heat transfer coefficients are $27,100 \frac{W}{m^2 K}$ and $3,134 \frac{W}{m^2 K}$ respectively. It is assumed a constant heat flow through the thermal bridge. Knowing external temperature is 7 degrees and internal temperature 28 degrees, can be calculated the heat transfer through the window:

$$Q_{trans} = U_w A_{facade} \Delta T \tag{K.1}$$

Where:

U_w	is the total heat transfer coefficient of the window, $[0,8706 W/m^2 K]$
A_{facade}	is the area of the glazing
ΔT	is the temperature difference between the external and internal temperature, [K]

Obtained heat flow is $77,48 W$. Knowing the temperature in the surface of the thermal bridge, thermal linear loss coefficient can be calculated as

$$Q_{trans} = \psi_{Line} L_{line} \Delta T \tag{K.2}$$

where the heat transfer coefficient for the thermal bridge is obtained, equal to $1,1122 \frac{W}{mK}$

CD L

1. Calibration folder
2. Matlab models
3. Measurements
4. Pictures
5. Report in PDF